
MARTIN–LUTHER–UNIVERSITÄT
HALLE–WITTENBERG
INSTITUT FÜR MATHEMATIK



DAE aspects of multibody system dynamics

M. Arnold

Report No. 01 (2016)

Editors:

Professors of the Institute for Mathematics, Martin Luther University Halle-Wittenberg.

Electronic version: see <http://www.mathematik.uni-halle.de/institut/reports/>

DAE aspects of multibody system dynamics

M. Arnold

Report No. 01 (2016)

Martin Arnold
Martin-Luther-Universität Halle-Wittenberg
Naturwissenschaftliche Fakultät II
Institut für Mathematik
Theodor-Lieser-Str. 5
D-06120 Halle/Saale, Germany
Email: martin.arnold@mathematik.uni-halle.de

DAE aspects of multibody system dynamics

Martin Arnold

Abstract The dynamical simulation of mechanical multibody systems has stimulated the development of theory and numerical methods for higher index differential-algebraic equations (DAEs) for more than three decades. The equations of motion are linearly implicit second order differential equations. For constrained systems, they form an index-3 DAE with a specific structure that is exploited in theoretical investigations as well as in the numerical solution. In the present survey paper, we give an introduction to this field of research with focus on classical and more recent solution techniques for the time integration of constrained mechanical systems in multibody system dynamics. Part of the material is devoted to topics of current research like multibody system models with nonlinear configuration spaces or systems with redundant constraints.

1 Introduction

Multibody system dynamics is a branch of technical mechanics that considers the dynamical interaction of rigid and flexible bodies in complex engineering systems [74]. Multibody system models are frequently used in such diverse fields of application like robotics, vehicle system dynamics, biomechanics, aerospace engineering and wind turbine design. They are composed of a finite number of rigid or flexible bodies and their connecting elements that are assumed to be massless [74, 75].

In engineering, the modelling of mechanical multibody systems follows a generic network approach [52] with basic elements like rigid bodies, flexible bodies, force elements and joints being available in model libraries. The interaction of these basic elements is described by equations of motion resulting from the principles of clas-

Martin Arnold

Martin Luther University Halle-Wittenberg, Institute of Mathematics, 06099 Halle (Saale), Germany, e-mail: martin.arnold@mathematik.uni-halle.de

sical mechanics [76]. The separate modelling of system components in this network approach is attractive from the viewpoint of model setup but results systematically in a redundant system description [52]. Constraints have to be added to guarantee a consistent state of the overall multibody system model.

Formally, these constrained systems could always be transformed to an analytically equivalent ordinary differential equation (ODE) introducing appropriate generalized coordinates [17]. The progress in analysis and numerical solution of differential-algebraic equations (DAEs) allows, however, to solve the constrained systems directly in terms of the original redundant coordinates which proves to be much more efficient than (semi-)analytical solution techniques being based on a minimum set of independent coordinates. A short historical review of these developments has recently been published in [83, Section 2.4].

Constrained multibody system models are challenging from the viewpoint of DAE theory since their index is three and index reduction techniques are mandatory for a numerically stable time integration by error controlled variable step size solvers. These index reduction techniques rely on time derivatives of the constrained equations that have a direct physical interpretation as hidden constraints at the level of velocity or acceleration coordinates [40]. Classical approaches like Baumgarte stabilization [21] or the stabilized index-2 formulation of the equations of motion in the sense of Gear, Gupta and Leimkuhler [44] have been developed a long time before the “boom days” of DAE theory [83] that started in the late 1980’s.

There is a rich literature on numerical methods in multibody dynamics [36, 88], in particular on time integration methods for constrained systems. The comprehensive survey in [50, Chapter VII] is an excellent reference in this field.

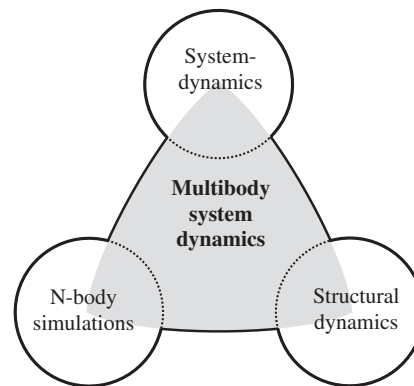


Fig. 1 Multibody system dynamics and related fields of dynamical analysis.

Multibody system dynamics is, however, much more than just the simulation of constrained N -body systems, see Fig. 1. In engineering, the methods and software tools of multibody system dynamics are used as integration platform for multidisciplinary simulation in nonlinear system dynamics [16]. The analysis of flexible

bodies provides a close link to structural mechanics. Specific aspects of such flexible multibody systems have been discussed recently from a mathematical viewpoint [82] and from the viewpoint of engineering [20]. The monograph of Géradin and Cardona [45] was an early attempt to bridge the gap between both disciplines.

The present paper considers some DAE aspects of multibody numerics being relevant to applications in engineering. It starts in Section 2 with an introduction to constrained systems studying systematically conditions for the existence and uniqueness of solutions for a large problem class of practical interest including systems with rank-deficient mass matrix and redundant constraints.

In Section 3, we consider systems with nonlinear configuration spaces representing the orientation of (rigid or flexible) bodies in space. The resulting model equations are substantially more complex than the ones that are typically discussed in the mathematical literature on multibody numerics. This section ends with a compact introduction to multibody formalisms that exploit the model topology for an efficient evaluation of the equations of motion in large scale engineering applications.

Section 4 provides a consistent introduction to DAE time integration methods in multibody dynamics that covers ODE based solution techniques like Runge-Kutta or linear multi-step methods [50] as well as Newmark type integrators from structural dynamics [45]. There is a special focus on the stabilized index-2 formulation of the equations of motion that may be considered as a quasi-standard in industrial multibody system simulation [11].

2 Constrained mechanical systems

In Lagrangian mechanics, the motion of a conservative mechanical system is characterized by a variational principle that takes into account the potential energy $U(\mathbf{q})$ and the kinetic energy

$$T(\mathbf{q}, \dot{\mathbf{q}}) := \frac{1}{2} \dot{\mathbf{q}}^\top \mathbf{M}(\mathbf{q}) \dot{\mathbf{q}}.$$

The potential energy results in potential forces $-\nabla U(\mathbf{q})$. It is formulated in terms of *position coordinates* $\mathbf{q}(t) \in \mathbb{R}^{n_q}$ that describe the configuration of the system and define *velocity coordinates* $\dot{\mathbf{q}}(t) := (d\mathbf{q}/dt)(t)$. Mass and inertia terms are summarized in the symmetric, positive semi-definite *mass matrix* $\mathbf{M}(\mathbf{q}) \in \mathbb{R}^{n_q \times n_q}$.

In the present section, we consider constrained systems and derive in Section 2.1 their equations of motion. These are classical results that may be found in any textbook on mechanics like, e.g., [17]. Sufficient conditions for the unique solvability of initial value problems are discussed in Section 2.2, see also [50, Section VII.1]. A more refined analysis is necessary for systems with rank-deficient mass matrix or rank-deficient constraint matrix that have recently found new interest in the literature [42] and will be studied in Section 2.3.

2.1 Equations of motion

The motion of a mechanical system may be subject to constraints in form of equations (*bilateral* constraints) or inequalities (*unilateral* constraints). In the present section, we consider *holonomic* constraints

$$\mathbf{g}(t, \mathbf{q}(t)) = \mathbf{0}, \quad (t \in [t_0, t_{\text{end}}]) \quad (1)$$

that have to be satisfied in the whole time interval of interest. For more general types of constraints, we refer to Section 3.2 below.

To derive the equations of motion from a variational principle, we summarize kinetic and potential energy in the Lagrangian

$$L(\mathbf{q}, \dot{\mathbf{q}}) := T(\mathbf{q}, \dot{\mathbf{q}}) - U(\mathbf{q}).$$

In the constrained case, we introduce *Lagrange multipliers* $\boldsymbol{\lambda}(t) \in \mathbb{R}^{n_\lambda}$ to couple $n_\lambda \leq n_q$ holonomic constraints (1) to $L(\mathbf{q}, \dot{\mathbf{q}})$ and consider the augmented action integral

$$\int_{t_0}^{t_{\text{end}}} \left(L(\mathbf{q}(t), \dot{\mathbf{q}}(t)) - (\mathbf{g}(t, \mathbf{q}(t)))^\top \boldsymbol{\lambda}(t) \right) dt.$$

According to Hamilton's principle of least action, the extremals of this functional coincide with the motion of the mechanical system. The Euler equations for this variational problem are given by

$$\frac{d}{dt} \left(\frac{\partial L}{\partial \dot{q}_k}(\mathbf{q}, \dot{\mathbf{q}}) \right) - \frac{\partial L}{\partial q_k}(\mathbf{q}, \dot{\mathbf{q}}) + \left(\frac{\partial \mathbf{g}}{\partial q_k}(\mathbf{q}) \right)^\top \boldsymbol{\lambda} = \mathbf{0}, \quad (k = 1, \dots, n_q) \quad (2)$$

with $\mathbf{g}(t, \mathbf{q}(t)) = \mathbf{0}$, see (1). In vector form, they may be summarized to

$$\mathbf{M}(\mathbf{q})\ddot{\mathbf{q}} = \mathbf{f}(\mathbf{q}, \dot{\mathbf{q}}) - \mathbf{G}^\top(t, \mathbf{q}) \boldsymbol{\lambda}, \quad (3a)$$

$$\mathbf{0} = \mathbf{g}(t, \mathbf{q}) \quad (3b)$$

with the *constraint matrix* $\mathbf{G}(t, \mathbf{q}) := (\partial \mathbf{g} / \partial \mathbf{q})(t, \mathbf{q}) \in \mathbb{R}^{n_\lambda \times n_q}$ and the *force vector*

$$\mathbf{f}(\mathbf{q}, \dot{\mathbf{q}}) := -\nabla_{\mathbf{q}} U(\mathbf{q}) + \nabla_{\mathbf{q}} T(\mathbf{q}, \dot{\mathbf{q}}) - \left(\frac{\partial}{\partial \dot{\mathbf{q}}} (\nabla_{\mathbf{q}} T(\mathbf{q}, \dot{\mathbf{q}})) \right)^\top \dot{\mathbf{q}}. \quad (4)$$

For systems with constant mass matrix \mathbf{M} , we just have $\mathbf{f}(\mathbf{q}, \dot{\mathbf{q}}) = -\nabla_{\mathbf{q}} U(\mathbf{q})$ since $\nabla_{\mathbf{q}} T(\mathbf{q}, \dot{\mathbf{q}}) \equiv \mathbf{0}$.

Example 1. The mathematical pendulum is a rather simple model problem that has been used already in the 1980's to study constrained mechanical systems from the viewpoint of DAE theory [40, 47]. It consists of a point mass $m > 0$ that moves under the influence of gravity and is forced by a massless rod of length $l > 0$ to keep a fixed distance to the origin, see Fig. 2.

The pendulum has one degree of freedom that is given by the angle α between rod and y -axis with $\alpha^* = 0$ denoting the equilibrium position, see Fig. 2. Taking

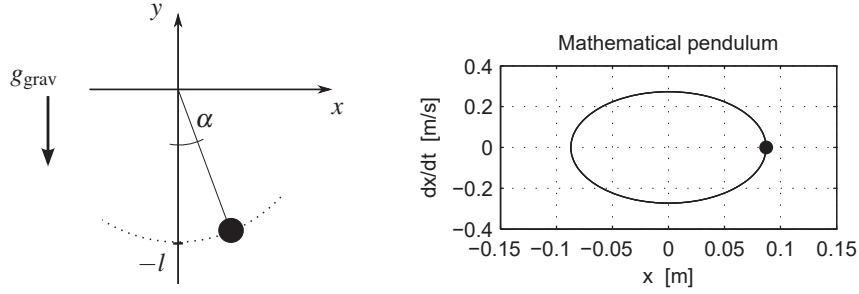


Fig. 2 Configuration and phase plot of the mathematical pendulum, Cartesian coordinates.

into account that $x = l \sin \alpha$, $y = -l \cos \alpha$ implies $\dot{x} = -l\dot{\alpha} \cos \alpha$ and $\dot{y} = -l\dot{\alpha} \sin \alpha$, we may express the kinetic energy $T = m(\dot{x}^2 + \dot{y}^2)/2$ and the potential energy $U = mg_{\text{grav}} y$ in terms of α and $\dot{\alpha}$:

$$T(\alpha, \dot{\alpha}) = \frac{ml^2}{2} \dot{\alpha}^2, \quad U(\alpha) = -mg_{\text{grav}} l \cos \alpha$$

with g_{grav} denoting the gravitational acceleration constant. The equations of motion (3) are given by the second order ordinary differential equation (ODE)

$$ml^2 \ddot{\alpha} = -mg_{\text{grav}} l \sin \alpha \quad \Rightarrow \quad \ddot{\alpha} = -\frac{g_{\text{grav}}}{l} \sin \alpha \quad (5)$$

since the position coordinates $\mathbf{q} = \alpha \in \mathbb{R}$ are not subject to constraints. All solutions of (5) are periodic. As a typical example, we show in Fig. 2 the phase plot (x, \dot{x}) for initial values $\alpha_0 = 5^\circ$, $\dot{\alpha}_0 = 0 \text{ rad/s}$ that are marked in the diagram by the dot at $x_0 = l \sin(5\pi/180)$, $\dot{x}_0 = 0 \text{ m/s}$. The physical model parameters are $m = 1.0 \text{ kg}$, $l = 1.0 \text{ m}$ and $g_{\text{grav}} = 9.81 \text{ m/s}^2$.

An analytically equivalent description of the mathematical pendulum is given by the Cartesian coordinates $\mathbf{q} = (x, y)^\top \in \mathbb{R}^2$ that are redundant and have to satisfy $x^2 + y^2 = l^2$ (Pythagorean theorem). Scaling this holonomic constraint by a factor of $1/2$, we get the equations of motion

$$m\ddot{x} = -x\lambda, \quad (6a)$$

$$m\ddot{y} = -mg_{\text{grav}} - y\lambda, \quad (6b)$$

$$0 = \frac{1}{2}(x^2 + y^2 - l^2), \quad (6c)$$

see (3). The mass matrix $\mathbf{M} = m\mathbf{I}_2$ is a constant multiple of the identity matrix $\mathbf{I}_2 \in \mathbb{R}^{2 \times 2}$. Force vector and constraint matrix are given by $\mathbf{f}(\mathbf{q}, \dot{\mathbf{q}}) = (0, -mg_{\text{grav}})^\top$ and $\mathbf{G}(\mathbf{q}) = (x, y) \in \mathbb{R}^{1 \times 2}$.

Example 1 illustrates that one and the same mechanical system may be represented by different sets of coordinates resulting in unconstrained systems like (5)

or constrained systems like (6). Obviously, the mathematical structure of the constrained equations (6) is more complex. On the other hand, the Cartesian coordinate approach is more flexible in the modelling of more complex systems as can be seen already from the model of a chain of $N \geq 2$ mathematical pendulums:

Example 2. Consider a chain of $N \geq 2$ point masses m being connected by massless rods of length l and attach the first point mass by another massless rod of length l to the origin $(x_0, y_0) = (0, 0)$. This chain of mathematical pendulums moves under the influence of gravity.

In the special case $N = 2$ we obtain the double pendulum that is depicted by the left plot of Fig. 3. Phase plots (x_1, \dot{x}_1) and (x_2, \dot{x}_2) illustrate the complex dynamical behaviour that is known to be chaotic. We started with zero initial velocities $\dot{\mathbf{q}}_0 = \mathbf{0}$ and an initial position $\mathbf{q}_0 = (x_1(t_0), y_1(t_0), x_2(t_0), y_2(t_0))^T$ that is defined by initial values for the angles α_i between rod “ i ” and the y -axis, ($i = 1, 2$), see Fig. 3. The physical parameter values are the same as in Example 1 and the initial values are set to $\alpha_1(t_0) = 5^\circ$, $\alpha_2(t_0) = 0^\circ$.

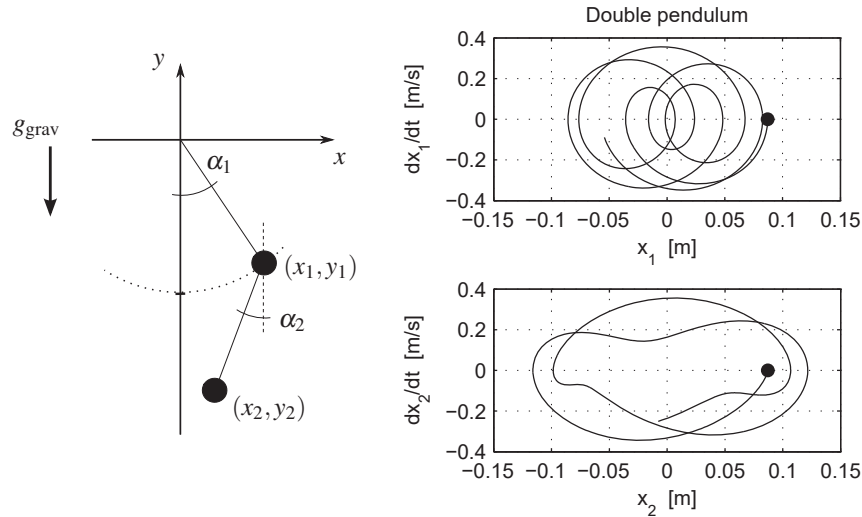


Fig. 3 Configuration and phase plots of a double pendulum, Cartesian coordinates.

To setup the equations of motion in the general case, we consider $N \geq 2$ point masses with Cartesian coordinates $\mathbf{q}_i = (x_i, y_i)^T$, ($i = 1, \dots, N$), and obtain a constrained system in $n_{\mathbf{q}} = 2N$ position coordinates $\mathbf{q} = (\mathbf{q}_1^T, \dots, \mathbf{q}_N^T)^T$ that are subject to $n_{\lambda} = N$ constraints $(x_i - x_{i-1})^2 + (y_i - y_{i-1})^2 = l^2$, ($i = 1, \dots, N$). Following step-by-step the analysis in Example 1, we get the kinetic energy $T(\mathbf{q}, \dot{\mathbf{q}}) = \sum_i m(\dot{x}_i^2 + \dot{y}_i^2)/2$, the potential energy $U(\mathbf{q}) = \sum_i m g_{\text{grav}} y_i$ and the equations of motion

$$m\ddot{x}_i = -(x_i - x_{i-1})\lambda_i + (x_{i+1} - x_i)\lambda_{i+1}, \quad (i = 1, \dots, N-1), \quad (7a)$$

$$m\ddot{x}_N = -(x_N - x_{N-1})\lambda_N, \quad (7b)$$

$$m\ddot{y}_i = -mg_{\text{grav}} - (y_i - y_{i-1})\lambda_i + (y_{i+1} - y_i)\lambda_{i+1}, \quad (i = 1, \dots, N-1), \quad (7c)$$

$$m\ddot{y}_N = -mg_{\text{grav}} - (y_N - y_{N-1})\lambda_N, \quad (7d)$$

$$0 = \frac{1}{2}((x_i - x_{i-1})^2 + (y_i - y_{i-1})^2 - l^2), \quad (i = 1, \dots, N) \quad (7e)$$

with Lagrange multipliers $\boldsymbol{\lambda} = (\lambda_1, \dots, \lambda_N)^\top \in \mathbb{R}^N$. Comparing (7) with the equations of motion in compact form (3), we see that the constraints (7e) define a vector valued function $\mathbf{g} = (g_1, \dots, g_N)^\top$ in (3b) that yields a sparse constraint matrix $\mathbf{G}(\mathbf{q}) = (G_{ij}(\mathbf{q}))_{i,j} \in \mathbb{R}^{N \times 2N}$ with non-zero elements

$$\begin{aligned} G_{i,2i-1}(\mathbf{q}) &= x_i - x_{i-1}, & G_{i,2i}(\mathbf{q}) &= y_i - y_{i-1}, & (i = 1, \dots, N), \\ G_{i,2i+1}(\mathbf{q}) &= -(x_{i+1} - x_i), & G_{i,2i+2}(\mathbf{q}) &= -(y_{i+1} - y_i), & (i = 1, \dots, N-1). \end{aligned}$$

The mass matrix $\mathbf{M}(\mathbf{q})$ and the force vector $\mathbf{f}(\mathbf{q}, \dot{\mathbf{q}})$ in the dynamical equations (3a) are given by $\mathbf{M} = \text{blockdiag}(\mathbf{M}_1, \dots, \mathbf{M}_N)$, $\mathbf{f} = (\mathbf{f}_1^\top, \dots, \mathbf{f}_N^\top)^\top$ with $\mathbf{M}_i = m\mathbf{I}_2$ and $\mathbf{f}_i(\mathbf{q}, \dot{\mathbf{q}}) = (0, -mg_{\text{grav}})^\top$, $(i = 1, \dots, N)$.

Cartesian coordinates are favourable to derive the equations of motion (7) since kinetic energy and potential energy are given in terms of $(x_i, y_i, \dot{x}_i, \dot{y}_i)$, $(i = 1, \dots, N)$. Mass matrix and constraint matrix are sparse. Furthermore, the mass matrix \mathbf{M} is constant and block-diagonal. The sparsity pattern of the constraint matrix $\mathbf{G}(\mathbf{q})$ corresponds to the coordinates of direct neighbours in the chain.

Example 2 illustrates that redundant position coordinates \mathbf{q} may help to speed-up the modelling process of complex systems. In principle such redundant coordinates \mathbf{q} and the corresponding constraints $\mathbf{g}(t, \mathbf{q}) = \mathbf{0}$ in (3) could be avoided choosing appropriate generalized coordinates. For larger systems, the use of such generalized coordinates is, however, often technically much more complicated than for simple model problems like the mathematical pendulum with equations of motion (5). As a typical example, we consider the double pendulum with the configuration being depicted in Fig. 3.

Example 3. Let α_i , $(i = 1, 2)$, denote the angle between rod “ i ” and the y-axis and use position coordinates $\mathbf{q} = (\alpha_1, \alpha_2)^\top \in \mathbb{R}^2$. We get

$$x_i = x_{i-1} + l \sin \alpha_i, \quad y_i = y_{i-1} - l \cos \alpha_i, \quad (i = 1, 2).$$

with $(x_0, y_0) = (0, 0)$ and may express the kinetic and potential energy in terms of $\mathbf{q}, \dot{\mathbf{q}}$ using $\dot{x}_1 = l\dot{\alpha}_1 \cos \alpha_1$, $\dot{x}_2 = \sum_i l\dot{\alpha}_i \cos \alpha_i$, $\dot{y}_1 = -l\dot{\alpha}_1 \sin \alpha_1$, $\dot{y}_2 = -\sum_i l\dot{\alpha}_i \sin \alpha_i$:

$$T(\mathbf{q}, \dot{\mathbf{q}}) = \sum_{i=1}^2 \frac{m}{2} (\dot{x}_i^2 + \dot{y}_i^2) = \frac{ml^2}{2} (\dot{\alpha}_1^2 + 2 \cos(\alpha_2 - \alpha_1) \dot{\alpha}_1 \dot{\alpha}_2 + \dot{\alpha}_2^2),$$

$$U(\mathbf{q}) = \sum_{i=1}^2 mg_{\text{grav}} y_i = -mg_{\text{grav}} l (2 \cos \alpha_1 + \cos \alpha_2).$$

Evaluating the force vector according to (4), we have to take into account the state dependent mass matrix $\mathbf{M}(\mathbf{q})$ that results in $\nabla_{\mathbf{q}}T(\mathbf{q}, \dot{\mathbf{q}}) \neq \mathbf{0}$. Then, the equations of motion are obtained in form of a linearly implicit second order system of ordinary differential equations with state dependent mass matrix $\mathbf{M}(\mathbf{q})$:

$$\begin{pmatrix} 2 & \cos(\alpha_2 - \alpha_1) \\ \cos(\alpha_2 - \alpha_1) & 1 \end{pmatrix} \begin{pmatrix} \ddot{\alpha}_1 \\ \ddot{\alpha}_2 \end{pmatrix} = \begin{pmatrix} -2 \frac{g_{\text{grav}}}{l} \sin \alpha_1 + \sin(\alpha_2 - \alpha_1) \dot{\alpha}_2^2 \\ -\frac{g_{\text{grav}}}{l} \sin \alpha_2 - \sin(\alpha_2 - \alpha_1) \dot{\alpha}_1^2 \end{pmatrix}.$$

For the double pendulum, these algebraic manipulations may still be performed by hand but for larger systems the use of computer algebra programs becomes mandatory. As an alternative, we will consider in Section 3.3 below a mixed coordinate formulation that allows to evaluate the accelerations $\ddot{\mathbf{q}}(t)$ numerically by a block Gauss elimination for a large sparse system of linear equations.

2.2 Existence and uniqueness

Holonomic constraints (1) restrict the configuration space at the level of position coordinates. They imply *hidden constraints* at the level of velocity coordinates $\dot{\mathbf{q}}$ that are obtained by differentiation of (1) w.r.t. t :

$$\mathbf{0} = \frac{d}{dt} \mathbf{g}(t, \mathbf{q}(t)) = \frac{\partial \mathbf{g}}{\partial t}(t, \mathbf{q}(t)) + \frac{\partial \mathbf{g}}{\partial \mathbf{q}}(t, \mathbf{q}(t)) \dot{\mathbf{q}}(t) = \mathbf{g}_t(t, \mathbf{q}) + \mathbf{G}(t, \mathbf{q}) \dot{\mathbf{q}}. \quad (8)$$

The second time derivative of the holonomic constraints (1) defines hidden constraints at the level of acceleration coordinates $\ddot{\mathbf{q}}$:

$$\mathbf{0} = \frac{d^2}{dt^2} \mathbf{g}(t, \mathbf{q}(t)) = \mathbf{g}_{tt}(t, \mathbf{q}) + 2\mathbf{g}_{tq}(t, \mathbf{q}) \dot{\mathbf{q}} + \mathbf{G}(t, \mathbf{q}) \ddot{\mathbf{q}} + \mathbf{g}_{qq}(t, \mathbf{q})(\dot{\mathbf{q}}, \dot{\mathbf{q}}) \quad (9)$$

with $\mathbf{g}_{iq}(t, \mathbf{q}) = \mathbf{G}_i(t, \mathbf{q})$. The curvature term $\mathbf{g}_{qq}(t, \mathbf{q})(\dot{\mathbf{q}}, \dot{\mathbf{q}})$ represents the second partial derivatives of the vector valued function $\mathbf{g}(t, \mathbf{q})$ w.r.t. its vector valued argument \mathbf{q} in the sense that

$$\mathbf{g}_{qq}(t, \mathbf{q})(\mathbf{w}, \mathbf{z}) = \frac{\partial}{\partial \mathbf{q}} (\mathbf{G}(t, \mathbf{q}) \mathbf{w}) \mathbf{z}, \quad (\mathbf{w}, \mathbf{z} \in \mathbb{R}^{nq}). \quad (10)$$

Here we assume tacitly that the constraint function \mathbf{g} is as often continuously differentiable as it is necessary to define the constraint matrix $\mathbf{G}(t, \mathbf{q})$ and to derive the hidden constraints (8) and (9). Appropriate smoothness assumptions will be specified in Theorem 1 below.

The hidden constraints (8) are part of the *derivative array* of DAE (3), see [26]. But they are not just the result of an abstract mathematical transformation but have a reasonable physical interpretation as well [40]. To discuss this aspect in more detail, we focus on *scleronomic* constraints

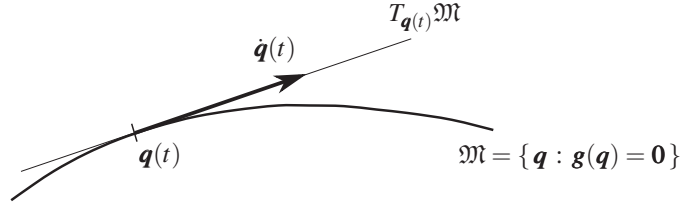


Fig. 4 Constraint manifold $\mathfrak{M} := \{ \mathbf{q} : \mathbf{g}(\mathbf{q}) = \mathbf{0} \}$ with tangent space $T_{\mathbf{q}}\mathfrak{M}$.

$$\mathbf{g}(\mathbf{q}) = \mathbf{0} \quad (11)$$

that do not depend explicitly on time t and restrict the configuration of the constrained system to the manifold

$$\mathfrak{M} := \{ \mathbf{q} : \mathbf{g}(\mathbf{q}) = \mathbf{0} \}. \quad (12)$$

For scleronomic constraints, the hidden constraints (8) and (9) are simplified because the partial derivatives w.r.t. t vanish identically:

$$\mathbf{0} = \mathbf{G}(\mathbf{q})\dot{\mathbf{q}}, \quad (13)$$

$$\mathbf{0} = \mathbf{G}(\mathbf{q})\ddot{\mathbf{q}} + \mathbf{g}_{\mathbf{q}\mathbf{q}}(\mathbf{q})(\dot{\mathbf{q}}, \dot{\mathbf{q}}). \quad (14)$$

Since $\ker \mathbf{G}(\mathbf{q})$ spans the tangent space $T_{\mathbf{q}}\mathfrak{M}$ of the manifold at point $\mathbf{q} \in \mathfrak{M}$, the hidden constraints (13) indicate that the velocity vector $\dot{\mathbf{q}}(t)$ is in the tangent space $T_{\mathbf{q}(t)}\mathfrak{M}$, see Fig. 4. Therefore, the solution $\mathbf{q}(t)$ remains in manifold \mathfrak{M} for all $t \in [t_0, t_{\text{end}}]$, see [71, 72].

Example 4. The mathematical pendulum is a model in the (x, y) -plane with a point mass moving in the one-dimensional manifold $\mathfrak{M} = \{ \mathbf{q} = (x, y)^\top : x^2 + y^2 = l^2 \}$, see Example 1. Manifold \mathfrak{M} is a circle and its tangent space $T_{\mathbf{q}}\mathfrak{M} \subset \mathbb{R}^2$ consists of all vectors being orthogonal to \mathbf{q} .

The trajectory $\mathbf{q}(t)$ will follow the circle iff $\dot{\mathbf{q}}(t) \in T_{\mathbf{q}(t)}\mathfrak{M}$, i.e., iff $0 = (\mathbf{q}(t))^\top \dot{\mathbf{q}}(t) = x(t)\dot{x}(t) + y(t)\dot{y}(t)$. This is exactly the hidden constraint (13) at the level of velocity coordinates that results from formal differentiation of constraint (6c). A second differentiation step yields the hidden constraint (14) at the level of acceleration coordinates:

$$0 = \frac{d}{dt}(x\dot{x} + y\dot{y}) = x\ddot{x} + y\ddot{y} + \dot{x}^2 + \dot{y}^2.$$

This equation may be solved w.r.t. the Lagrange multiplier λ since $\ddot{x} = -x\lambda/m$, $\ddot{y} = -y\lambda/m$, see (6a,b):

$$\lambda = \lambda(x, \dot{x}, y, \dot{y}) := m \frac{-g_{\text{grav}}y + \dot{x}^2 + \dot{y}^2}{x^2 + y^2} = m \frac{-g_{\text{grav}}y + \dot{x}^2 + \dot{y}^2}{l^2}. \quad (15)$$

The dynamical equations (6a,b) with λ being substituted by $\lambda(x, \dot{x}, y, \dot{y})$ according to (15) define a system of second order ODEs for variables x and y that is analytically equivalent to the constrained system.

Initial values $(x_0, \dot{x}_0, y_0, \dot{y}_0, \lambda_0)$ for the constrained system (6) have to be consistent with the constraint (6c) at position level and with its counterparts (13) and (14) at the level of velocity and acceleration coordinates:

$$x_0^2 + y_0^2 = l^2, \quad x_0 \dot{x}_0 + y_0 \dot{y}_0 = 0, \quad \lambda_0 = \lambda(x_0, \dot{x}_0, y_0, \dot{y}_0).$$

Example 4 shows that holonomic constraints (1) and the corresponding hidden constraints (8), (9) define conditions on initial values $\mathbf{q}_0 = \mathbf{q}(t_0)$, $\dot{\mathbf{q}}_0 = \dot{\mathbf{q}}(t_0)$, $\boldsymbol{\lambda}_0 = \boldsymbol{\lambda}(t_0)$. We will discuss these conditions for constrained systems

$$\mathbf{M}(t, \mathbf{q}) \ddot{\mathbf{q}} = \mathbf{f}(t, \mathbf{q}, \dot{\mathbf{q}}) - \mathbf{G}^\top(t, \mathbf{q}) \boldsymbol{\lambda}, \quad (16a)$$

$$\mathbf{0} = \mathbf{g}(t, \mathbf{q}) \quad (16b)$$

with $\mathbf{G}(t, \mathbf{q}) = (\partial \mathbf{g} / \partial \mathbf{q})(t, \mathbf{q})$. This problem class is slightly more general than (3) and covers time dependent force terms \mathbf{f} as well as condensed mass matrices $\mathbf{M}(t, \mathbf{q})$ that result from the application of multibody formalisms to systems with rheonomic joint equations, see Section 3.3.

Remark 1. In some textbooks, the argument t in the equations of motion (3) and (16) is omitted to keep the notation compact. In the ODE case, this is justified by the observation that any second order system $\ddot{\mathbf{x}} = \mathbf{f}(t, \mathbf{x}, \dot{\mathbf{x}})$ in \mathbb{R}^k is equivalent to an autonomous system $\ddot{\tilde{\mathbf{x}}} = \tilde{\mathbf{f}}(\tilde{\mathbf{x}}, \dot{\tilde{\mathbf{x}}})$ in \mathbb{R}^{k+1} with $\tilde{\mathbf{x}} := (t, \mathbf{x}^\top)^\top$, $\tilde{\mathbf{f}} := (0, \mathbf{f}^\top)^\top$, $\tilde{\mathbf{x}}_0 := (t_0, \mathbf{x}_0^\top)^\top$, $\dot{\tilde{\mathbf{x}}}_0 := (1, \dot{\mathbf{x}}_0^\top)^\top$, see. e.g., [49, Section II.2] for the corresponding transformation in the case of first order ODEs.

Applying this transformation formally to constrained systems (16) with *rheonomic* constraints $\mathbf{0} = \mathbf{g}(t, \mathbf{q})$, we obtain $\bar{\mathbf{q}} = (t, \mathbf{q}^\top)^\top$, scleronomic constraints $\mathbf{0} = \bar{\mathbf{g}}(\bar{\mathbf{q}}) := \mathbf{g}(t, \mathbf{q})$ and a constraint Jacobian $(\partial \bar{\mathbf{g}} / \partial \bar{\mathbf{q}})(\bar{\mathbf{q}})$ that is composed of the constraint matrix $\mathbf{G}(t, \mathbf{q}) = (\partial \mathbf{g} / \partial \mathbf{q})(t, \mathbf{q})$ and the partial derivatives $(\partial \mathbf{g} / \partial t)(t, \mathbf{q})$ that do not appear in (16). Therefore, the structure of the equations of motion (16) gets lost by the transformation to an autonomous system in coordinates $\bar{\mathbf{q}} = (t, \mathbf{q}^\top)^\top$ if $\partial \mathbf{g} / \partial t \neq \mathbf{0}$. That's why we will consider the equations of motion in their original non-autonomous form (16).

The dynamical equations (16a) and the hidden constraints (9) may be summarized to a system of $n_q + n_\lambda$ linear equations in $\ddot{\mathbf{q}}$ and $\boldsymbol{\lambda}$:

$$\begin{pmatrix} \mathbf{M}(t, \mathbf{q}) & \mathbf{G}^\top(t, \mathbf{q}) \\ \mathbf{G}(t, \mathbf{q}) & \mathbf{0} \end{pmatrix} \begin{pmatrix} \ddot{\mathbf{q}} \\ \boldsymbol{\lambda} \end{pmatrix} = \begin{pmatrix} \mathbf{f}(t, \mathbf{q}, \dot{\mathbf{q}}) \\ -\mathbf{g}_{qq}(t, \mathbf{q})(\dot{\mathbf{q}}, \dot{\mathbf{q}}) - 2\mathbf{g}_{tq}(t, \mathbf{q})\dot{\mathbf{q}} - \mathbf{g}_{tt}(t, \mathbf{q}) \end{pmatrix}. \quad (17)$$

For any given arguments $t, \mathbf{q}, \dot{\mathbf{q}}$ the Lagrange multipliers $\boldsymbol{\lambda} = \boldsymbol{\lambda}(t, \mathbf{q}, \dot{\mathbf{q}})$ are uniquely defined by this block structured system if the 2×2 block matrix at the left hand side of (17) is non-singular.

Lemma 1. Consider a symmetric, positive semi-definite matrix $\mathbf{M} \in \mathbb{R}^{k \times k}$ and a matrix $\mathbf{G} \in \mathbb{R}^{m \times k}$ with $\text{rank } \mathbf{G} = m \leq k$. If \mathbf{M} is positive definite at the null space of \mathbf{G} then matrix

$$\begin{pmatrix} \mathbf{M} & \mathbf{G}^\top \\ \mathbf{G} & \mathbf{0} \end{pmatrix} \quad (18)$$

is non-singular.

Proof. The terms $\boldsymbol{\xi}^\top \mathbf{M} \boldsymbol{\xi}$ and $\|\mathbf{G} \boldsymbol{\xi}\|_2^2$ are non-negative for all vectors $\boldsymbol{\xi} \in \mathbb{R}^k$ since matrix \mathbf{M} is positive semi-definite and $\|\mathbf{G} \boldsymbol{\xi}\|_2 \geq 0$. Furthermore, $\|\mathbf{G} \boldsymbol{\xi}\|_2 = 0$ implies $\mathbf{G} \boldsymbol{\xi} = \mathbf{0}$ and $\boldsymbol{\xi} \in \ker \mathbf{G}$, i.e., $\boldsymbol{\xi} = \mathbf{0}$ or $\boldsymbol{\xi}^\top \mathbf{M} \boldsymbol{\xi} > 0$ because \mathbf{M} is positive definite at $\ker \mathbf{G}$. Taking into account that

$$\boldsymbol{\xi}^\top \mathbf{M} \boldsymbol{\xi} + \|\mathbf{G} \boldsymbol{\xi}\|_2^2 = \boldsymbol{\xi}^\top (\mathbf{M} + \mathbf{G}^\top \mathbf{G}) \boldsymbol{\xi}$$

we see that the symmetric matrix $\mathbf{M} + \mathbf{G}^\top \mathbf{G} \in \mathbb{R}^{k \times k}$ is positive definite. Therefore, its inverse is well defined and matrix $\mathbf{G}(\mathbf{M} + \mathbf{G}^\top \mathbf{G})^{-1} \mathbf{G}^\top \in \mathbb{R}^{m \times m}$ is symmetric, positive definite for any matrix \mathbf{G} of full rank $m \leq k$. The assertion of the lemma follows from a block factorization of the 2×2 block matrix in three non-singular factors:

$$\begin{pmatrix} \mathbf{M} & \mathbf{G}^\top \\ \mathbf{G} & \mathbf{0} \end{pmatrix} = \begin{pmatrix} \mathbf{I} & -\mathbf{G}^\top \\ \mathbf{0} & \mathbf{I} \end{pmatrix} \begin{pmatrix} \mathbf{M} + \mathbf{G}^\top \mathbf{G} & \mathbf{0} \\ \mathbf{G} & -\mathbf{I} \end{pmatrix} \begin{pmatrix} \mathbf{I} & (\mathbf{M} + \mathbf{G}^\top \mathbf{G})^{-1} \mathbf{G}^\top \\ \mathbf{0} & \mathbf{G}(\mathbf{M} + \mathbf{G}^\top \mathbf{G})^{-1} \mathbf{G}^\top \end{pmatrix}. \quad \blacksquare$$

Theorem 1. Consider vectors $\mathbf{q}_0, \dot{\mathbf{q}}_0 \in \mathbb{R}^{n_q}$ that satisfy at $t = t_0$ the (hidden) constraints at the levels of position and velocity coordinates:

$$\mathbf{0} = \mathbf{g}(t_0, \mathbf{q}_0) = \mathbf{G}(t_0, \mathbf{q}_0) \dot{\mathbf{q}}_0 + \mathbf{g}_t(t_0, \mathbf{q}_0). \quad (19)$$

We assume that functions $\mathbf{M}(t, \mathbf{q})$, $\mathbf{f}(t, \mathbf{q}, \dot{\mathbf{q}})$ and $\mathbf{g}(t, \mathbf{q})$ are well-defined and continuous in a neighbourhood of $(t_0, \mathbf{q}_0, \dot{\mathbf{q}}_0)$ with $\mathbf{g}(t, \mathbf{q})$ being two times continuously differentiable. Furthermore, functions \mathbf{M} , \mathbf{f} and the second (partial) derivatives of \mathbf{g} are assumed to satisfy Lipschitz conditions w.r.t. arguments \mathbf{q} and $\dot{\mathbf{q}}$.

If the constraint matrix $\mathbf{G}(t_0, \mathbf{q}_0)$ has full rank n_λ and the mass matrix $\mathbf{M}(t_0, \mathbf{q}_0)$ is symmetric, positive semi-definite and positive definite at $\ker \mathbf{G}(t_0, \mathbf{q}_0)$ then there is a uniquely defined vector $\boldsymbol{\lambda}_0 \in \mathbb{R}^{n_\lambda}$ such that the initial value problem

$$\mathbf{q}(t_0) = \mathbf{q}_0, \quad \dot{\mathbf{q}}(t_0) = \dot{\mathbf{q}}_0, \quad \boldsymbol{\lambda}(t_0) = \boldsymbol{\lambda}_0 \quad (20)$$

for the constrained system (16) is locally uniquely solvable.

Proof. The assumptions on $\mathbf{M}(t_0, \mathbf{q}_0)$ and $\mathbf{G}(t_0, \mathbf{q}_0)$ imply that the 2×2 block matrix at the left hand side of (17) is non-singular for arguments $t = t_0$, $\mathbf{q} = \mathbf{q}_0$, see Lemma 1. Therefore, this block matrix is non-singular for any arguments (t, \mathbf{q}) in a neighbourhood of (t_0, \mathbf{q}_0) since functions \mathbf{M} and \mathbf{G} are continuous w.r.t. t and \mathbf{q} , see [46, Lemma 2.3.3]. In this neighbourhood, the system of linear equations (17) is uniquely solvable w.r.t. $\ddot{\mathbf{q}}$ and $\boldsymbol{\lambda}$ and defines continuous functions \mathbf{a} and $\boldsymbol{\lambda}$ such that

$$\ddot{\mathbf{q}} = \mathbf{a}(t, \mathbf{q}, \dot{\mathbf{q}}), \quad \boldsymbol{\lambda} = \boldsymbol{\lambda}(t, \mathbf{q}, \dot{\mathbf{q}}).$$

The initial value problem $\mathbf{q}(t_0) = \mathbf{q}_0$, $\dot{\mathbf{q}}(t_0) = \dot{\mathbf{q}}_0$ for the second order ODE $\ddot{\mathbf{q}}(t) = \mathbf{a}(t, \mathbf{q}(t), \dot{\mathbf{q}}(t))$ is locally uniquely solvable since the right hand side \mathbf{a} satisfies a Lipschitz condition w.r.t. \mathbf{q} and $\dot{\mathbf{q}}$. The solution $\mathbf{q}(t)$ of this ODE initial value problem satisfies the dynamical equations (16a) with $\boldsymbol{\lambda} := \boldsymbol{\lambda}(t, \mathbf{q}(t), \dot{\mathbf{q}}(t))$ since these equations are represented by the first block row in (17). The initial value for the Lagrange multipliers is uniquely defined by $\boldsymbol{\lambda}_0 := \boldsymbol{\lambda}(t_0, \mathbf{q}_0, \dot{\mathbf{q}}_0)$.

To verify the constraint equations (16b), we consider the constraint residual $\boldsymbol{\gamma}(t) := \mathbf{g}(t, \mathbf{q}(t))$ and its time derivatives

$$\begin{aligned} \dot{\boldsymbol{\gamma}}(t) &= \mathbf{g}_t(t, \mathbf{q}(t)) + \mathbf{G}(t, \mathbf{q}(t))\dot{\mathbf{q}}(t), \\ \ddot{\boldsymbol{\gamma}}(t) &= \mathbf{g}_{tt}(t, \mathbf{q}(t)) + 2\mathbf{g}_{tq}(t, \mathbf{q}(t))\dot{\mathbf{q}}(t) + \mathbf{G}(t, \mathbf{q}(t))\ddot{\mathbf{q}}(t) + \mathbf{g}_{qq}(t, \mathbf{q}(t))(\dot{\mathbf{q}}(t), \dot{\mathbf{q}}(t)), \end{aligned}$$

see (1), (8), (9). The second block row of (17) shows that the residual $\ddot{\boldsymbol{\gamma}}(t)$ in the hidden constraints (9) at the level of acceleration coordinates vanishes identically. Hence, $\boldsymbol{\gamma}(t)$ solves the second order ODE $\ddot{\boldsymbol{\gamma}}(t) = \mathbf{0}$ with initial values $\boldsymbol{\gamma}(t_0) = \mathbf{g}(t_0, \mathbf{q}_0) = \mathbf{0}$ and $\dot{\boldsymbol{\gamma}}(t_0) = \mathbf{G}(t_0, \mathbf{q}_0)\dot{\mathbf{q}}_0 + \mathbf{g}_t(t_0, \mathbf{q}_0) = \mathbf{0}$, see (19). Since this solution is unique, we get $\boldsymbol{\gamma}(t) \equiv \mathbf{0}$ and therefore also $\mathbf{g}(t, \mathbf{q}(t)) \equiv \mathbf{0}$. I.e., the constraint equations (16b) are satisfied in the whole time interval of interest and functions $\mathbf{q}(t)$, $\boldsymbol{\lambda}(t, \mathbf{q}(t), \dot{\mathbf{q}}(t))$ solve the initial value problem $\mathbf{q}(t_0) = \mathbf{q}_0$, $\dot{\mathbf{q}}(t_0) = \dot{\mathbf{q}}_0$, $\boldsymbol{\lambda}(t_0) = \boldsymbol{\lambda}_0 = \boldsymbol{\lambda}(t_0, \mathbf{q}_0, \dot{\mathbf{q}}_0)$ for the constrained system (16). ■

Definition 1. Initial values $\mathbf{q}_0, \dot{\mathbf{q}}_0 \in \mathbb{R}^{n_q}$, $\boldsymbol{\lambda}_0 \in \mathbb{R}^{n_\lambda}$ are *consistent* with the equations of motion (16) if \mathbf{q}_0 and $\dot{\mathbf{q}}_0$ satisfy the (hidden) constraints at the levels of position and velocity coordinates, see (19), and there is a vector $\ddot{\mathbf{q}}_0$ such that $\ddot{\mathbf{q}} = \ddot{\mathbf{q}}_0$, $\boldsymbol{\lambda} = \boldsymbol{\lambda}_0$ solve the system of linear equations (17) with $t := t_0$, $\mathbf{q} := \mathbf{q}_0$, $\dot{\mathbf{q}} := \dot{\mathbf{q}}_0$.

Remark 2. a) For any consistent initial values $\mathbf{q}_0, \dot{\mathbf{q}}_0, \boldsymbol{\lambda}_0$, the initial value problem $\mathbf{q}(t_0) = \mathbf{q}_0$, $\dot{\mathbf{q}}(t_0) = \dot{\mathbf{q}}_0$, $\boldsymbol{\lambda}(t_0) = \boldsymbol{\lambda}_0$ for DAE (16) is locally uniquely solvable if $\text{rank } \mathbf{G}(t_0, \mathbf{q}_0) = n_\lambda$, $\mathbf{M}(t_0, \mathbf{q}_0)$ is symmetric positive semi-definite and positive definite at $\ker \mathbf{G}(t_0, \mathbf{q}_0)$ and functions \mathbf{M} , \mathbf{f} and \mathbf{g} satisfy appropriate smoothness assumptions, see Theorem 1.

b) Following a *coordinate partitioning* approach [89], consistent initial values $\mathbf{q}_0, \dot{\mathbf{q}}_0, \boldsymbol{\lambda}_0$ may be obtained from any pair of vectors $\bar{\mathbf{q}}_0, \hat{\mathbf{q}}_0 \in \mathbb{R}^{n_q}$ provided that $\|\mathbf{g}(t_0, \bar{\mathbf{q}}_0)\| \leq \delta$ with a sufficiently small constant $\delta > 0$: The full rank assumption on the constraint matrix \mathbf{G} allows to select in a first step n_λ linearly independent column vectors of $\mathbf{G}(t_0, \bar{\mathbf{q}}_0)$. There is a matrix $\hat{\mathbf{P}} \in \mathbb{R}^{n_q \times n_\lambda}$ being composed of n_λ unit vectors such that $\mathbf{G}(t_0, \bar{\mathbf{q}}_0)\hat{\mathbf{P}} \in \mathbb{R}^{n_\lambda \times n_\lambda}$ is non-singular.

In the second step, vector $\mathbf{q}_0 \in \mathbb{R}^{n_q}$ is decomposed into $n_q - n_\lambda$ independent coordinates $\bar{\mathbf{P}}^\top \mathbf{q}_0 \in \mathbb{R}^{n_q - n_\lambda}$ and n_λ dependent coordinates $\hat{\mathbf{q}}_0 := \hat{\mathbf{P}}^\top \mathbf{q}_0 \in \mathbb{R}^{n_\lambda}$ with a matrix $\bar{\mathbf{P}} \in \mathbb{R}^{n_q \times (n_q - n_\lambda)}$ that is defined such that $\mathbf{P} := (\bar{\mathbf{P}} \hat{\mathbf{P}}) \in \mathbb{R}^{n_q \times n_q}$ forms a permutation matrix, i.e., $\mathbf{I}_{n_q} = \mathbf{P}\mathbf{P}^\top = \bar{\mathbf{P}}\bar{\mathbf{P}}^\top + \hat{\mathbf{P}}\hat{\mathbf{P}}^\top$. Finally, we fix $\bar{\mathbf{P}}^\top \mathbf{q}_0 := \bar{\mathbf{P}}^\top \bar{\mathbf{q}}_0$ and get consistent position coordinates $\mathbf{q}_0 = \mathbf{P}\mathbf{P}^\top \mathbf{q}_0 := \bar{\mathbf{P}}\bar{\mathbf{P}}^\top \bar{\mathbf{q}}_0 + \hat{\mathbf{P}}\hat{\mathbf{q}}_0$ solving

$$\mathbf{0} = \mathbf{g}(t_0, \bar{\mathbf{P}}\bar{\mathbf{P}}^\top \bar{\mathbf{q}}_0 + \hat{\mathbf{P}}\hat{\mathbf{q}}_0) \quad (21)$$

w.r.t. $\hat{\mathbf{q}}_0 \in \mathbb{R}^{n_\lambda}$. According to the Implicit function theorem, Eqs. (21) are locally uniquely solvable if $\|\mathbf{g}(t_0, \bar{\mathbf{q}}_0)\| \leq \delta \ll 1$ since

$$\frac{\partial \mathbf{g}}{\partial \hat{\mathbf{q}}_0}(t_0, \bar{\mathbf{q}}_0) = \frac{\partial \mathbf{g}}{\partial \mathbf{q}}(t_0, \bar{\mathbf{q}}_0) \frac{\partial \mathbf{q}_0}{\partial \hat{\mathbf{q}}_0}(\bar{\mathbf{q}}_0) = \mathbf{G}(t_0, \bar{\mathbf{q}}_0) \hat{\mathbf{P}}$$

is non-singular by construction.

In the same way, consistent initial values $\dot{\mathbf{q}}_0 = \bar{\mathbf{P}}\bar{\mathbf{P}}^\top \bar{\mathbf{q}}_0 + \hat{\mathbf{P}}\hat{\mathbf{q}}_0$ with $\hat{\mathbf{q}}_0 \in \mathbb{R}^{n_\lambda}$ are obtained from the system of n_λ linear equations

$$\mathbf{0} = \mathbf{G}(t_0, \mathbf{q}_0)\dot{\mathbf{q}}_0 + \mathbf{g}_t(t_0, \mathbf{q}_0) = \mathbf{G}(t_0, \mathbf{q}_0)\bar{\mathbf{P}}\bar{\mathbf{P}}^\top \bar{\mathbf{q}}_0 + \mathbf{G}(t_0, \mathbf{q}_0)\hat{\mathbf{P}}\hat{\mathbf{q}}_0 + \mathbf{g}_t(t_0, \mathbf{q}_0)$$

provided that $\mathbf{G}(t_0, \mathbf{q}_0)\hat{\mathbf{P}}$ is non-singular as well. At the end, the 2×2 block system (17) yields consistent initial values $\boldsymbol{\lambda}_0$ for the Lagrange multipliers.

Remark 3. a) For the index analysis, the equations of motion (16) are transformed to an equivalent first order DAE introducing velocity coordinates $\mathbf{v}(t) := \dot{\mathbf{q}}(t)$ and substituting $\dot{\mathbf{q}} \rightarrow \mathbf{v}$, $\ddot{\mathbf{q}} \rightarrow \dot{\mathbf{v}}$. With the assumptions of Theorem 1, functions $\dot{\mathbf{v}}(t) = \dot{\ddot{\mathbf{q}}}(t)$ and $\boldsymbol{\lambda}(t)$ are obtained from the system of linear equations (17) that contains the second time derivative of the holonomic constraints (16b).

The 2×2 block matrix in (17) is non-singular and does not depend on \mathbf{v} , $\dot{\mathbf{v}}$ and $\boldsymbol{\lambda}$. Therefore, the time derivative of (17) may be solved w.r.t. $\dot{\mathbf{v}}$ and $\dot{\boldsymbol{\lambda}}$ providing an explicit expression for $\dot{\boldsymbol{\lambda}}$ that utilizes the *third* time derivative of (16b). Consequently, the differentiation index of the equivalent first order system is (at most) three [47, 60].

b) For positive definite mass matrices $\mathbf{M}(t, \mathbf{q})$, the dynamical equations (16a) may formally be solved w.r.t. $\ddot{\mathbf{q}} = \dot{\mathbf{v}}$ resulting in the first order DAE

$$\dot{\mathbf{q}} = \mathbf{v}, \tag{22a}$$

$$\dot{\mathbf{v}} = [\mathbf{M}^{-1}\mathbf{f}](t, \mathbf{q}, \mathbf{v}) - [\mathbf{M}^{-1}\mathbf{G}^\top](t, \mathbf{q})\boldsymbol{\lambda}, \tag{22b}$$

$$\mathbf{0} = \mathbf{g}(t, \mathbf{q}) \tag{22c}$$

that is of Hessenberg form [26]. For full rank matrices \mathbf{G} and symmetric, positive definite matrices \mathbf{M} , matrix $\mathbf{GM}^{-1}\mathbf{G}^\top$ is non-singular and (22b) implies

$$\boldsymbol{\lambda} = \mathbf{f}_0(t, \mathbf{q}, \mathbf{v}) - [(\mathbf{GM}^{-1}\mathbf{G}^\top)^{-1}](t, \mathbf{q}) \cdot \mathbf{G}(t, \mathbf{q})\dot{\mathbf{v}} \tag{23}$$

with an appropriate function \mathbf{f}_0 . The time derivative of (23) shows that $\dot{\boldsymbol{\lambda}}(t)$ is composed of functions depending on t , \mathbf{q} , \mathbf{v} and $\dot{\mathbf{v}} = [\mathbf{M}^{-1}\mathbf{f}] - [\mathbf{M}^{-1}\mathbf{G}^\top]\boldsymbol{\lambda}$ and of the vector $\mathbf{G}(t, \mathbf{q})\dot{\mathbf{v}}$ that is pre-multiplied by the non-singular matrix $-(\mathbf{GM}^{-1}\mathbf{G}^\top)^{-1}$.

Since $\mathbf{G}(t, \mathbf{q})\dot{\mathbf{v}}$ can not be obtained from DAE (22) and its first two time derivatives, the differentiation index of DAE (22) is larger than two. Taking into account the upper bound from part a) of this remark, we see that the equations of motion (16) form an index-3 DAE if $\mathbf{M}(t, \mathbf{q})$ is symmetric and positive definite. Note, that differentiation index and perturbation index of (16) coincide since the equivalent first order system is of Hessenberg form [30, 47].

The analytical transformation of the equations of motion (16) to the Hessenberg form index-3 DAE (22) is a common approach in DAE theory. This transformation is essentially based on the assumption that the mass matrix \mathbf{M} is symmetric, positive definite [26, 50, 58]. However, the existence and uniqueness result in Theorem 1 is not restricted to this problem class but applies as well to a class of model equations (16) with rank-deficient mass matrix \mathbf{M} . In this more general setting, the structure of (16) is more complex and its index may be less than three [12]:

Example 5. A (pathological) example of problems with rank-deficient mass matrix \mathbf{M} are constrained systems (16) with $\mathbf{M}(t, \mathbf{q}) = \mathbf{0}_{n_q \times n_q}$. This matrix is positive semi-definite and it is positive definite at $\ker \mathbf{G}(t, \mathbf{q})$ if $n_q = n_\lambda$ and $\mathbf{G}(t, \mathbf{q})$ is non-singular. For such systems, there is no need to consider the 2×2 block system (17) since the Lagrange multipliers $\boldsymbol{\lambda}(t) = [\mathbf{G}^{-\top} \mathbf{f}](t, \mathbf{q}(t), \dot{\mathbf{q}}(t))$ are directly defined by the dynamical equations (16a).

The differentiation index of the corresponding first order system in variables \mathbf{q} , $\mathbf{v} := \dot{\mathbf{q}}$ and $\boldsymbol{\lambda}$ is two [12]. If \mathbf{G} is non-singular, $\mathbf{M} \equiv \mathbf{0}$ and \mathbf{f} is independent of $\dot{\mathbf{q}}$, then (16) defines even an index-1 DAE (in variables \mathbf{q} and $\boldsymbol{\lambda}$):

$$\mathbf{0} = \mathbf{f}(t, \mathbf{q}) - \mathbf{G}^\top(t, \mathbf{q}) \boldsymbol{\lambda}, \quad \mathbf{0} = \mathbf{g}(t, \mathbf{q}).$$

2.3 Positive semi-definite mass matrices, rank deficient constraint matrices

In engineering applications, there are certain types of position coordinates \mathbf{q} that result systematically in constrained systems (16) with rank-deficient mass matrix, see [42, 64, 86] and the references therein. From the viewpoint of physics, the kinetic energy $T = 0.5 \dot{\mathbf{q}}^\top \mathbf{M} \dot{\mathbf{q}}$ should define a positive semi-definite quadratic form and any non-zero velocity increment being compatible with the hidden constraints (8) should result in a positive contribution to T , see [42]. Both properties of T are achieved by the assumptions of Lemma 1 that considers symmetric, positive semi-definite mass matrices \mathbf{M} being positive definite at $\ker \mathbf{G}$.

These assumptions imply that the augmented matrix $\mathbf{M} + \mathbf{G}^\top \mathbf{G}$ with $\text{rank } \mathbf{G} = n_\lambda$ is symmetric, positive definite [45, Section 10.2] and the 2×2 block matrix in (18) is non-singular, see Lemma 1. For a more detailed analysis, we decouple in the present section the nullspace of \mathbf{M} from its orthogonal complement and consider furthermore systems with rank deficient constraint matrix \mathbf{G} resulting from redundant constraints (16b) that are typical of some algorithms for computer-aided setup of complex, three dimensional multibody system models [39, 42].

Lötstedt [59] pointed out that equations of motion (16) with consistent, but redundant constraints (16b) do not define unique Lagrange multipliers $\boldsymbol{\lambda}(t)$. Nevertheless, the constraint forces $-\mathbf{G}^\top \boldsymbol{\lambda}$ and the position coordinates $\mathbf{q}(t)$ are well defined. Modeling aspects and analytical aspects of equations of motion (16) with rank deficient mass matrix or rank deficient constraint matrix have recently been studied in great detail by García de Jalón and Gutiérrez-López [42]. They also refer

to the work of Fraćzek and Wojtyra [39] who have shown that the uniqueness of $\mathbf{q}(t)$ can not longer be guaranteed if the dynamical equations (16a) depend nonlinearly on $\boldsymbol{\lambda}$ (and the constraints (16b) are redundant), see also the more general and more abstract analysis of overdetermined and underdetermined DAEs by Kunkel and Mehrmann [58].

The internal structure of equations of motion (16) with rank deficient mass matrix \mathbf{M} or rank deficient constraint matrix \mathbf{G} may be studied conveniently by a decomposition of the 2×2 block matrix in (18) that takes into account nontrivial nullspaces $\ker \mathbf{M}$ and $\ker \mathbf{G}$:

Lemma 2. Consider matrices $\mathbf{M} \in \mathbb{R}^{k \times k}$ and $\mathbf{G} \in \mathbb{R}^{m \times k}$ with $\text{rank} \mathbf{M} = r \leq k$ and $\text{rank} \mathbf{G} = s \leq m \leq k$. If \mathbf{M} is symmetric, positive semi-definite and positive definite at $\ker \mathbf{G}$ then there are non-singular matrices $\mathbf{U} \in \mathbb{R}^{k \times k}$ and $\mathbf{Q} \in \mathbb{R}^{m \times m}$ such that

$$\left(\begin{array}{c|c} \mathbf{M} & \mathbf{G}^\top \\ \hline \mathbf{G} & \mathbf{0} \end{array} \right) = \left(\begin{array}{c|c} \mathbf{U} & \mathbf{0} \\ \hline \mathbf{0} & \mathbf{Q} \end{array} \right) \left(\begin{array}{cc|ccc} \mathbf{0} & \mathbf{0} & \mathbf{0} & \mathbf{0} & \mathbf{I}_{k-r} \\ \mathbf{0} & \bar{\mathbf{M}} & \bar{\mathbf{G}}^\top & \mathbf{0} & \mathbf{0} \\ \hline \mathbf{0} & \bar{\mathbf{G}} & \mathbf{0} & \mathbf{0} & \mathbf{0} \\ \mathbf{0} & \mathbf{0} & \mathbf{0} & \mathbf{0} & \mathbf{0} \\ \mathbf{I}_{k-r} & \mathbf{0} & \mathbf{0} & \mathbf{0} & \mathbf{0} \end{array} \right) \left(\begin{array}{c|c} \mathbf{U}^\top & \mathbf{0} \\ \hline \mathbf{0} & \mathbf{Q}^\top \end{array} \right) \quad (24)$$

with a non-singular matrix $\bar{\mathbf{M}} \in \mathbb{R}^{r \times r}$ and a matrix $\bar{\mathbf{G}} \in \mathbb{R}^{(s-(k-r)) \times r}$ that has full rank $s - (k - r)$.

Proof. If $r = \text{rank} \mathbf{M} < k$ then the nullspace of \mathbf{M} is non-trivial and there is an orthonormal basis $\{\mathbf{u}_1, \dots, \mathbf{u}_{k-r}\}$ of $\ker \mathbf{M}$. Summarizing these basis vectors in a matrix $\bar{\mathbf{U}} := (\mathbf{u}_1, \dots, \mathbf{u}_{k-r}) \in \mathbb{R}^{k \times (k-r)}$, we may define a matrix $\bar{\mathbf{U}} \in \mathbb{R}^{k \times r}$ such that $\hat{\mathbf{U}} := (\bar{\mathbf{U}} \bar{\mathbf{U}}) \in \mathbb{R}^{k \times k}$ is orthogonal. Since $\mathbf{M}\bar{\mathbf{U}} = \mathbf{0}_{k \times (k-r)}$ and $\hat{\mathbf{U}}^\top \mathbf{M} \hat{\mathbf{U}}$ is symmetric, we get

$$\hat{\mathbf{U}}^\top \mathbf{M} \hat{\mathbf{U}} = \begin{pmatrix} \bar{\mathbf{U}}^\top \\ \mathbf{0}^\top \end{pmatrix} \begin{pmatrix} \mathbf{0} & \mathbf{M} \bar{\mathbf{U}} \end{pmatrix} = \begin{pmatrix} \mathbf{0} & \mathbf{0} \\ \mathbf{0} & \bar{\mathbf{M}} \end{pmatrix} \quad (25)$$

with the matrix $\bar{\mathbf{M}} := \bar{\mathbf{U}}^\top \mathbf{M} \bar{\mathbf{U}} \in \mathbb{R}^{r \times r}$ that is non-singular because of $\text{rank} \bar{\mathbf{M}} = \text{rank} \hat{\mathbf{U}}^\top \mathbf{M} \hat{\mathbf{U}} = \text{rank} \mathbf{M} = r$.

The column vectors of $\mathbf{G}\bar{\mathbf{U}} \in \mathbb{R}^{m \times (k-r)}$ are linearly independent since otherwise there would be a vector $\boldsymbol{\zeta} \in \mathbb{R}^{k-r}$ with $\boldsymbol{\zeta} \neq \mathbf{0}$ and $\mathbf{0} = (\mathbf{G}\bar{\mathbf{U}})\boldsymbol{\zeta} = \mathbf{G}(\bar{\mathbf{U}}\boldsymbol{\zeta})$, i.e., $\boldsymbol{\xi} := \bar{\mathbf{U}}\boldsymbol{\zeta} \in \ker \mathbf{G} \setminus \{\mathbf{0}\}$. Since \mathbf{M} is positive definite at $\ker \mathbf{G}$, we would get $0 < \boldsymbol{\xi}^\top \mathbf{M} \boldsymbol{\xi} = \boldsymbol{\zeta}^\top \bar{\mathbf{U}}^\top \mathbf{M} \bar{\mathbf{U}} \boldsymbol{\zeta}$ which contradicts $\text{span} \bar{\mathbf{U}} = \ker \mathbf{M}$.

Because of $\text{rank} \mathbf{G}\bar{\mathbf{U}} = k - r \leq m$, there is a QR factorization

$$\mathbf{G}\bar{\mathbf{U}} = \bar{\mathbf{Q}} \begin{pmatrix} \bar{\mathbf{R}} \\ \mathbf{0} \end{pmatrix}$$

with an orthogonal matrix $\bar{\mathbf{Q}} \in \mathbb{R}^{m \times m}$ and a non-singular matrix $\bar{\mathbf{R}} \in \mathbb{R}^{(k-r) \times (k-r)}$, see, e.g., [46]. We get

$$\bar{\mathbf{Q}}^\top \mathbf{G} \hat{\mathbf{U}} = \begin{pmatrix} \bar{\mathbf{R}} & \bar{\bar{\mathbf{G}}} \\ \mathbf{0} & \hat{\mathbf{G}} \end{pmatrix} = \begin{pmatrix} \mathbf{0} & \bar{\mathbf{R}} \\ \mathbf{I}_{m-(k-r)} & \mathbf{0} \end{pmatrix} \begin{pmatrix} \mathbf{0} & \hat{\mathbf{G}} \\ \mathbf{I}_{k-r} & \mathbf{0} \end{pmatrix} \begin{pmatrix} \mathbf{I}_{k-r} & \bar{\mathbf{R}}^{-1} \bar{\bar{\mathbf{G}}} \\ \mathbf{0} & \mathbf{I}_r \end{pmatrix} \quad (26)$$

with matrices $\hat{\mathbf{G}} \in \mathbb{R}^{(m-(k-r)) \times r}$ and $\bar{\bar{\mathbf{G}}} \in \mathbb{R}^{(k-r) \times r}$. The right hand side of (26) is a product of three block matrices. Since the first and the last factor are non-singular, we get

$$\text{rank } \hat{\mathbf{G}} + \text{rank } \mathbf{I}_{k-r} = \text{rank } \bar{\bar{\mathbf{Q}}}^\top \mathbf{G} \hat{\mathbf{U}} = \text{rank } \mathbf{G} = s,$$

i.e., $\text{rank } \hat{\mathbf{G}} = s - (k-r) \leq m - (k-r)$. If matrix \mathbf{G} has full rank m , then $\hat{\mathbf{G}}$ has full rank as well and we define $\bar{\mathbf{G}} := \hat{\mathbf{Q}} \hat{\mathbf{G}}$ with the identity matrix $\hat{\mathbf{Q}} := \mathbf{I}_{m-(k-r)}$, see [12]. Otherwise, matrix $\hat{\mathbf{G}}$ is rank deficient and $s - (k-r)$ linearly independent row vectors may be selected by some pivoting strategy that results in a decomposition

$$\hat{\mathbf{G}} = \hat{\mathbf{Q}} \begin{pmatrix} \bar{\mathbf{G}} \\ \mathbf{0} \end{pmatrix}$$

with non-singular $\hat{\mathbf{Q}} \in \mathbb{R}^{(m-(k-r)) \times (m-(k-r))}$ and a matrix $\bar{\mathbf{G}} \in \mathbb{R}^{(s-(k-r)) \times r}$ of full rank $s - (k-r)$. Inserting this expression in (26), we get

$$\mathbf{G} = \mathbf{Q} \begin{pmatrix} \mathbf{0} & \bar{\mathbf{G}} \\ \mathbf{0} & \mathbf{0} \\ \mathbf{I}_{k-r} & \mathbf{0} \end{pmatrix} \mathbf{U}^\top$$

and non-singular transformation matrices

$$\mathbf{Q} := \bar{\mathbf{Q}} \begin{pmatrix} \mathbf{0} & \bar{\mathbf{R}} \\ \hat{\mathbf{Q}} & \mathbf{0} \end{pmatrix} \in \mathbb{R}^{m \times m}, \quad \mathbf{U} := \hat{\mathbf{U}} \begin{pmatrix} \mathbf{I}_{k-r} & \mathbf{0} \\ (\bar{\mathbf{R}}^{-1} \bar{\bar{\mathbf{G}}})^\top & \mathbf{I}_r \end{pmatrix} \in \mathbb{R}^{k \times k}.$$

To complete the proof, we observe that (25) implies

$$\mathbf{M} = \hat{\mathbf{U}} \begin{pmatrix} \mathbf{0} & \mathbf{0} \\ \mathbf{0} & \bar{\mathbf{M}} \end{pmatrix} \hat{\mathbf{U}}^\top = \mathbf{U} \begin{pmatrix} \mathbf{0} & \mathbf{0} \\ \mathbf{0} & \bar{\mathbf{M}} \end{pmatrix} \mathbf{U}^\top$$

since the second factor in the definition of \mathbf{U} is block lower triangular and satisfies

$$\begin{pmatrix} \mathbf{I}_{k-r} & \mathbf{0} \\ (\bar{\mathbf{R}}^{-1} \bar{\bar{\mathbf{G}}})^\top & \mathbf{I}_r \end{pmatrix} \begin{pmatrix} \mathbf{0} & \mathbf{0} \\ \mathbf{0} & \bar{\mathbf{M}} \end{pmatrix} \begin{pmatrix} \mathbf{I}_{k-r} & \bar{\mathbf{R}}^{-1} \bar{\bar{\mathbf{G}}} \\ \mathbf{0} & \mathbf{I}_r \end{pmatrix} = \begin{pmatrix} \mathbf{0} & \mathbf{0} \\ \mathbf{0} & \bar{\mathbf{M}} \end{pmatrix}. \quad \blacksquare$$

Remark 4. Consider equations of motion (16) with linear holonomic constraints $\mathbf{0} = \mathbf{G}\mathbf{q} - \mathbf{z}(t)$ and constant matrices \mathbf{M}, \mathbf{G} that satisfy the assumptions of Lemma 2 with $k = n_q, m = n_\lambda$. The matrix factorization (24) suggests to multiply the dynamical equations (16a) and the constraint equations (16b) by \mathbf{U}^{-1} and \mathbf{Q}^{-1} , respectively, to decompose the 2×2 block system (17) into

$$\bar{\bar{\lambda}} = \bar{\bar{f}}, \quad (27a)$$

$$\begin{pmatrix} \bar{\mathbf{M}} & \bar{\mathbf{G}}^\top \\ \bar{\mathbf{G}} & \mathbf{0} \end{pmatrix} \begin{pmatrix} \bar{\bar{q}} \\ \bar{\bar{\lambda}} \end{pmatrix} = \begin{pmatrix} \bar{\bar{f}} \\ -\bar{\bar{g}}_{qq}(\dot{q}, \dot{q}) - 2\bar{\bar{g}}_{iq}\dot{q} - \bar{\bar{g}}_{tt} \end{pmatrix} = \begin{pmatrix} \bar{\bar{f}} \\ \bar{\bar{z}} \end{pmatrix}, \quad (27b)$$

$$\mathbf{0} = -\hat{\mathbf{g}}_{qq}(\dot{q}, \dot{q}) - 2\hat{\mathbf{g}}_{iq}\dot{q} - \hat{\mathbf{g}}_{tt} = \hat{\bar{z}}, \quad (27c)$$

$$\bar{\bar{q}} = -\bar{\bar{g}}_{qq}(\dot{q}, \dot{q}) - 2\bar{\bar{g}}_{iq}\dot{q} - \bar{\bar{g}}_{tt} = \bar{\bar{z}} \quad (27d)$$

with

$$\mathbf{U}^{-1}\mathbf{f} = \begin{pmatrix} \bar{\bar{f}} \\ \bar{\bar{f}} \end{pmatrix}, \quad \mathbf{Q}^{-1}\mathbf{g} = \begin{pmatrix} \bar{\bar{g}} \\ \hat{\mathbf{g}} \end{pmatrix}, \quad \mathbf{Q}^{-1}\mathbf{z} = \begin{pmatrix} \bar{\bar{z}} \\ \hat{\mathbf{z}} \end{pmatrix}, \quad \mathbf{U}^\top\mathbf{q} = \begin{pmatrix} \bar{\bar{q}} \\ \bar{\bar{q}} \end{pmatrix}, \quad \mathbf{Q}^\top\boldsymbol{\lambda} = \begin{pmatrix} \bar{\bar{\lambda}} \\ \hat{\boldsymbol{\lambda}} \end{pmatrix},$$

functions $\bar{q}, \bar{f} \in \mathbb{R}^r$, functions $\bar{q}, \bar{\lambda}, \bar{f}, \bar{g}, \bar{z} \in \mathbb{R}^{k-r}$, functions $\bar{\lambda}, \bar{g}, \bar{z} \in \mathbb{R}^{s-(k-r)}$, functions $\hat{\lambda}, \hat{g}, \hat{z} \in \mathbb{R}^{m-s}$ and $r = \text{rank } \mathbf{M}$, $s = \text{rank } \mathbf{G}$.

If the mass matrix \mathbf{M} is symmetric, positive definite and \mathbf{G} has full rank, then we have $\mathbf{q} = \bar{q}$, $\boldsymbol{\lambda} = \bar{\lambda}$ and the 2×2 block system (17) coincides with (27b). If \mathbf{M} is rank deficient, then $k-r$ components of the Lagrange multipliers $\boldsymbol{\lambda}$ are explicitly defined by the $k-r$ algebraic equations (27a) that do not depend on any derivatives of the constraint function \mathbf{g} , see Example 5. Furthermore, there are $k-r$ second order ODEs (27d) for $k-r$ components of \mathbf{q} . The solution components $\bar{q} \in \mathbb{R}^r$ and $\bar{\lambda} \in \mathbb{R}^{s-(k-r)}$ are defined by the 2×2 block system (27b) with the symmetric, positive definite reduced mass matrix $\bar{\mathbf{M}}$ and a reduced constraint matrix $\bar{\mathbf{G}}$ that has full rank $s - (k-r)$.

A rank deficient constraint matrix \mathbf{G} indicates holonomic constraints (16b) that are either redundant or inconsistent. In (27), this fact is reflected by $m-s$ equations $\hat{\bar{z}}(t) = \mathbf{0}$, see (27c). If the compatibility conditions (27c) are violated, then there is no solution of the equations of motion since the holonomic constraints $\mathbf{0} = \mathbf{G}\mathbf{q} - \mathbf{z}(t)$ are not consistent.

For redundant constraints, the position coordinates \mathbf{q} are uniquely defined by the solution (\bar{q}, \bar{q}) of (27b,d) and the compatibility conditions (27c) are satisfied in the whole time interval of interest. Eqs. (27a,b) define $s = \text{rank } \mathbf{G}$ components of the Lagrange multipliers $\boldsymbol{\lambda} \in \mathbb{R}^m$ with $m = n_\lambda$. The remaining $m-s$ components are summarized in the vector $\hat{\boldsymbol{\lambda}} \in \mathbb{R}^{m-s}$ that does not at all appear in the decoupled equations of motion (27).

In the nonlinear case, the characterization of (consistent) redundant constraints (16b) is technically more challenging than in the linear setting of Remark 4. To avoid state dependent transformation matrices $\mathbf{U}(t, \mathbf{q})$, $\mathbf{Q}(t, \mathbf{q})$, we follow a local approach that is tailored to the existence and uniqueness result in Theorem 2 below:

Definition 2. Consider equations of motion (16) with n_λ holonomic constraints $\mathbf{g}(t, \mathbf{q}) = \mathbf{0}$ and a constraint matrix $\mathbf{G}(t, \mathbf{q}) := (\partial \mathbf{g} / \partial \mathbf{q})(t, \mathbf{q}) \in \mathbb{R}^{n_\lambda \times n_q}$ that has constant rank in a neighbourhood $\mathcal{U}(t^*, \mathbf{q}^*)$ of a given point $(t^*, \mathbf{q}^*) \in [t_0, t_{\text{end}}] \times \mathbb{R}^{n_q}$:

$$\text{rank } \mathbf{G}(t, \mathbf{q}) = s \leq n_\lambda \leq n_q, \quad ((t, \mathbf{q}) \in \mathcal{U}(t^*, \mathbf{q}^*)).$$

The constraints $\mathbf{g}(t, \mathbf{q}) = \mathbf{0}$ are said to be *redundant* (in $\mathcal{U}(t^*, \mathbf{q}^*)$) if $\tilde{\mathbf{Q}}\mathbf{g}(t, \mathbf{q}) = \mathbf{0}$ implies $\mathbf{g}(t, \mathbf{q}) = \mathbf{0}$ for any constant matrix $\tilde{\mathbf{Q}} \in \mathbb{R}^{s \times n_\lambda}$ with $\text{rank}(\tilde{\mathbf{Q}}\mathbf{G}(t^*, \mathbf{q}^*)) = s$.

Theorem 2. Consider equations of motion (16) with functions $\mathbf{M}, \mathbf{f}, \mathbf{g}$ satisfying all assumptions of Theorem 1 except the full rank assumption on $\mathbf{G}(t_0, \mathbf{q}_0)$.

a) If the holonomic constraints (16b) are redundant in a neighbourhood \mathcal{U}_0 of (t_0, \mathbf{q}_0) then there is a vector $\boldsymbol{\lambda}_0 \in \mathbb{R}^{n_\lambda}$ such that the initial value problem (20) for the constrained system (16) is locally solvable. The solution $\mathbf{q}(t)$ is locally uniquely defined and independent of the choice of $\boldsymbol{\lambda}_0$.

b) With these assumptions, the differentiation index and the perturbation index of (16) are bounded by three. For symmetric, positive definite mass matrices $\mathbf{M}(t_0, \mathbf{q}_0)$, the variables \mathbf{q} and $\dot{\mathbf{q}}$ are solutions of an equivalent index-3 DAE in Hessenberg form.

Proof. Applying Lemma 2 with (constant) matrices $\mathbf{M} := \mathbf{M}(t_0, \mathbf{q}_0)$, $\mathbf{G} := \mathbf{G}(t_0, \mathbf{q}_0)$, we get the matrix decomposition (24) and (constant) non-singular transformation matrices \mathbf{U} and \mathbf{Q} .

The idea of the proof is to delete in (16) all terms corresponding to the 4th block row and to the 4th block column of the 5×5 block matrix in (24) and to show that the solution of this reduced system solves the original equations of motion (16) as well. We define

$$\tilde{\mathbf{Q}} := \begin{pmatrix} \mathbf{I}_{s-(k-r)} & \mathbf{0} & \mathbf{0} \\ \mathbf{0} & \mathbf{0} & \mathbf{I}_{k-r} \end{pmatrix} \mathbf{Q}^{-1} \in \mathbb{R}^{s \times m}, \quad \tilde{\mathbf{g}}(t, \mathbf{q}) := \tilde{\mathbf{Q}}\mathbf{g}(t, \mathbf{q})$$

with $k = n_q$, $m = n_\lambda$, $r = \text{rank } \mathbf{M}(t_0, \mathbf{q}_0)$, $s = \text{rank } \mathbf{G}(t_0, \mathbf{q}_0)$ and get

$$\tilde{\mathbf{G}}(t_0, \mathbf{q}_0) := \frac{\partial \tilde{\mathbf{g}}}{\partial \mathbf{q}}(t_0, \mathbf{q}_0) = \tilde{\mathbf{Q}}\mathbf{G}(t_0, \mathbf{q}_0) = \begin{pmatrix} \mathbf{0} & \tilde{\mathbf{G}}(t_0, \mathbf{q}_0) \\ \mathbf{I}_{k-r} & \mathbf{0} \end{pmatrix} \mathbf{U}^\top \quad (28)$$

with a matrix $\tilde{\mathbf{G}}(t_0, \mathbf{q}_0) \in \mathbb{R}^{(s-(k-r)) \times (k-r)}$ of full rank $s - (k - r)$, see Lemma 2.

Eq. (28) shows that the left multiplication by $\tilde{\mathbf{Q}}$ selects $s = \text{rank } \mathbf{G}$ linearly independent row vectors of $\mathbf{G}(t_0, \mathbf{q}_0)$, i.e., all $m = n_\lambda$ row vectors of $\mathbf{G}(t_0, \mathbf{q}_0)$ may be represented by a linear combination of the row vectors of matrix $\tilde{\mathbf{G}}(t_0, \mathbf{q}_0) \in \mathbb{R}^{s \times k}$ and there is a matrix $\tilde{\tilde{\mathbf{Q}}}(t_0, \mathbf{q}_0) \in \mathbb{R}^{m \times s}$ such that

$$\mathbf{G}(t_0, \mathbf{q}_0) = \tilde{\tilde{\mathbf{Q}}}(t_0, \mathbf{q}_0) \tilde{\mathbf{G}}(t_0, \mathbf{q}_0). \quad (29)$$

The continuity of the matrix valued functions $\mathbf{G}(t, \mathbf{q})$ and $\tilde{\mathbf{G}}(t, \mathbf{q})$ implies that there is a (sufficiently small) neighbourhood \mathcal{U}_0 of (t_0, \mathbf{q}_0) such that $\text{rank } \tilde{\mathbf{G}}(t, \mathbf{q}) = \text{rank } \mathbf{G}(t, \mathbf{q}) = s$ and

$$\mathbf{G}(t, \mathbf{q}) = \tilde{\tilde{\mathbf{Q}}}(t, \mathbf{q}) \tilde{\mathbf{G}}(t, \mathbf{q}) \quad (30)$$

with $\tilde{\tilde{\mathbf{Q}}}(t, \mathbf{q}) \in \mathbb{R}^{m \times s}$ for all $(t, \mathbf{q}) \in \mathcal{U}_0$. This matrix $\tilde{\tilde{\mathbf{Q}}}(t, \mathbf{q})$ has to have full rank s since the left multiplication of (30) by $\tilde{\mathbf{Q}}$ results in a matrix of rank s .

The matrix factorization (30) allows to express the constraint forces $-\mathbf{G}^\top(t, \mathbf{q}) \boldsymbol{\lambda}$

in terms of $-\tilde{\mathbf{G}}^\top(t, \mathbf{q}) \tilde{\boldsymbol{\lambda}}$ with $\tilde{\boldsymbol{\lambda}} = \tilde{\mathbf{Q}}^\top(t, \mathbf{q}) \boldsymbol{\lambda} \in \mathbb{R}^s$. On the other hand, we have $-\mathbf{G}^\top(t, \mathbf{q}) \boldsymbol{\lambda} = -\tilde{\mathbf{G}}^\top(t, \mathbf{q}) \tilde{\boldsymbol{\lambda}}$ for all $\boldsymbol{\lambda} \in \mathbb{R}^m$ satisfying

$$\boldsymbol{\lambda} = [\tilde{\mathbf{Q}}(\tilde{\mathbf{Q}}^\top \tilde{\mathbf{Q}})^{-1}] (t, \mathbf{q}) \tilde{\boldsymbol{\lambda}} + \hat{\boldsymbol{\lambda}} \quad (31)$$

with some $\hat{\boldsymbol{\lambda}} \in \ker \tilde{\mathbf{Q}}^\top(t, \mathbf{q})$. The nullspace of $\tilde{\mathbf{Q}}^\top(t, \mathbf{q})$ has dimension $m - s$. It is non-trivial if the constraint matrix $\mathbf{G}(t, \mathbf{q})$ is rank deficient. In that case, the variables $\hat{\boldsymbol{\lambda}}$ are left undefined by the constrained system (16), see also the corresponding discussion for systems with constant matrices \mathbf{M} and \mathbf{G} in Remark 4.

Because of (29), we have $\ker \tilde{\mathbf{G}}(t_0, \mathbf{q}_0) \subset \ker \mathbf{G}(t_0, \mathbf{q}_0)$ and the mass matrix $\mathbf{M}(t_0, \mathbf{q}_0)$ is positive definite at the nullspace of $\tilde{\mathbf{G}}(t_0, \mathbf{q}_0)$. Furthermore, function $\tilde{\mathbf{g}}(t, \mathbf{q})$ satisfies the smoothness assumptions of Theorem 1 since the matrix decomposition (24) was evaluated for matrices \mathbf{M} , \mathbf{G} with *fixed* arguments $t = t_0$, $\mathbf{q} = \mathbf{q}_0$. Therefore, we may apply Theorem 1 to the reduced system

$$\mathbf{M}(t, \mathbf{q}) \dot{\mathbf{q}} = \mathbf{f}(t, \mathbf{q}, \dot{\mathbf{q}}) - \tilde{\mathbf{G}}^\top(t, \mathbf{q}) \tilde{\boldsymbol{\lambda}}, \quad (32a)$$

$$\mathbf{0} = \tilde{\mathbf{g}}(t, \mathbf{q}) \quad (32b)$$

and get a locally uniquely defined solution $\mathbf{q}(t)$ with initial values $\mathbf{q}(t_0) = \mathbf{q}_0$, $\dot{\mathbf{q}}(t_0) = \dot{\mathbf{q}}_0$. In \mathcal{U}_0 , the s linearly independent constraints (32b) of the reduced system imply the $m \geq s$ redundant constraints (16b) of the original equations of motion, see Definition 2. Furthermore, the reduced system (32) defines unique Lagrange multipliers $\tilde{\boldsymbol{\lambda}}(t) \in \mathbb{R}^s$ and the set of all solutions $\boldsymbol{\lambda}(t) \in \mathbb{R}^m$ according to (31).

To prove part b) of the Theorem, we apply the index analysis of Remark 3 to the reduced system (32). ■

3 From constrained mechanical systems to multibody system dynamics

Mechanical multibody systems are composed of a finite number of rigid or flexible bodies being connected by *joints* that restrict the relative motion of bodies w.r.t. each other and by *force elements* like springs, dampers or actuators that cause forces and momenta acting on the interconnected bodies but do not restrict the degrees of freedom of their relative motion. The mass of a multibody system is concentrated in the bodies and the connecting elements are idealized to be massless. After space discretization of the flexible components, the mechanical state of the system may be characterized by elements of a finite dimensional configuration space that describe the position and orientation of all bodies and the elastic deformation of the flexible parts.

The equations of motion follow systematically from principles of classical mechanics that result in linearly implicit systems of second order differential equations. Efficient time integration methods in multibody numerics are essentially based on

the specific mathematical structure of these model equations. Discussing this structure, we started in Section 2 at a rather basic level with constrained systems of point masses. The modelling of rigid body systems is substantially more complex since the orientation of the bodies in 2-D or 3-D has to be taken into account which may result in nonlinear configuration spaces, see Section 3.1. There is a rich literature on the general structure of model equations in multibody system dynamics that is shortly summarized in Section 3.2. Finally, we consider in Section 3.3 some specific algorithms of multibody dynamics that exploit the topology of a multibody system model to speed-up the evaluation of the model equations.

3.1 Configuration of rigid body systems

The configuration of rigid bodies is characterized by their position and orientation in space. For simplicity, we restrict ourselves in the present section to the discussion of systems in \mathbb{R}^3 (*spatial systems*). *Planar* systems may be considered as a special case of this general setting with position coordinates being restricted to a two-dimensional subspace.

In \mathbb{R}^3 , the position of body $(\bullet)^{(i)}$ is described by coordinates $\mathbf{x}^{(i)} \in \mathbb{R}^3$ and its orientation may be represented conveniently by a rotation matrix

$$\mathbf{R}^{(i)} \in \text{SO}(3) = \{ \mathbf{R} \in \mathbb{R}^{3 \times 3} : \mathbf{R}^\top \mathbf{R} = \mathbf{I}_3, \det \mathbf{R} = +1 \}.$$

The special orthogonal group $\text{SO}(3)$ is a subgroup of the general linear group $\text{GL}(3) = \{ \mathbf{A} : \mathbf{A} \in \mathbb{R}^{3 \times 3} : \det \mathbf{A} \neq 0 \}$ and forms a three-dimensional differentiable manifold in \mathbb{R}^9 . *Lie group* theory provides the analytical framework for differential equations on such manifolds with group structure. The interested reader is referred to [48, Chapter IV] for a compact introduction and to [53] for a comprehensive survey of analytical and numerical aspects of differential equations on finite dimensional Lie groups.

Remark 5. a) The Lie group structure of configuration spaces may be exploited explicitly in the time integration of the equations of motion, see, e.g., [23, 28, 32, 85]. Position vector $\mathbf{x} \in \mathbb{R}^3$ and rotation matrix $\mathbf{R} \in \text{SO}(3)$ are either combined in the direct product $G = \text{SO}(3) \times \mathbb{R}^3$ with group operation

$$(\mathbf{R}_a, \mathbf{x}_a) \circ (\mathbf{R}_b, \mathbf{x}_b) = (\mathbf{R}_a \mathbf{R}_b, \mathbf{x}_a + \mathbf{x}_b)$$

or in the semi-direct product $G = \text{SE}(3) := \text{SO}(3) \ltimes \mathbb{R}^3$ with group operation

$$(\mathbf{R}_a, \mathbf{x}_a) \circ (\mathbf{R}_b, \mathbf{x}_b) = (\mathbf{R}_a \mathbf{R}_b, \mathbf{R}_a \mathbf{x}_b + \mathbf{x}_a),$$

see [27] and the more detailed discussions in [13] and [65]. With these notations, the configuration space of a rigid N -body system is given by the direct products $(\text{SO}(3) \times \mathbb{R}^3)^N$ or $(\text{SE}(3))^N$, respectively.

b) The inherent nonlinear structure of the configuration space results in nontrivial kinematic relations that express the time derivatives of the position coordinates $q = (\mathbf{x}, \mathbf{R}) \in G$ in terms of velocity coordinates \mathbf{v} . The Lie group structure of G implies $\dot{q}(t) \in T_{q(t)}G$ with T_qG denoting the tangent space. Taking into account the linear structure of T_qG , the velocity coordinates \mathbf{v} are defined by elements of a linear space \mathbb{R}^k . For a single rigid body, we get

$$\dot{\mathbf{x}}(t) = \mathbf{u}(t) = \mathbf{R}(t)\mathbf{U}(t) \quad (33a)$$

with $\mathbf{u}(t)$ and $\mathbf{U}(t)$ denoting the translation velocity w.r.t. an inertial and a body-attached frame, respectively. The corresponding angular velocities $\boldsymbol{\omega}$ (inertial frame) and $\boldsymbol{\Omega}$ (body-attached frame) are related by

$$\tilde{\boldsymbol{\omega}}(t) = \mathbf{R}(t)\tilde{\boldsymbol{\Omega}}(t)\mathbf{R}^\top(t)$$

with $(\tilde{\bullet}) : \mathbb{R}^3 \rightarrow \mathfrak{so}(3) = \{\mathbf{A} \in \mathbb{R}^{3 \times 3} : \mathbf{A} + \mathbf{A}^\top = \mathbf{0}\}$ denoting the *tilde operator* that maps $\boldsymbol{\Omega} \in \mathbb{R}^3$ to the skew-symmetric matrix

$$\tilde{\boldsymbol{\Omega}} := \begin{pmatrix} 0 & -\Omega_3 & \Omega_2 \\ \Omega_3 & 0 & -\Omega_1 \\ -\Omega_2 & \Omega_1 & 0 \end{pmatrix}$$

and represents the vector product $\mathbf{p} \times \mathbf{q}$ in \mathbb{R}^3 in the sense that $\tilde{\mathbf{p}}\mathbf{q} = \mathbf{p} \times \mathbf{q}$ for any vectors $\mathbf{p}, \mathbf{q} \in \mathbb{R}^3$. The kinematic relations for \mathbf{R} are given by

$$\dot{\mathbf{R}}(t) = \tilde{\boldsymbol{\omega}}(t)\mathbf{R}(t) = \mathbf{R}(t)\tilde{\boldsymbol{\Omega}}(t). \quad (33b)$$

Eqs. (33) allow to represent the time derivative of $q = (\mathbf{x}, \mathbf{R}) \in G$ by a velocity vector $\mathbf{v} \in \mathbb{R}^6$ being composed of translation velocity and angular velocity (either in the inertial or in the body-attached frame).

The structural difference between the kinematic relations (33) and the more classical setting $\dot{q}(t) = \mathbf{v}(t)$ in linear spaces, see (22a), is given by the Lie group ODE (33b) on $\text{SO}(3)$. In the following, we will discuss analytical and numerical aspects of these equations and will assume that the angular velocities are defined in the body-attached frame. As a typical model problem, we consider a slowly rotating heavy top with its tip being fixed to the origin:

Example 6. In the gravity field, the kinetic and potential energy of a spinning top of mass m are given by [27]

$$T = \frac{1}{2} m \dot{\mathbf{x}}^\top \dot{\mathbf{x}} + \frac{1}{2} \boldsymbol{\Omega}^\top \mathbf{J} \boldsymbol{\Omega}, \quad U = -\mathbf{x}^\top m \boldsymbol{\gamma} \quad \text{with} \quad \boldsymbol{\gamma} = \begin{pmatrix} 0 \\ 0 \\ -g_{\text{grav}} \end{pmatrix}$$

and the gravitational acceleration constant g_{grav} . Here, the tensor of inertia \mathbf{J} is defined w.r.t. the center of mass in the body-attached frame. If this center of mass has

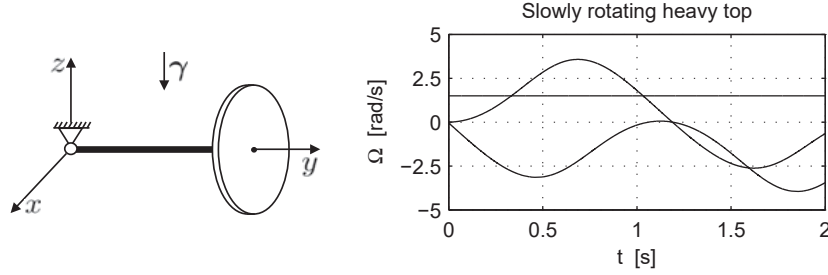


Fig. 5 Configuration and angular velocity of a slowly rotating heavy top [28], see also [45].

position $\mathbf{X} \in \mathbb{R}^3$ for the reference configuration $\mathbf{R} = \mathbf{I}_3$ then its current position in the inertial frame is given by $\mathbf{x}(t) = \mathbf{R}(t)\mathbf{X}$ since the tip of the top is fixed at the origin, see Fig. 5. This constraint implies $\dot{\mathbf{x}}(t) = \dot{\mathbf{R}}(t)\mathbf{X} = \mathbf{R}(t)\dot{\boldsymbol{\Omega}}(t)\mathbf{X}$, see (33b), and we get $\dot{\mathbf{x}} = -\mathbf{R}\tilde{\mathbf{X}}\boldsymbol{\Omega}$, $\dot{\mathbf{x}}^\top = -\boldsymbol{\Omega}^\top \tilde{\mathbf{X}}^\top \mathbf{R}^\top = \boldsymbol{\Omega}^\top \tilde{\mathbf{X}}\mathbf{R}^\top$ and

$$T = \frac{1}{2} \boldsymbol{\Omega}^\top (\mathbf{J} - m\tilde{\mathbf{X}}\tilde{\mathbf{X}}) \boldsymbol{\Omega}, \quad U = -\mathbf{X}^\top \mathbf{R}^\top m\boldsymbol{\gamma}.$$

In Section 2.1, we discussed the derivation of the equations of motion in linear configuration spaces using Hamilton's principle of least action. For nonlinear configuration spaces, the nonlinear kinematic relations (33b) have to be taken into account [27]. For the heavy top problem we obtain equations of motion

$$\dot{\mathbf{R}} = \mathbf{R}\tilde{\boldsymbol{\Omega}}, \quad (34a)$$

$$\tilde{\mathbf{J}}\dot{\boldsymbol{\Omega}} + \boldsymbol{\Omega} \times \tilde{\mathbf{J}}\boldsymbol{\Omega} = \mathbf{X} \times \mathbf{R}^\top m\boldsymbol{\gamma} \quad (34b)$$

with $\tilde{\mathbf{J}} := \mathbf{J} - m\tilde{\mathbf{X}}\tilde{\mathbf{X}}$ denoting the moment of inertia w.r.t. the origin [28]. The right plot of Fig. 5 shows the angular velocity $\boldsymbol{\Omega}(t)$ for model parameters $m = 15.0 \text{ kg}$, $\tilde{\mathbf{J}} = \text{diag}(15.234375, 0.46875, 15.234375) \text{ kg} \cdot \text{m}^2$, $g_{\text{grav}} = 9.81 \text{ m/s}^2$ and initial values

$$\mathbf{R}(0) = \begin{pmatrix} 0 & 0 & 1 \\ 0 & 1 & 0 \\ -1 & 0 & 0 \end{pmatrix}, \quad \boldsymbol{\Omega}(0) = \begin{pmatrix} 0 \\ 1.5 \\ -0.0461538 \end{pmatrix} \frac{\text{rad}}{\text{s}}.$$

The direct time discretization of Lie group ODEs by Lie group integrators is a challenging topic of active research. In practical applications it is, however, more common to use parametrizations of the rotation matrix by elements of a linear space.

Remark 6. a) There is no *global* parametrization of $\text{SO}(3)$ by elements of \mathbb{R}^3 but small deviations from a nominal state may be described very efficiently by three Euler angles [75]. Euler angles define a decomposition of the rotation matrix into a sequence of three *elementary* rotations about axes of coordinates. A common sequence of such elementary rotations is given by

$$\mathbf{R}(\mathbf{q}_R) = \begin{pmatrix} \cos \psi & -\sin \psi & 0 \\ \sin \psi & \cos \psi & 0 \\ 0 & 0 & 1 \end{pmatrix} \begin{pmatrix} \cos \theta & 0 & \sin \theta \\ 0 & 1 & 0 \\ -\sin \theta & 0 & \cos \theta \end{pmatrix} \begin{pmatrix} \cos \phi & -\sin \phi & 0 \\ \sin \phi & \cos \phi & 0 \\ 0 & 0 & 1 \end{pmatrix}$$

with angles ϕ (precession), θ (nutation) and ψ (spin) that are summarized in a parameter vector $\mathbf{q}_R = (\phi, \theta, \psi)^\top \in \mathbb{R}^3$.

For $\theta = \theta^* = 0$, this parametrization gets singular since only the sum $\phi + \psi$ is well defined in this case and there is a continuum of parameter vectors \mathbf{q}_R yielding one and the same rotation matrix $\mathbf{R}(\mathbf{q}_R)$. In engineering applications, such singular configurations are avoided switching to an alternative sequence of elementary rotations whenever $|\theta|$ gets too small [75].

b) Beyond the singularities, we may insert the parametrization $\mathbf{R}(\mathbf{q}_R(t))$ into the kinematic relations (33b) to get a linear relation between $\dot{\mathbf{q}}_R$ and the angular velocity $\boldsymbol{\Omega}$:

$$\sum_{j=1}^3 \frac{\partial \mathbf{R}}{\partial q_{R,j}}(\mathbf{q}_R(t)) \dot{q}_{R,j}(t) = \frac{d}{dt} \mathbf{R}(\mathbf{q}_R(t)) = \mathbf{R}(\mathbf{q}_R(t)) \tilde{\boldsymbol{\Omega}}(t).$$

This equation can be summarized in matrix-vector form

$$\mathbf{H}_0(\mathbf{q}_R(t)) \dot{\mathbf{q}}_R(t) = \boldsymbol{\Omega}(t) \quad (35)$$

using the matrix valued function $\mathbf{H}_0(\mathbf{q}_R) = (h_{ij}(\mathbf{q}_R))_{i,j} \in \mathbb{R}^{3 \times 3}$ that is defined by its elements

$$h_{ij}(\mathbf{q}_R) := \frac{1}{2} \left((\mathbf{R}^\top(\mathbf{q}_R) \frac{\partial \mathbf{R}}{\partial q_{R,j}}(\mathbf{q}_R))_{l_{i+2}, l_{i+1}} - (\mathbf{R}^\top(\mathbf{q}_R) \frac{\partial \mathbf{R}}{\partial q_{R,i}}(\mathbf{q}_R))_{l_{i+1}, l_{i+2}} \right)$$

with indices $l_1 = l_4 = 1$, $l_2 = l_5 = 2$, $l_3 = 3$. Straightforward computations yield [75]

$$\mathbf{H}_0(\mathbf{q}_R) = \mathbf{H}_0(\phi, \theta, \psi) = \begin{pmatrix} -\cos \phi \sin \theta & \sin \phi & 0 \\ \sin \phi \sin \theta & \cos \phi & 0 \\ \cos \theta & 0 & 1 \end{pmatrix} \in \mathbb{R}^{3 \times 3}.$$

c) The linear relation $\mathbf{H}_0(\mathbf{q}_R) \dot{\mathbf{q}}_R = \boldsymbol{\Omega}$, see (35), may be used to eliminate for all bodies $(\bullet)^{(i)}$ the angular velocity $\boldsymbol{\Omega}^{(i)}$ and its time derivative in the equations of motion resulting in a second order system (3) with configuration variables $\mathbf{q} \in \mathbb{R}^{6N}$ being composed of the position coordinates $\mathbf{x}^{(i)}$ and the vectors of Euler angles $\mathbf{q}_R^{(i)}$ for all N bodies in the rigid body system.

d) Alternatively, the kinematic relations (33b) may be substituted by

$$\dot{\mathbf{q}}_R(t) = \mathbf{H}_0^{-1}(\mathbf{q}_R(t)) \boldsymbol{\Omega}(t) \quad (36)$$

resulting in a system of first order differential equations in terms of position coordinates $\mathbf{q} \in \mathbb{R}^{n_q}$ and velocity coordinates $\mathbf{v} \in \mathbb{R}^{n_v}$.

For the heavy top model of Example 6, these coordinates are given by $\mathbf{q} = \mathbf{q}_R$, $\mathbf{v} = \boldsymbol{\Omega}$ with $n_q = n_v = 3$ and position coordinates $\mathbf{q} = \mathbf{q}_R = (\phi, \theta, \psi)^\top$ that are

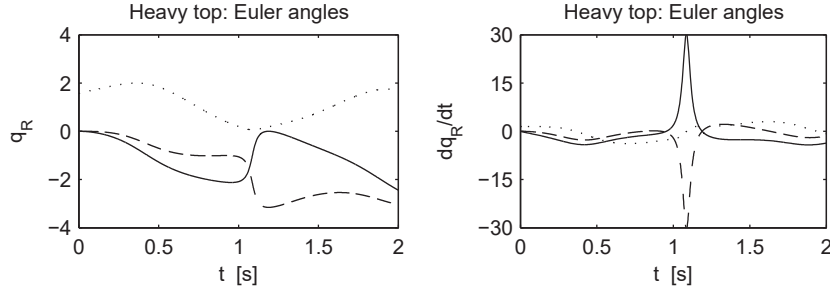


Fig. 6 Parametrization of the heavy top model by Euler angles: precession ϕ (dashed line), nutation θ (dotted line), spin ψ (solid line).

shown in the left plot of Fig. 6. The nutation $\theta(t)$ has its minimum value $\theta(t^*) = 0.059 \text{ rad} = 3.4^\circ$ at $t = t^* \approx 1.1 \text{ s}$ without reaching the singular configuration at $\theta^* = 0$. The rapid changes of ϕ and ψ in a neighbourhood of $t = t^*$ may, however, result in (very) small time step sizes in an error controlled variable step size solver. The right plots of Figs. 5 and 6 illustrate that $\max_t \|\dot{\mathbf{q}}_{\mathbf{R}}(t)\|$ is larger by a factor of 10 than the corresponding maximum value $\max_t \|\boldsymbol{\Omega}(t)\|$ of the angular velocity $\boldsymbol{\Omega}$.

e) For a rigid body system with N bodies, the kinematic equations (33a) and (36) may be summarized to $\dot{\mathbf{q}} = \mathbf{H}(\mathbf{q})\mathbf{v}$ with position coordinates \mathbf{q} being defined by $\mathbf{x}^{(i)}$, $\mathbf{q}_{\mathbf{R}}^{(i)}$, ($i = 1, \dots, N$), and velocity coordinates \mathbf{v} that summarize the corresponding velocity terms $\mathbf{U}^{(i)}$ and $\boldsymbol{\Omega}^{(i)}$ (or their counterparts $\mathbf{u}^{(i)}$, $\boldsymbol{\omega}^{(i)}$ in the inertial frame). The equations of motion get the form (22) with (22a) being substituted by

$$\dot{\mathbf{q}} = \mathbf{H}(\mathbf{q})\mathbf{v}. \quad (37)$$

The parametrization by Euler angles is quite popular in multibody dynamics but fails systematically for systems with large rotations. In that case, parametrizations without singularities prove to be favourable. According to [85], “... it is now well established that the optimal singularity free parametrization is defined in terms of the (four) unit quaternion parameters.”

Remark 7. a) Unit quaternions may be interpreted as normalized elements of \mathbb{R}^4 :

$$\mathbb{Q} = \{ \mathbf{p} = (p_0, p_1, p_2, p_3)^\top \in \mathbb{R}^4 : \|\mathbf{p}\|_2 = 1 \}.$$

Identifying the *scalar* part p_0 of quaternion \mathbf{p} with the quaternion $(p_0, 0, 0, 0)^\top$ and its *vector* part $\mathbf{p} = (p_1, p_2, p_3)^\top$ with the quaternion $(0, p_1, p_2, p_3)^\top$, we get $\mathbf{p} = p_0 + \mathbf{p}$ and its conjugate $\mathbf{p}^* := p_0 - \mathbf{p}$.

b) The multiplication of two quaternions $\mathbf{p} = p_0 + \mathbf{p}$ and $\mathbf{q} = q_0 + \mathbf{q}$ is defined by

$$\mathbf{q} * \mathbf{p} = q_0 p_0 - \mathbf{q} \cdot \mathbf{p} + q_0 \mathbf{p} + p_0 \mathbf{q} + \mathbf{q} \times \mathbf{p}$$

and allows a very compact and computationally efficient representation of rotations in terms of unit quaternions [75]. Identifying a given vector $\mathbf{w} \in \mathbb{R}^3$ with the quaternion $0 + \mathbf{w}$, we get $\mathbf{w}^p := \mathbf{R}(p)\mathbf{w}$ by

$$\begin{pmatrix} 0 \\ \mathbf{w}^p \end{pmatrix} = \begin{pmatrix} 0 \\ \mathbf{w} \end{pmatrix}^p := p * \begin{pmatrix} 0 \\ \mathbf{w} \end{pmatrix} * p^*$$

and the parametrization

$$\mathbf{R}(p) = \begin{pmatrix} p_0^2 + p_1^2 - p_2^2 - p_3^2 & 2p_1p_2 - 2p_0p_3 & 2p_1p_3 + 2p_0p_2 \\ 2p_1p_2 + 2p_0p_3 & p_0^2 - p_1^2 + p_2^2 - p_3^2 & 2p_2p_3 - 2p_0p_1 \\ 2p_1p_3 - 2p_0p_2 & 2p_2p_3 + 2p_0p_1 & p_0^2 - p_1^2 - p_2^2 + p_3^2 \end{pmatrix}$$

of rotation matrices $\mathbf{R}(p)$ in terms of unit quaternions $p = (p_0, p_1, p_2, p_3)^\top \in \mathbb{Q}$.

c) As in Remark 6b), we may express the angular velocity $\boldsymbol{\Omega}$ in terms of the time derivative of the parameter vector, see (35):

$$\boldsymbol{\Omega} = \mathbf{H}_0(p)\dot{p} \quad \text{with} \quad \mathbf{H}_0(p) = \mathbf{H}_0(p_0, \mathbf{p}) = (-2\mathbf{p}, 2p_0\mathbf{I} - 2\tilde{\mathbf{p}}) \in \mathbb{R}^{3 \times 4}. \quad (38)$$

In that way, the equations of motion are obtained as second order system (3) with configuration variables $\mathbf{q} \in \mathbb{R}^{7N}$ being composed of the position coordinates $\mathbf{x}^{(i)}$ and the vectors of unit quaternions $p^{(i)}$ for all N bodies in the rigid body system, see also Remark 6c). The normalization of the unit quaternions may be guaranteed by N constraints (3b) with $g_i(\mathbf{q}) := \|p^{(i)}\|_2^2 - 1$, ($i = 1, \dots, N$).

d) The normalization condition for a unit quaternion p implies a hidden constraint

$$0 = \frac{d}{dt} ((p(t))^\top p(t) - 1) = 2(p(t))^\top \dot{p}(t) = 2p_0(t)\dot{p}_0(t) + 2(\mathbf{p}(t))^\top \dot{\mathbf{p}}(t)$$

that may be combined with (38) to

$$\begin{pmatrix} 2p_0 & 2\mathbf{p}^\top \\ -2\mathbf{p} & 2p_0\mathbf{I} - 2\tilde{\mathbf{p}} \end{pmatrix} \dot{p} = \begin{pmatrix} 0 \\ \boldsymbol{\Omega} \end{pmatrix}.$$

These 4 linear equations in terms of $\dot{p} = (\dot{p}_0, \dot{p}_1, \dot{p}_2, \dot{p}_3)^\top$ yield kinematic relations

$$\dot{p}(t) = \mathbf{H}(p(t))\boldsymbol{\Omega}(t) \quad \text{with} \quad \mathbf{H}(p) := \frac{1}{2} \begin{pmatrix} -\mathbf{p}^\top \\ p_0\mathbf{I} + \tilde{\mathbf{p}} \end{pmatrix} \in \mathbb{R}^{4 \times 3}, \quad (39)$$

position coordinates $p \in \mathbb{R}^4$ and velocity coordinates $\boldsymbol{\Omega} \in \mathbb{R}^3$, see [75].

Fig. 7 shows simulation results for the heavy top model of Example 6. The components of p vary smoothly and without singularities in time. The comparison of the right plots in Figs. 5 and 7 shows that the maximum amplitude of \dot{p} is of the same size as the one of $\boldsymbol{\Omega}$. In time integration, the normalization condition $\|p\|_2 = 1$ may be enforced conveniently re-normalizing the numerical solution $p_n \approx p(t_n)$ after each successful time step.

e) For a rigid body system with N bodies, the kinematic equations (33a) and (39)

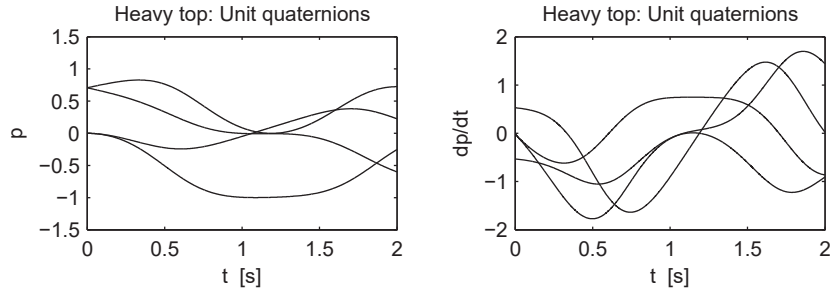


Fig. 7 Parametrization of the heavy top model by unit quaternions. Left plot: $p(t)$, right plot $\dot{p}(t)$.

are again summarized in compact form: $\dot{\mathbf{q}} = \mathbf{H}(\mathbf{q})\mathbf{v}$. Note, that the different dimensions of p and $\boldsymbol{\Omega}$ result in a *rectangular* matrix $\mathbf{H}(\mathbf{q}) \in \mathbb{R}^{7N \times 6N}$ since the position coordinates \mathbf{q} are defined by $\mathbf{x}^{(i)}$, $p^{(i)}$, ($i = 1, \dots, N$), and the velocity coordinates \mathbf{v} are composed of the velocity terms $\mathbf{U}^{(i)}$ and $\boldsymbol{\Omega}^{(i)}$ (or their counterparts $\mathbf{u}^{(i)}$, $\boldsymbol{\omega}^{(i)}$ in the inertial frame). As in Remark 6e), we get equations of motion of the form (22) with (22a) being substituted by $\dot{\mathbf{q}} = \mathbf{H}(\mathbf{q})\mathbf{v}$, see (37).

The mathematical structure of the configuration space for flexible bodies is very similar to the one for rigid body systems if the flexible body is discretized in space by finite elements (or finite differences). Following the *finite element approach* to flexible multibody dynamics [45], the configuration variables describe the nodal translations and rotations.

An alternative approach is based on (modal) model reduction and considers small elastic deformations w.r.t. a *floating frame of reference* that describes large translations and rotations of the flexible body in space [77, 78]. Here, the configuration variables of each flexible body are composed of coordinates describing the position and orientation of its (floating) frame of reference and modal coordinates describing the (small) deformations w.r.t. this reference frame. As before, the basic mathematical structure of configuration space and equations of motion is the one that is known from rigid body systems.

For a more detailed discussion of flexible multibody systems we refer to the rich literature in this field including monographs like [20, 45, 77, 79, 82].

3.2 Model equations in multibody system dynamics

The state variables of a mechanical multibody system model describe the position and orientation of all bodies, the elastic deformation of the flexible components and the internal state of all force elements. Parametrizing the rotation matrices by elements of a linear space we get position coordinates $\mathbf{q} \in \mathbb{R}^{nq}$ with time derivatives that depend linearly on velocity coordinates $\mathbf{v} \in \mathbb{R}^{nv}$, see Section 3.1. Position and

velocity coordinates have either one and the same dimension $n_q = n_v$ or the dimension of \mathbf{q} exceeds the one of \mathbf{v} and the position coordinates are subject to $n_q - n_v > 0$ invariants

$$\mathbf{0} = \boldsymbol{\gamma}(\mathbf{q}) \quad (40)$$

representing, e.g., the normalization of unit quaternions.

The internal state of force elements is characterized by continuous state variables $\mathbf{c}(t) \in \mathbb{R}^{n_c}$ and by time-discrete state variables $\mathbf{r}_j \in \mathbb{R}^{n_r}$ that remain constant in each sampling interval $[T_j, T_{j+1}) \in [t_0, t_{\text{end}}]$. The state variables represent, e.g., hydraulic and electronic system components or control structures [11, 36]. They are subject to changes according to first order ODEs

$$\dot{\mathbf{c}} = \mathbf{d}(t, \mathbf{q}, \mathbf{s}, \mathbf{v}, \mathbf{c}, \mathbf{r}_j, \mathbf{w}, \boldsymbol{\lambda}, \boldsymbol{\eta})$$

and (time-)discrete state equations

$$\mathbf{r}_{j+1} = \mathbf{a}(\mathbf{r}_j, \mathbf{r}_{j-1}, \dots, T_{j+1}, \mathbf{q}, \mathbf{s}, \mathbf{v}, \mathbf{c}, \mathbf{w}, \boldsymbol{\lambda}, \boldsymbol{\eta}). \quad (41)$$

The right hand sides \mathbf{d} and \mathbf{a} depend on $t, \mathbf{q}, \mathbf{v}, \mathbf{c}, \mathbf{r}_j$ and on Lagrange multipliers $\boldsymbol{\lambda}$ and $\boldsymbol{\eta}$ that correspond to holonomic and to non-holonomic constraints, respectively.

They may depend furthermore on additional algebraic variables \mathbf{s} and \mathbf{w} that are introduced for a more convenient model setup in industrial applications [11, 73, 84]. Contact point coordinates $\mathbf{s} \in \mathbb{R}^{n_s}$ are used in the modelling of contact conditions to determine the position of contact points on the surfaces of contacting bodies. They are implicitly defined by a system of n_s nonlinear equations

$$\mathbf{0} = \mathbf{h}(t, \mathbf{q}, \mathbf{s}) \quad (42a)$$

with non-singular Jacobian $\partial \mathbf{h} / \partial \mathbf{s}$. In the same way, coordinates $\mathbf{w} \in \mathbb{R}^{n_w}$ are implicitly defined by a system of n_w nonlinear equations

$$\mathbf{0} = \mathbf{b}(t, \mathbf{q}, \mathbf{s}, \mathbf{v}, \mathbf{c}, \mathbf{r}_j, \mathbf{w}, \boldsymbol{\lambda}, \boldsymbol{\eta}) \quad (42b)$$

with non-singular Jacobian $\partial \mathbf{b} / \partial \mathbf{w}$. Variables of this type are used, e.g., in the modelling of joint friction that results in force vectors \mathbf{f} depending nonlinearly on the constraint forces [73].

If there are bodies in the multibody system model that are permanently in contact then their relative motion is restricted by contact conditions that contribute to the holonomic constraints

$$\mathbf{0} = \mathbf{g}(t, \mathbf{q}, \mathbf{s}), \quad (43)$$

see [11, 84]. The structure of these constraint equations is slightly more complex than in the classical setting of Section 2.1, see (1). Formally, the contact point coordinates \mathbf{s} in (43) could be eliminated applying the implicit function theorem to (42a) resulting in

$$\mathbf{0} = \bar{\mathbf{g}}(t, \mathbf{q}) := \mathbf{g}(t, \mathbf{q}, \mathbf{s}(t, \mathbf{q}))$$

with $\mathbf{s} = \mathbf{s}(t, \mathbf{q})$ being implicitly defined by

$$\mathbf{0} = \mathbf{h}(t, \mathbf{q}, \mathbf{s}(t, \mathbf{q})).$$

Implicit differentiation yields

$$\mathbf{0} = \frac{\partial \mathbf{h}}{\partial \mathbf{q}}(t, \mathbf{q}, \mathbf{s}) + \frac{\partial \mathbf{h}}{\partial \mathbf{s}}(t, \mathbf{q}, \mathbf{s}) \frac{\partial \mathbf{s}}{\partial \mathbf{q}}(t, \mathbf{q})$$

and

$$\mathbf{0} = \frac{\partial \mathbf{h}}{\partial t}(t, \mathbf{q}, \mathbf{s}) + \frac{\partial \mathbf{h}}{\partial \mathbf{q}}(t, \mathbf{q}, \mathbf{s}) \dot{\mathbf{q}}(t) + \frac{\partial \mathbf{h}}{\partial \mathbf{s}}(t, \mathbf{q}, \mathbf{s}) \dot{\mathbf{s}}(t).$$

Therefore, the constraint matrix is given by

$$\begin{aligned} \mathbf{G}(t, \mathbf{q}, \mathbf{s}) &= \bar{\mathbf{G}}(t, \mathbf{q}) = \frac{\partial \bar{\mathbf{g}}}{\partial \mathbf{q}}(t, \mathbf{q}) = \frac{\mathbf{D}\mathbf{g}}{\mathbf{D}\mathbf{q}}(t, \mathbf{q}, \mathbf{s}(t, \mathbf{q})) \\ &= \frac{\partial \mathbf{g}}{\partial \mathbf{q}}(t, \mathbf{q}, \mathbf{s}) + \frac{\partial \mathbf{g}}{\partial \mathbf{s}}(t, \mathbf{q}, \mathbf{s}) \frac{\partial \mathbf{s}}{\partial \mathbf{q}}(t, \mathbf{q}) = \left[\frac{\partial \mathbf{g}}{\partial \mathbf{q}} - \frac{\partial \mathbf{g}}{\partial \mathbf{s}} \left(\frac{\partial \mathbf{h}}{\partial \mathbf{s}} \right)^{-1} \frac{\partial \mathbf{h}}{\partial \mathbf{q}} \right](t, \mathbf{q}, \mathbf{s}) \end{aligned}$$

and the hidden constraints at the level of velocity coordinates get the form

$$\begin{aligned} \mathbf{0} &= \frac{d}{dt} \mathbf{g}(t, \mathbf{q}(t), \mathbf{s}(t)) = \frac{\partial \mathbf{g}}{\partial t}(t, \mathbf{q}, \mathbf{s}) + \frac{\partial \mathbf{g}}{\partial \mathbf{q}}(t, \mathbf{q}, \mathbf{s}) \dot{\mathbf{q}}(t) + \frac{\partial \mathbf{g}}{\partial \mathbf{s}}(t, \mathbf{q}, \mathbf{s}) \dot{\mathbf{s}}(t) \\ &= \left[\frac{\partial \mathbf{g}}{\partial t} - \frac{\partial \mathbf{g}}{\partial \mathbf{s}} \left(\frac{\partial \mathbf{h}}{\partial \mathbf{s}} \right)^{-1} \frac{\partial \mathbf{h}}{\partial t} \right](t, \mathbf{q}, \mathbf{s}) + \left[\frac{\partial \mathbf{g}}{\partial \mathbf{q}} - \frac{\partial \mathbf{g}}{\partial \mathbf{s}} \left(\frac{\partial \mathbf{h}}{\partial \mathbf{s}} \right)^{-1} \frac{\partial \mathbf{h}}{\partial \mathbf{q}} \right](t, \mathbf{q}, \mathbf{s}) \dot{\mathbf{q}}(t), \\ &= \mathbf{g}^{(l)}(t, \mathbf{q}, \mathbf{s}) + \mathbf{G}(t, \mathbf{q}, \mathbf{s}) \dot{\mathbf{q}}(t) = \bar{\mathbf{g}}^{(l)}(t, \mathbf{q}, \mathbf{s}) + \mathbf{G}(t, \mathbf{q}, \mathbf{s}) \mathbf{H}(\mathbf{q}) \mathbf{v}, \end{aligned}$$

with $\mathbf{g}^{(l)}$ summarizing the partial derivatives of \mathbf{g} and \mathbf{h} w.r.t. t , see (8) and (37). In the dynamical equations, the holonomic constraints (43) result in constraint forces $-\mathbf{H}^\top(\mathbf{q}) \mathbf{G}^\top(t, \mathbf{q}, \mathbf{s}) \boldsymbol{\lambda}$ with Lagrange multipliers $\boldsymbol{\lambda} \in \mathbb{R}^{n_\lambda}$. Additional constraint forces $-\mathbf{K}^\top(t, \mathbf{q}, \mathbf{s}) \boldsymbol{\eta}$ with Lagrange multipliers $\boldsymbol{\eta} \in \mathbb{R}^{n_k}$ correspond to n_k non-holonomic constraints that are assumed to be in Pfaffian form $\mathbf{0} = \mathbf{K}(t, \mathbf{q}, \mathbf{s}) \mathbf{v} + \mathbf{k}_0(t, \mathbf{q}, \mathbf{s})$, see [20].

With all these notations, the multibody system model equations may be summarized in a hybrid system of discrete state equations (41) and differential-algebraic equations

$$\dot{\mathbf{q}} = \mathbf{H}(\mathbf{q}) \mathbf{v}, \quad (44a)$$

$$\mathbf{M}(t, \mathbf{q}) \dot{\mathbf{v}} = \mathbf{f}(t, \mathbf{q}, \mathbf{s}, \mathbf{v}, \mathbf{c}, \mathbf{r}_j, \mathbf{w}, \boldsymbol{\lambda}, \boldsymbol{\eta}) - \mathbf{H}^\top(\mathbf{q}) \mathbf{G}^\top(t, \mathbf{q}, \mathbf{s}) \boldsymbol{\lambda} - \mathbf{K}^\top(t, \mathbf{q}, \mathbf{s}) \boldsymbol{\eta}, \quad (44b)$$

$$\dot{\mathbf{c}} = \mathbf{d}(t, \mathbf{q}, \mathbf{s}, \mathbf{v}, \mathbf{c}, \mathbf{r}_j, \mathbf{w}, \boldsymbol{\lambda}, \boldsymbol{\eta}), \quad (44c)$$

$$\mathbf{0} = \mathbf{b}(t, \mathbf{q}, \mathbf{s}, \mathbf{v}, \mathbf{c}, \mathbf{r}_j, \mathbf{w}, \boldsymbol{\lambda}, \boldsymbol{\eta}), \quad (44d)$$

$$\mathbf{0} = \mathbf{h}(t, \mathbf{q}, \mathbf{s}), \quad (44e)$$

$$\mathbf{0} = \mathbf{g}(t, \mathbf{q}, \mathbf{s}), \quad (44f)$$

$$\mathbf{0} = \mathbf{K}(t, \mathbf{q}, \mathbf{s}) \mathbf{v} + \mathbf{k}_0(t, \mathbf{q}, \mathbf{s}) \quad (44g)$$

that describe the evolution of all time-continuous state variables for $t \in [T_j, T_{j+1})$.

Existence and uniqueness of solutions for DAE (44) may be studied along the lines of the analysis in Section 2.2 provided that the terms

$$\frac{\partial \mathbf{f}}{\partial \boldsymbol{\lambda}} - \frac{\partial \mathbf{f}}{\partial \mathbf{w}} \left(\frac{\partial \mathbf{b}}{\partial \mathbf{w}} \right)^{-1} \frac{\partial \mathbf{b}}{\partial \boldsymbol{\lambda}} \quad \text{and} \quad \frac{\partial \mathbf{f}}{\partial \boldsymbol{\eta}} - \frac{\partial \mathbf{f}}{\partial \mathbf{w}} \left(\frac{\partial \mathbf{b}}{\partial \mathbf{w}} \right)^{-1} \frac{\partial \mathbf{b}}{\partial \boldsymbol{\eta}}$$

are sufficiently small [61]. Essential assumptions for the existence of a locally uniquely defined solution are known from Theorem 1: The symmetric, positive semi-definite mass matrix $\mathbf{M}(t, \mathbf{q})$ is assumed to have full rank at the nullspace of the extended constraint matrix

$$\begin{pmatrix} \mathbf{G}(t, \mathbf{q}, \mathbf{s}) \mathbf{H}(\mathbf{q}) \\ \mathbf{K}(t, \mathbf{q}, \mathbf{s}) \end{pmatrix}$$

and this matrix has to have full rank. With these assumptions, the index of DAE (44) is bounded by three, see Remark 3a.

Note, that the full rank assumption on $\mathbf{G}(t, \mathbf{q}, \mathbf{s}) \mathbf{H}(\mathbf{q})$ would be violated if the invariants (40) would be considered in the holonomic constraints (44f) since $\mathbf{0} \equiv \boldsymbol{\gamma}(\mathbf{q}(t))$ and the kinematic equations $\dot{\mathbf{q}} = \mathbf{H}(\mathbf{q}) \mathbf{v}$, see (44a), imply

$$\mathbf{0}_{n_q - n_v} = \frac{d}{dt} \boldsymbol{\gamma}(\mathbf{q}(t)) = \frac{\partial \boldsymbol{\gamma}}{\partial \mathbf{q}}(\mathbf{q}(t)) \dot{\mathbf{q}}(t) = \frac{\partial \boldsymbol{\gamma}}{\partial \mathbf{q}}(\mathbf{q}) \mathbf{H}(\mathbf{q}) \mathbf{v}$$

for any velocity coordinates $\mathbf{v} \in \mathbb{R}^{n_v}$, i.e., $(\partial \boldsymbol{\gamma} / \partial \mathbf{q})(\mathbf{q}) \mathbf{H}(\mathbf{q}) \equiv \mathbf{0}_{(n_q - n_v) \times n_v}$.

As an alternative, $n_q - n_v$ linearly independent invariants (40) with a Jacobian $(\partial \boldsymbol{\gamma} / \partial \mathbf{q})(\mathbf{q})$ of full rank could be enforced in time integration substituting the kinematic equations (44a) by

$$\dot{\mathbf{q}} = \mathbf{H}(\mathbf{q}) \mathbf{v} - \left(\frac{\partial \boldsymbol{\gamma}}{\partial \mathbf{q}}(\mathbf{q}) \right)^\top \boldsymbol{\mu}, \quad (45a)$$

$$\mathbf{0} = \boldsymbol{\gamma}(\mathbf{q}) \quad (45b)$$

with artificial multipliers $\boldsymbol{\mu} \in \mathbb{R}^{n_q - n_v}$, see [43]. These new variables vanish identically for the analytical solution since $(\partial \boldsymbol{\gamma} / \partial \mathbf{q})(\mathbf{q}) \mathbf{H}(\mathbf{q}) = \mathbf{0}$ implies

$$\begin{aligned} \mathbf{0} &= \frac{d}{dt} \boldsymbol{\gamma}(\mathbf{q}(t)) = \frac{\partial \boldsymbol{\gamma}}{\partial \mathbf{q}}(\mathbf{q}(t)) \dot{\mathbf{q}}(t) = \frac{\partial \boldsymbol{\gamma}}{\partial \mathbf{q}}(\mathbf{q}) \left(\mathbf{H}(\mathbf{q}) \mathbf{v} - \left(\frac{\partial \boldsymbol{\gamma}}{\partial \mathbf{q}}(\mathbf{q}) \right)^\top \boldsymbol{\mu} \right) \\ &= - \frac{\partial \boldsymbol{\gamma}}{\partial \mathbf{q}}(\mathbf{q}) \left(\frac{\partial \boldsymbol{\gamma}}{\partial \mathbf{q}}(\mathbf{q}) \right)^\top \boldsymbol{\mu}. \end{aligned}$$

and $(\partial \boldsymbol{\gamma} / \partial \mathbf{q})(\partial \boldsymbol{\gamma} / \partial \mathbf{q})^\top$ is non-singular by assumption. For the numerical solution, the correction term $-(\partial \boldsymbol{\gamma} / \partial \mathbf{q})^\top \boldsymbol{\mu}$ in (45a) remains typically in the size of the discretization error [43].

3.3 Multibody formalisms and topological solvers

In Section 2.1, we considered conservative systems being characterized by potential forces $-\nabla U(\mathbf{q})$ and used Hamilton's principle of least action to derive the equations of motion (3). Formally, this approach may be generalized to non-conservative systems including, e.g., dissipative terms and actuator forces. In engineering applications it is, however, more common to use equilibrium conditions for forces and momenta for deriving the equations of motion of complex multibody systems [75, 76].

These *Newton-Euler equations* are formulated most conveniently in an inertial frame using absolute coordinates. To simplify the notation, we restrict ourselves in the present section to linear configuration spaces and consider (absolute) position coordinates $\mathbf{p}_i(t) \in \mathbb{R}^{d_i}$, ($i = 1, \dots, N$), for the N bodies of the multibody system. Position and orientation of a rigid body $(\bullet)^{(i)}$ are described by $\mathbf{p}_i \in \mathbb{R}^6$ for 3-D models ($d_i = 6$, see Section 3.1) and by $\mathbf{p}_i \in \mathbb{R}^3$ in the 2-D case. For point masses, the (absolute) position may be characterized by Cartesian coordinates $\mathbf{p}_i \in \mathbb{R}^{d_i}$ with $d_i = 3$ in 3-D and $d_i = 2$ in 2-D, see, e.g., Example 1.

In this body-oriented modelling framework, the interaction of bodies may be described by *force elements* and by *joints* [52, 76]. Force elements represent, e.g., spring-damper elements and actuators and contribute in the mathematical model to the force vector \mathbf{f} .

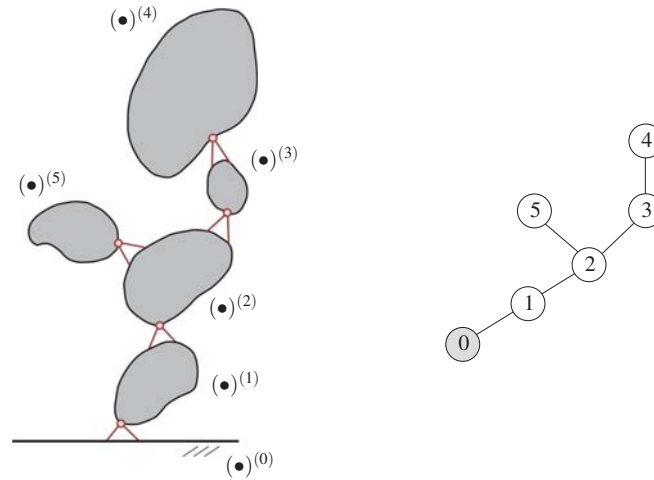


Fig. 8 Topology and labelled graph of a multibody system model with $N = 5$ bodies, see [6].

Joints restrict the relative motion of (two) bodies w.r.t. each other and result in (holonomic) constraints (1). Therefore, the basic internal structure of the DAE model equations (3) is characterized by the *topology* of the multibody system in terms of bodies and joints. The topology of a system with N bodies is represented

by a labelled graph with $N + 1$ vertices for the (rigid or flexible) bodies $(\bullet)^{(i)}$, ($i = 1, \dots, N$), and an extra (virtual) body $(\bullet)^{(0)}$ that is inertially fixed and stands for the inertial system. Two vertices of the graph are connected by an edge if and only if the corresponding bodies in the multibody system model are connected by a joint restricting their relative motion, see Fig. 8.

In dynamical simulation, the topology of the multibody system model is exploited to evaluate the equations of motion efficiently. An early reference in this field is the work of Featherstone who developed an algorithm to evaluate the equations of motion for a tree structured system of N bodies with $\mathcal{O}(N)$ complexity [38], see also [24]. Such *multibody formalisms* may be interpreted as a block Gauss elimination for an augmented set of equations of motion, see, e.g., [62, 90] and the references therein. From the viewpoint of numerical linear algebra, these algorithms define *topological solvers* [88] for large systems of linear equations (17) with sparse matrices \mathbf{M} and \mathbf{G} .

As a typical example, we consider in the present section a multibody formalism for tree structured systems that is based on a mixed coordinate formulation. The equations of motion are reduced to a second order ODE in joint coordinates \mathbf{q} with a right hand side that may be evaluated with $\mathcal{O}(N)$ complexity. These results have recently been published in a slightly more general setting in [6, 7]. They are essentially based on the work of Lubich et al. [62] and Eich-Soellner, Führer [36].

The graph of a tree structured multibody system is acyclic, i.e., it is free of loops. Furthermore, it is connected and may be ordered such that there is a *root vertex* and all vertices except this root vertex have a uniquely defined predecessor. It is assumed that the root vertex corresponds to the (inertially fixed) *root body* $(\bullet)^{(0)}$ and that the other vertices are labelled such that the labels are monotonically increasing along each branch of the kinematic tree.

With these assumptions, all bodies $(\bullet)^{(i)}$, ($i = 1, \dots, N$), have a uniquely defined predecessor $(\bullet)^{(\pi_i)}$ and the labels satisfy $\pi_i < i$. Each body $(\bullet)^{(i)}$ may have (direct) successors $(\bullet)^{(j)}$ being characterized by $\pi_j = i$ or, equivalently, by $j \in I_i := \{k : \pi_k = i\}$ with an index set I_i that represents the set of all successors of a given body $(\bullet)^{(i)}$ in the multibody system model. Bodies without successors ($I_i = \emptyset$) correspond to leafs of the kinematic tree and are therefore called “leaf bodies”. The tree structured system in Fig. 8 has the two leaf bodies $(\bullet)^{(4)}$ and $(\bullet)^{(5)}$ and we have $I_1 = \{2\}$, $I_2 = \{3, 5\}$, $I_3 = \{4\}$ since $\pi_1 = 0$, $\pi_2 = 1$, $\pi_3 = \pi_5 = 2$ and $\pi_4 = 3$.

Position and orientation of body $(\bullet)^{(i)}$ are characterized by the (absolute) position coordinates $\mathbf{p}_i(t) \in \mathbb{R}^{d_i}$. The *relative* position and orientation of body $(\bullet)^{(i)}$ w.r.t. its predecessor $(\bullet)^{(\pi_i)}$ is characterized by joint coordinates $\mathbf{q}_i(t) \in \mathbb{R}^{n_i}$ representing the n_i degrees of freedom of the joint connecting $(\bullet)^{(i)}$ with $(\bullet)^{(\pi_i)}$:

$$\mathbf{0} = \mathbf{k}_i(\mathbf{p}_i, \mathbf{p}_{\pi_i}, \mathbf{q}_i, t). \quad (46)$$

Here and in the following we assume that (46) is locally uniquely solvable w.r.t. \mathbf{p}_i and that the Jacobian $\mathbf{K}_i = \partial \mathbf{k}_i / \partial \mathbf{p}_i$ is non-singular along the solution. In its most simple form, Eq. (46) defines \mathbf{p}_i explicitly by $\mathbf{p}_i(t) = \mathbf{r}_i(\mathbf{p}_{\pi_i}(t), \mathbf{q}_i(t), t)$ resulting in $\mathbf{K}_i = \mathbf{I}_{d_i}$.

The kinematic relations (46) at the level of position coordinates imply relations at the level of velocity and acceleration coordinates that may formally be obtained by (total) differentiation of (46) w.r.t. time t , see (8) and (9):

$$\mathbf{0} = \frac{d}{dt} \mathbf{k}_i(\mathbf{p}_i(t), \mathbf{p}_{\pi_i}(t), \mathbf{q}_i(t), t) = \mathbf{K}_i \dot{\mathbf{p}}_i + \mathbf{H}_i \dot{\mathbf{p}}_{\pi_i} + \mathbf{J}_i \dot{\mathbf{q}}_i + \mathbf{k}_i^{(I)}(\mathbf{p}_0, \mathbf{p}, \mathbf{q}, t), \quad (47)$$

$$\mathbf{0} = \mathbf{K}_i \ddot{\mathbf{p}}_i + \mathbf{H}_i \ddot{\mathbf{p}}_{\pi_i} + \mathbf{J}_i \ddot{\mathbf{q}}_i + \mathbf{k}_i^{(II)}(\mathbf{p}_0, \dot{\mathbf{p}}_0, \mathbf{p}, \dot{\mathbf{p}}, \mathbf{q}, \dot{\mathbf{q}}, t) \quad (48)$$

with

$$\mathbf{K}_i := \frac{\partial \mathbf{k}_i}{\partial \mathbf{p}_i} \in \mathbb{R}^{d_i \times d_i}, \quad \mathbf{H}_i := \frac{\partial \mathbf{k}_i}{\partial \mathbf{p}_{\pi_i}} \in \mathbb{R}^{d_i \times d_i}, \quad \mathbf{J}_i := \frac{\partial \mathbf{k}_i}{\partial \mathbf{q}_i} \in \mathbb{R}^{d_i \times n_i}. \quad (49)$$

It is assumed that the joint coordinates $\mathbf{q}_i(t)$ are defined such that all Jacobians \mathbf{J}_i have full column rank: $\text{rank } \mathbf{J}_i = n_i \leq d_i$. Functions $\mathbf{k}_i^{(I)} := \partial \mathbf{k}_i / \partial t$ and $\mathbf{k}_i^{(II)}$ summarize partial time derivatives and all lower order terms in the first and second time derivative of (46), respectively. They may depend on the (absolute) coordinates \mathbf{p}_0 of the root body, on the absolute coordinates $\mathbf{p} := (\mathbf{p}_1, \dots, \mathbf{p}_N)$ of the remaining N bodies in the system, on the corresponding joint coordinates $\mathbf{q} := (\mathbf{q}_1, \dots, \mathbf{q}_N)$ and on $\dot{\mathbf{p}}_0$, $\dot{\mathbf{p}}$ and $\dot{\mathbf{q}}$.

In recursive multibody formalisms, the position and velocity of the root body ($\mathbf{p}_0(t)$, $\dot{\mathbf{p}}_0(t)$) as well as all joint coordinates $\mathbf{q}_i(t)$, $\dot{\mathbf{q}}_i(t)$, ($i = 1, \dots, N$), at a current time t are assumed to be given. Starting from the root body, the absolute position and velocity coordinates $\mathbf{p}_i(t)$, $\dot{\mathbf{p}}_i(t)$ of all N bodies $(\bullet)^{(i)}$, ($i = 1, \dots, N$), may then be computed recursively using (46) and (47), respectively, (*forward recursion*).

The equilibrium conditions for forces and momenta are formulated for each individual body $(\bullet)^{(i)}$ using its absolute coordinates \mathbf{p}_i :

$$\mathbf{M}_i \ddot{\mathbf{p}}_i + \mathbf{K}_i^\top \boldsymbol{\mu}_i + \sum_{j \in I_i} \mathbf{H}_j^\top \boldsymbol{\mu}_j = \mathbf{f}_i, \quad (i = 1, \dots, N). \quad (50)$$

They contain the reaction forces of the joints connecting body $(\bullet)^{(i)}$ with its predecessor ($\mathbf{K}_i^\top \boldsymbol{\mu}_i$) and with its successors in the kinematic tree ($\mathbf{H}_j^\top \boldsymbol{\mu}_j$, $j \in I_i$). All remaining forces and momenta acting on body $(\bullet)^{(i)}$ are summarized in the force vector $\mathbf{f}_i = \mathbf{f}_i(\mathbf{p}, \dot{\mathbf{p}}, \mathbf{q}, \dot{\mathbf{q}}, t) \in \mathbb{R}^{d_i}$. The body mass matrix $\mathbf{M}_i \in \mathbb{R}^{d_i \times d_i}$ contains mass and inertia tensor of body $(\bullet)^{(i)}$ and is assumed to be symmetric, positive definite. For a discussion of rank-deficient body mass matrices \mathbf{M}_i we refer to [7].

The specific structure of the joint reaction forces with Lagrange multipliers $\boldsymbol{\mu}_i(t) \in \mathbb{R}^{d_i}$ that satisfy

$$\mathbf{J}_i^\top \boldsymbol{\mu}_i = \mathbf{0}, \quad (i = 1, \dots, N), \quad (51)$$

results from the joint equations (46) and from d'Alembert's principle since the virtual work of constraint forces vanishes for all (virtual) displacements being compatible with (46). In (51), matrix \mathbf{J}_i denotes the Jacobian of the constraint function \mathbf{k}_i w.r.t. joint coordinates $\mathbf{q}_i \in \mathbb{R}^{n_i}$, see (49).

Eqs. (48), (51) and the equilibrium conditions (50) are linear in $\ddot{\mathbf{p}}, \ddot{\mathbf{q}}$ and $\boldsymbol{\mu}$. They may be summarized in a large sparse system of the form (17) with $(\ddot{\mathbf{q}}, \boldsymbol{\lambda})$ being substituted by $((\ddot{\mathbf{p}}^\top, \ddot{\mathbf{q}}^\top)^\top, \boldsymbol{\mu})$. The block diagonal mass matrix \mathbf{M} is of size $(n_p + n_q) \times (n_p + n_q)$. It has rank n_p since the non-zero blocks on the main diagonal are given by the symmetric, positive definite body mass matrices \mathbf{M}_i , $(i = 1, \dots, N)$. The non-zero blocks of the constraint matrix \mathbf{G} result from the Jacobians $\mathbf{K}_i, \mathbf{H}_i, \mathbf{J}_i$, $(i = 1, \dots, N)$, see (49).

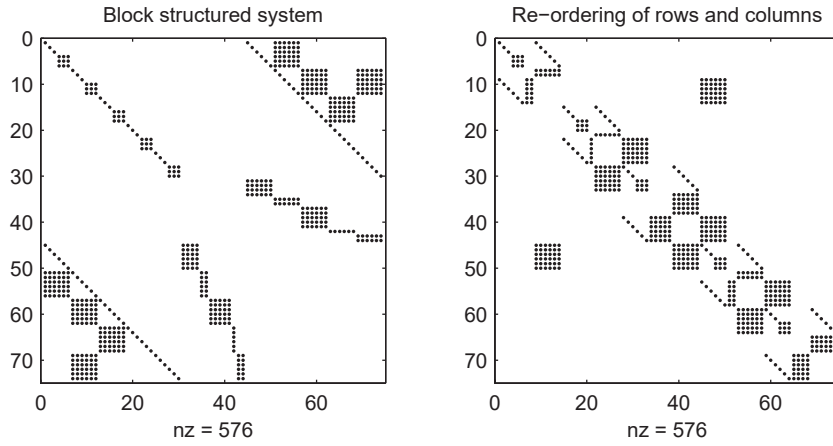


Fig. 9 Sparsity pattern of matrix (18) for a mixed coordinate formulation of the tree structured system of Fig. 8. Left plot: Original structure (18). Right plot: Structure after re-ordering of rows and columns according to the system's topology, see Example 7.

Example 7. The left plot of Fig. 9 shows the sparsity pattern of matrix (18) for a 3-D version of the tree structured system in Fig. 8 with $N = 5$ rigid bodies ($d_i = 6$) and joint coordinates \mathbf{q}_i of dimension $n_1 = 4, n_2 = 2, n_3 = 5, n_4 = 1, n_5 = 2$. The body mass matrices are given by $\mathbf{M}_i = \text{blockdiag}(m_i \mathbf{I}_3, \boldsymbol{\Theta}_i)$ with $m_i \in \mathbb{R}$ and $\boldsymbol{\Theta}_i \in \mathbb{R}^{3 \times 3}$ denoting mass and inertia tensor of body $(\bullet)^{(i)}$, $(i = 1, \dots, N)$. With kinematic relations $\mathbf{p}_i(t) = \mathbf{r}_i(\mathbf{p}_{\pi_i}(t), \mathbf{q}_i(t), t)$, we get Jacobians $\mathbf{K}_i = \mathbf{I}_6$, $(i = 1, \dots, N)$.

To reduce the bandwidth of this sparse symmetric matrix, rows and columns are re-ordered according to the system's topology. This may be achieved by the vector of unknowns $\mathbf{x} = (\mathbf{x}_N^\top, \mathbf{x}_{N-1}^\top, \dots, \mathbf{x}_1^\top)^\top$ with $\mathbf{x}_i \in \mathbb{R}^{12+n_i}$ summarizing the unknowns $\ddot{\mathbf{p}}_i, \ddot{\mathbf{q}}_i$ and $\boldsymbol{\mu}_i$ that correspond to body $(\bullet)^{(i)}$. Then we obtain an $N \times N$ block structured system with non-singular diagonal blocks $\mathbf{A}_i \in \mathbb{R}^{(12+n_i) \times (12+n_i)}$, $(i = N, N-1, \dots, 1)$:

$$\mathbf{x}_i := \begin{pmatrix} \ddot{\mathbf{p}}_i \\ \ddot{\mathbf{q}}_i \\ \boldsymbol{\mu}_i \end{pmatrix}, \quad \mathbf{A}_i := \begin{pmatrix} \mathbf{M}_i & \mathbf{0} & \mathbf{K}_i^\top \\ \mathbf{0} & \mathbf{0} & \mathbf{J}_i^\top \\ \mathbf{K}_i & \mathbf{J}_i & \mathbf{0} \end{pmatrix}.$$

For chain structured systems, this re-ordered matrix is block-tridiagonal. In a tree structured system, each ramification yields an extra non-zero block below this block-tridiagonal band (accompanied by its transposed in the upper triangle).

This sparsity structure is illustrated by the right plot of Fig. 9 that shows a 5×5 block structure with diagonal blocks of dimension 14×14 , 13×13 , 17×17 , 14×14 and 16×16 . The non-zero off-diagonal blocks in block row 4, block column 1 and in block row 1, block column 4 correspond to the ramification of the kinematic tree at body $(\bullet)^{(2)}$ that has *two* successors $(\bullet)^{(3)}$ and $(\bullet)^{(5)}$. (Note, that block column i is multiplied by vector \mathbf{x}_{N+1-i} since $\mathbf{x} = (\mathbf{x}_N^\top, \mathbf{x}_{N-1}^\top, \dots, \mathbf{x}_1^\top)^\top$).

The mixed coordinate formulation results in sparse systems (17) for the accelerations $\ddot{\mathbf{p}}, \ddot{\mathbf{q}}$ and the Lagrange multipliers $\boldsymbol{\mu}$. Example 7 shows how to re-arrange rows and columns of matrix (18) to get a sparse $N \times N$ block structure reflecting the system's topology. Lubich et al. [62] combine this approach with a block Gauss elimination to compute $\ddot{\mathbf{p}}, \ddot{\mathbf{q}}$ and $\boldsymbol{\mu}$ with $\mathcal{O}(N)$ complexity.

In engineering, such structure exploiting algorithms have been formulated such that all intermediate results have a straightforward physical interpretation ($\mathcal{O}(N)$ -formalisms): We start with the observation that the equilibrium conditions (50) get a simpler form for leaf bodies $(\bullet)^{(i)}$ since $I_i = \{j : \pi_j = i\} = \emptyset$ in that case. We obtain

$$\bar{\mathbf{M}}_i \mathbf{K}_i \ddot{\mathbf{p}}_i + \boldsymbol{\mu}_i = \bar{\mathbf{f}}_i \quad (52)$$

with $\bar{\mathbf{f}}_i := \mathbf{K}_i^{-\top} \mathbf{f}_i$, $\mathbf{K}_i^{-\top} := (\mathbf{K}_i^\top)^{-1}$ and the symmetric, positive definite mass matrix $\bar{\mathbf{M}}_i := \mathbf{K}_i^{-\top} \mathbf{M}_i \mathbf{K}_i^{-1}$. Eqs. (48), (51) and (52) define a system of $2d_i + n_i$ linear equations that may be solved w.r.t. $\ddot{\mathbf{p}}_i, \ddot{\mathbf{q}}_i$ and $\boldsymbol{\mu}_i$:

Lemma 3. *Consider the system of linear equations*

$$\bar{\mathbf{M}}_i \mathbf{K}_i \ddot{\mathbf{p}}_i + \boldsymbol{\mu}_i = \bar{\mathbf{f}}_i, \quad (53a)$$

$$\mathbf{J}_i^\top \boldsymbol{\mu}_i = \mathbf{0}, \quad (53b)$$

$$\mathbf{K}_i \ddot{\mathbf{p}}_i + \mathbf{H}_i \ddot{\mathbf{p}}_{\pi_i} + \mathbf{J}_i \ddot{\mathbf{q}}_i + \mathbf{k}_i^{(\text{II})} = \mathbf{0} \quad (53c)$$

with matrices $\bar{\mathbf{M}}_i, \mathbf{K}_i, \mathbf{H}_i \in \mathbb{R}^{d \times d}$, $\mathbf{J}_i \in \mathbb{R}^{d \times n}$ and vectors $\ddot{\mathbf{p}}_i, \boldsymbol{\mu}_i, \bar{\mathbf{f}}_i, \ddot{\mathbf{p}}_{\pi_i}, \mathbf{k}_i^{(\text{II})} \in \mathbb{R}^d$, $\ddot{\mathbf{q}}_i \in \mathbb{R}^n$. If $\bar{\mathbf{M}}_i$ is symmetric, positive definite, \mathbf{K}_i is non-singular and \mathbf{J}_i has full rank $n \leq d$ then (53) may be solved w.r.t. $\ddot{\mathbf{p}}_i, \boldsymbol{\mu}_i, \ddot{\mathbf{q}}_i$ resulting in

$$\ddot{\mathbf{q}}_i = -(\mathbf{J}_i^\top \bar{\mathbf{M}}_i \mathbf{J}_i)^{-1} \mathbf{J}_i^\top \bar{\mathbf{f}}_i - (\mathbf{J}_i^\top \bar{\mathbf{M}}_i \mathbf{J}_i)^{-1} \mathbf{J}_i^\top \bar{\mathbf{M}}_i (\mathbf{H}_i \ddot{\mathbf{p}}_{\pi_i} + \mathbf{k}_i^{(\text{II})}), \quad (54a)$$

$$\ddot{\mathbf{p}}_i = -\mathbf{K}_i^{-1} (\bar{\mathbf{H}}_i \ddot{\mathbf{p}}_{\pi_i} + \bar{\mathbf{k}}_i^{(\text{II})}), \quad (54b)$$

$$\boldsymbol{\mu}_i = \bar{\mathbf{f}}_i + \bar{\mathbf{M}}_i \bar{\mathbf{H}}_i \ddot{\mathbf{p}}_{\pi_i} + \bar{\mathbf{M}}_i \bar{\mathbf{k}}_i^{(\text{II})} \quad (54c)$$

with

$$\tilde{\mathbf{H}}_i := (\mathbf{I}_d - \mathbf{J}_i(\mathbf{J}_i^\top \tilde{\mathbf{M}}_i \mathbf{J}_i)^{-1} \mathbf{J}_i^\top \tilde{\mathbf{M}}_i) \mathbf{H}_i, \quad (55a)$$

$$\tilde{\mathbf{k}}_i^{(\text{II})} := (\mathbf{I}_d - \mathbf{J}_i(\mathbf{J}_i^\top \tilde{\mathbf{M}}_i \mathbf{J}_i)^{-1} \mathbf{J}_i^\top \tilde{\mathbf{M}}_i) \mathbf{k}_i^{(\text{II})} - \mathbf{J}_i(\mathbf{J}_i^\top \tilde{\mathbf{M}}_i \mathbf{J}_i)^{-1} \mathbf{J}_i^\top \tilde{\mathbf{f}}_i. \quad (55b)$$

Proof. If $\tilde{\mathbf{M}}_i \in \mathbb{R}^{d \times d}$ is symmetric, positive definite and $\mathbf{J}_i \in \mathbb{R}^{d \times n}$ has full rank then matrix $\mathbf{J}_i^\top \tilde{\mathbf{M}}_i \mathbf{J}_i \in \mathbb{R}^{n \times n}$ is symmetric, positive definite as well and left multiplication of (53c) by $(\mathbf{J}_i^\top \tilde{\mathbf{M}}_i \mathbf{J}_i)^{-1} \mathbf{J}_i^\top \tilde{\mathbf{M}}_i$ yields

$$\ddot{\mathbf{q}}_i = -(\mathbf{J}_i^\top \tilde{\mathbf{M}}_i \mathbf{J}_i)^{-1} \mathbf{J}_i^\top \tilde{\mathbf{M}}_i \mathbf{K}_i \ddot{\mathbf{p}}_i - (\mathbf{J}_i^\top \tilde{\mathbf{M}}_i \mathbf{J}_i)^{-1} \mathbf{J}_i^\top \tilde{\mathbf{M}}_i (\mathbf{H}_i \ddot{\mathbf{p}}_{\pi_i} + \mathbf{k}_i^{(\text{II})}). \quad (56)$$

Taking into account that left multiplication of (53a) by \mathbf{J}_i^\top results in

$$\mathbf{J}_i^\top \tilde{\mathbf{f}}_i = \mathbf{J}_i^\top \tilde{\mathbf{M}}_i \mathbf{K}_i \ddot{\mathbf{p}}_i + \mathbf{J}_i^\top \boldsymbol{\mu}_i = \mathbf{J}_i^\top \tilde{\mathbf{M}}_i \mathbf{K}_i \ddot{\mathbf{p}}_i,$$

see (53b), we may substitute the first term in the right hand side of (56) by $-(\mathbf{J}_i^\top \tilde{\mathbf{M}}_i \mathbf{J}_i)^{-1} \mathbf{J}_i^\top \tilde{\mathbf{f}}_i$ and get the explicit expression (54a) for $\ddot{\mathbf{q}}_i$. This explicit expression is used to obtain assertion (54b) multiplying (53c) from the left by matrix \mathbf{K}_i^{-1} . Finally, assertion (54c) is seen to be a straightforward consequence of (53a) and (54b). ■

For leaf bodies $(\bullet)^{(i)}$, the equilibrium conditions (50) were transformed straightforwardly to the simpler form (52). Lemma 3 allows to get by induction these condensed equilibrium conditions with suitable $\tilde{\mathbf{M}}_i, \tilde{\mathbf{f}}_i$ for *all* bodies $(\bullet)^{(i)}$ of the tree structured system: Let us assume that the equilibrium conditions of all direct successors $(\bullet)^{(j)}$ of body $(\bullet)^{(i)}$ are given in form (52), i.e.,

$$\tilde{\mathbf{M}}_j \mathbf{K}_j \ddot{\mathbf{p}}_j + \boldsymbol{\mu}_j = \tilde{\mathbf{f}}_j, \quad (j \in I_i).$$

Applying Lemma 3 to body $(\bullet)^{(j)}$ we obtain

$$\boldsymbol{\mu}_j = \tilde{\mathbf{f}}_j + \tilde{\mathbf{M}}_j \tilde{\mathbf{H}}_j \ddot{\mathbf{p}}_i + \tilde{\mathbf{M}}_j \tilde{\mathbf{k}}_j^{(\text{II})}$$

since $\pi_j = i$ if $(\bullet)^{(j)}$ is a direct successor of $(\bullet)^{(i)}$, see (54c). Inserting this expression in (50), we get after left-multiplication by $\mathbf{K}_i^{-\top}$ the condensed equilibrium conditions (52) with

$$\begin{aligned} \tilde{\mathbf{M}}_i &:= \mathbf{K}_i^{-\top} \mathbf{M}_i \mathbf{K}_i^{-1} + \sum_{j \in I_i} \mathbf{K}_i^{-\top} \mathbf{H}_j^\top \tilde{\mathbf{M}}_j \tilde{\mathbf{H}}_j \mathbf{K}_i^{-1} \\ &= \mathbf{K}_i^{-\top} \mathbf{M}_i \mathbf{K}_i^{-1} + \sum_{j \in I_i} \mathbf{K}_i^{-\top} \mathbf{H}_j^\top (\tilde{\mathbf{M}}_j - \tilde{\mathbf{M}}_j \mathbf{J}_j (\mathbf{J}_j^\top \tilde{\mathbf{M}}_j \mathbf{J}_j)^{-1} \mathbf{J}_j^\top \tilde{\mathbf{M}}_j) \mathbf{H}_j \mathbf{K}_i^{-1}, \quad (57a) \end{aligned}$$

$$\begin{aligned} \tilde{\mathbf{f}}_i &:= \mathbf{K}_i^{-\top} \mathbf{f}_i + \sum_{j \in I_i} \mathbf{K}_i^{-\top} \mathbf{H}_j^\top (\tilde{\mathbf{f}}_j + \tilde{\mathbf{M}}_j \mathbf{k}_j^{(\text{II})}) \\ &= \mathbf{K}_i^{-\top} \mathbf{f}_i - \sum_{j \in I_i} \mathbf{K}_i^{-\top} \mathbf{H}_j^\top (\mathbf{I}_{d_i} - \tilde{\mathbf{M}}_j \mathbf{J}_j (\mathbf{J}_j^\top \tilde{\mathbf{M}}_j \mathbf{J}_j)^{-1} \mathbf{J}_j^\top) (\tilde{\mathbf{f}}_j + \tilde{\mathbf{M}}_j \mathbf{k}_j^{(\text{II})}). \quad (57b) \end{aligned}$$

The condensed mass matrix $\bar{\mathbf{M}}_i$ in (57a) is symmetric, positive definite since it is composed of the symmetric, positive definite matrix $\mathbf{K}_i^{-\top} \mathbf{M}_i \mathbf{K}_i^{-1}$ and a finite sum of symmetric, positive semi-definite matrices [7, Lemma 1]. Starting from the leaf bodies and following all branches of the kinematic tree to the root, the compact form (52) of the equilibrium conditions may be obtained recursively for all N bodies $(\bullet)^{(i)}$ of the multibody system (*backward recursion*).

From the viewpoint of numerical linear algebra we may interpret the transformation of the equilibrium conditions (50) to their condensed form (52) as a block Gauss elimination that transforms sparse block structured matrices like the one in the right plot of Fig. 9 to upper block triangular form. From the viewpoint of physics, we observe that the condensed mass matrix $\bar{\mathbf{M}}_i$ in (52) summarizes in compact form the mass and inertia terms of body $(\bullet)^{(i)}$ and all its successors in the kinematic tree. The condensed force vector $\bar{\mathbf{f}}_i$ represents the corresponding forces and momenta.

Since the backward recursion results in condensed equilibrium conditions (52) for all N bodies of the multibody system, we may use Lemma 3 to verify that $\ddot{\mathbf{p}}_i = \mathbf{a}_i$, ($i = 1, \dots, N$), with vector valued functions \mathbf{a}_i that are recursively defined by

$$\mathbf{a}_0 := \ddot{\mathbf{p}}_0 = \mathbf{0}, \quad (58a)$$

$$\mathbf{a}_i := -\mathbf{K}_i^{-1} (\bar{\mathbf{H}}_i \mathbf{a}_{\pi_i} + \bar{\mathbf{k}}_i^{(\text{II})}), \quad (i = 1, \dots, N), \quad (58b)$$

see (54b). This *2nd forward recursion* exploits the assumption that the root body $(\bullet)^{(0)}$ is inertially fixed such that the sequence $(\mathbf{a}_i)_i$ may be initialized by (58a).

The recursive multibody formalism is completed using the explicit expression (54a) for the accelerations $\ddot{\mathbf{q}}_i$, ($i = 1, \dots, N$), from Lemma 3:

$$\ddot{\mathbf{q}}_i = -(\mathbf{J}_i^\top \bar{\mathbf{M}}_i \mathbf{J}_i)^{-1} \mathbf{J}_i^\top \bar{\mathbf{f}}_i - (\mathbf{J}_i^\top \bar{\mathbf{M}}_i \mathbf{J}_i)^{-1} \mathbf{J}_i^\top \bar{\mathbf{M}}_i (\mathbf{H}_i \mathbf{a}_{\pi_i} + \mathbf{k}_i^{(\text{II})}). \quad (59)$$

The recursive multibody formalism is summarized in Table 1. It is an *explicit* $\mathcal{O}(N)$ -formalism since the right hand side of an explicit 2nd order ODE

$$\ddot{\mathbf{q}}(t) = \boldsymbol{\varphi}(t, \mathbf{q}(t), \dot{\mathbf{q}}(t)) \quad (60)$$

for the joint coordinates $\mathbf{q}(t)$ is evaluated with a complexity that grows linearly with the number N of bodies in the tree structured multibody system.

Alternatively, the equations of motion may be evaluated in residual form

$$\mathbf{r}(t, \mathbf{q}(t), \dot{\mathbf{q}}(t), \ddot{\mathbf{q}}(t)) = \mathbf{0}$$

with

$$\mathbf{r}(t, \mathbf{q}, \dot{\mathbf{q}}, \ddot{\mathbf{q}}) := \mathbf{M}(t, \mathbf{q}) \ddot{\mathbf{q}} - \mathbf{f}(t, \mathbf{q}, \dot{\mathbf{q}}). \quad (61)$$

Residual formalisms [37] evaluate the residual $\mathbf{r}(t, \mathbf{q}, \dot{\mathbf{q}}, \ddot{\mathbf{q}})$ for given arguments t , \mathbf{q} , $\dot{\mathbf{q}}$ and for a given estimate of $\ddot{\mathbf{q}}$ more efficiently than the explicit formalism of Table 1. In time integration, they have to be combined with implicit integrators

Table 1 Explicit $\mathcal{O}(N)$ -formalism.

Data:	$t, \mathbf{q}(t), \dot{\mathbf{q}}(t), \mathbf{p}_0(t), \dot{\mathbf{p}}_0(t)$
Result:	$\ddot{\mathbf{q}} = \ddot{\mathbf{q}}(t, \mathbf{q}, \dot{\mathbf{q}}, \mathbf{p}_0, \dot{\mathbf{p}}_0)$
Step 1:	<i>First forward recursion.</i> Start at the root body $(\bullet)^{(0)}$ and follow the branches of the kinematic tree to evaluate recursively the absolute position and velocity coordinates $\mathbf{p}_i = \mathbf{p}_i(t, \mathbf{q}_i, \mathbf{p}_{\pi_i})$ and $\dot{\mathbf{p}}_i = \dot{\mathbf{p}}_i(t, \mathbf{q}_i, \dot{\mathbf{q}}_i, \mathbf{p}_{\pi_i}, \dot{\mathbf{p}}_{\pi_i})$, ($i = 1, \dots, N$), according to (46) and (47).
Step 2:	<i>Backward recursion.</i> Start at the leaf bodies and proceed along the branches of the kinematic tree to evaluate recursively the condensed mass matrices $\bar{\mathbf{M}}_i$ and the condensed force vectors $\bar{\mathbf{f}}_i$, ($i = N, N-1, \dots, 1$), according to (57).
Step 3:	<i>Second forward recursion.</i> Set $\mathbf{a}_0 := \mathbf{0}$ and follow the branches of the kinematic tree to evaluate recursively the acceleration terms $\mathbf{a}_i = \mathbf{a}_i(t, \mathbf{q}, \dot{\mathbf{q}}, \mathbf{p}_0, \dot{\mathbf{p}}_0)$, ($i = 1, \dots, N$), according to (58b).
Step 4:	<i>Function evaluation.</i> $\ddot{\mathbf{q}}_i = -(\mathbf{J}_i^\top \bar{\mathbf{M}}_i \mathbf{J}_i)^{-1} \mathbf{J}_i^\top \bar{\mathbf{f}}_i - (\mathbf{J}_i^\top \bar{\mathbf{M}}_i \mathbf{J}_i)^{-1} \mathbf{J}_i^\top \bar{\mathbf{M}}_i (\mathbf{H}_i \mathbf{a}_{\pi_i} + \mathbf{k}_i^{(H)}), \quad (i = 1, \dots, N).$

like DASSL [26] that are tailored to implicit differential equations in residual form. Since the linearly implicit structure of the residual in (61) may result in frequent re-evaluations of the iteration matrix in the implicit integrator, the overall performance of explicit formalisms in time integration is, however, often superior [14, 73].

Explicit formalisms and residual formalisms are tailored to tree structured systems. Multibody system models with closed kinematical loops are beyond this problem class since the loops result in cycles in the corresponding graph. Formally, such a more complex model may be transformed to tree structure cutting virtually the loop-closing joints to get a simplified model with tree structure [19]. For this simplified model, the right hand side $\boldsymbol{\varphi}$ in (60) and the residual \mathbf{r} in (61) are evaluated with $\mathcal{O}(N)$ complexity by multibody formalisms for tree structured systems. Finally, the virtually cut joints are considered in the equations of motion (16) by holonomic constraints (16b).

4 Time integration methods for constrained mechanical systems

The time integration of constrained mechanical systems was a topic of very active research in the 1980's and 1990's. The interested reader may find a comprehensive introduction to this subject in [50, Chapter VII].

Early approaches in this field were based on the direct application of ODE time discretization methods to the constrained equations of motion (16), see [31, 67]. We will discuss time integration methods of this type and their limitations and shortcomings in Section 4.1. The robustness and numerical stability of numerical methods for higher index DAEs may be improved substantially by an analytical index reduction

before time discretization. In Section 4.2, we will consider index reduction and projection techniques for constrained mechanical systems.

To omit technical and implementation details we focus in the present section on equations of motion of the form

$$\mathbf{M}(\mathbf{q})\ddot{\mathbf{q}} = \mathbf{f}(\mathbf{q}, \dot{\mathbf{q}}) - \mathbf{G}^\top(\mathbf{q})\boldsymbol{\lambda}, \quad (62a)$$

$$\mathbf{0} = \mathbf{g}(\mathbf{q}) \quad (62b)$$

with a constraint matrix $\mathbf{G}(\mathbf{q}) = (\partial/\partial\mathbf{q})\mathbf{g}(\mathbf{q})$ of full rank and a symmetric, positive semi-definite mass matrix $\mathbf{M}(\mathbf{q})$ that is positive definite on the nullspace of $\mathbf{G}(\mathbf{q})$. With these assumptions, the index of (62) is less than or equal to three. For positive definite mass matrices $\mathbf{M}(\mathbf{q})$, the system is analytically equivalent to an index-3 DAE in Hessenberg form, see Section 2.2.

4.1 Direct time discretization of the constrained equations of motion

For time discretization, the equations of motion (62) may either be considered as a second order DAE in terms of \mathbf{q} and $\boldsymbol{\lambda}$ or as a first order DAE in terms of \mathbf{q} , \mathbf{v} and $\boldsymbol{\lambda}$ with $\mathbf{v}(t) := \dot{\mathbf{q}}(t)$ denoting the velocity coordinates, see Section 2.2.

Time integration of second order systems by Newmark type methods

The numerical solution of unconstrained systems

$$\mathbf{M}(\mathbf{q})\ddot{\mathbf{q}} = \mathbf{f}(\mathbf{q}, \dot{\mathbf{q}}) \quad (63)$$

by Newmark type methods is quite popular in structural dynamics and flexible multibody dynamics [45]. In its most general form this class of integrators is given by the *generalized- α method* that was originally introduced for linear systems $\mathbf{M}\ddot{\mathbf{q}} + \mathbf{D}\dot{\mathbf{q}} + \mathbf{K}\mathbf{q} = \mathbf{r}(t)$ with \mathbf{M} , \mathbf{D} , \mathbf{K} denoting the (constant) mass, damping and stiffness matrix [33].

For nonlinear systems (63) with state dependent mass matrix $\mathbf{M}(\mathbf{q})$, we follow the approach of Brüls [8] who proposed to update the numerical solution $(\mathbf{q}_n, \dot{\mathbf{q}}_n, \ddot{\mathbf{q}}_n) \approx (\mathbf{q}(t_n), \dot{\mathbf{q}}(t_n), \ddot{\mathbf{q}}(t_n))$ in time step $t_n \rightarrow t_{n+1} = t_n + h$ by

$$\mathbf{q}_{n+1} = \mathbf{q}_n + h\dot{\mathbf{q}}_n + h^2(0.5 - \beta)\mathbf{a}_n + h^2\beta\mathbf{a}_{n+1}, \quad (64a)$$

$$\dot{\mathbf{q}}_{n+1} = \dot{\mathbf{q}}_n + h(1 - \gamma)\mathbf{a}_n + h\gamma\mathbf{a}_{n+1} \quad (64b)$$

with acceleration like vectors \mathbf{a}_n that are defined by a weighted linear combination

$$(1 - \alpha_m)\mathbf{a}_{n+1} + \alpha_m\mathbf{a}_n = (1 - \alpha_f)\ddot{\mathbf{q}}_{n+1} + \alpha_f\ddot{\mathbf{q}}_n \quad (64c)$$

such that the equilibrium conditions

$$\mathbf{M}(\mathbf{q}_{n+1})\ddot{\mathbf{q}}_{n+1} = \mathbf{f}(\mathbf{q}_{n+1}, \dot{\mathbf{q}}_{n+1}) \quad (65)$$

at $t = t_{n+1}$ are satisfied.

The method is characterized by the algorithmic parameters α_f , α_m , β and γ . It has local truncation errors of size $\mathcal{O}(h^3)$ in the update formulae (64a,b) for position and velocity coordinates if $\gamma = 0.5 - (\alpha_m - \alpha_f)$. In structural dynamics, the remaining free parameters α_f , α_m and β are adjusted such that the numerical solution for the scalar linear test equation $\ddot{q} + \omega^2 q = 0$ is stable for all time step sizes $h > 0$ and a user prescribed damping ratio $\rho_\infty \in [0, 1]$ is achieved in the limit case $h\omega \rightarrow \infty$, see [33].

An alternative definition of algorithmic parameters goes back to the work of Hilber, Hughes and Taylor [51] who considered method (64), (65) for systems (63) with constant mass matrix \mathbf{M} . In these *HHT- α methods*, the parameters α_f , α_m are given by $\alpha_f = -\alpha \in [0, 1/3]$ and $\alpha_m = 0$ and the update of vectors \mathbf{a}_n is simplified to

$$\mathbf{M}\mathbf{a}_{n+1} = (1 + \alpha)\mathbf{f}(\mathbf{q}_{n+1}, \dot{\mathbf{q}}_{n+1}) - \alpha\mathbf{f}(\mathbf{q}_n, \dot{\mathbf{q}}_n), \quad (66)$$

see (64c) and (65). With parameters $\gamma = 0.5 - \alpha$, $\beta = (1 - \alpha)^2/4$, the local truncation errors in (64a,b) are of size $\mathcal{O}(h^3)$ and the method is unconditionally stable for the linear test equation [45].

For the direct application of generalized- α methods to constrained systems (62), the time-discrete equilibrium conditions (65) are substituted by

$$\mathbf{M}(\mathbf{q}_{n+1})\ddot{\mathbf{q}}_{n+1} = \mathbf{f}(\mathbf{q}_{n+1}, \dot{\mathbf{q}}_{n+1}) - \mathbf{G}^\top(\mathbf{q}_{n+1})\boldsymbol{\lambda}_{n+1}, \quad (67a)$$

$$\mathbf{0} = \mathbf{g}(\mathbf{q}_{n+1}), \quad (67b)$$

see [8] and the earlier work of Cardona and Géradin [31] and Negrut et al. [66] who applied HHT- α methods to constrained systems (62) with constant mass matrix \mathbf{M} . In each time step, the numerical solution is defined implicitly by linear update formulae (64) and nonlinear equilibrium conditions (67). Taking into account the linear equations (64), we may express \mathbf{q}_{n+1} , $\dot{\mathbf{q}}_{n+1}$, $\ddot{\mathbf{q}}_{n+1}$ and \mathbf{a}_{n+1} in terms of the scaled increment

$$\Delta\mathbf{q}_n := \dot{\mathbf{q}}_n + h(0.5 - \beta)\mathbf{a}_n + h\beta\mathbf{a}_{n+1} \quad (68a)$$

in the position update (64a) and get

$$\mathbf{q}_{n+1} = \mathbf{q}_{n+1}(\Delta\mathbf{q}_n) = \mathbf{q}_n + h\Delta\mathbf{q}_n, \quad (68b)$$

$$\mathbf{a}_{n+1} = \mathbf{a}_{n+1}(\Delta\mathbf{q}_n) = \frac{1}{\beta h}(\Delta\mathbf{q}_n - \dot{\mathbf{q}}_n - (0.5 - \beta)h\mathbf{a}_n), \quad (68c)$$

$$\dot{\mathbf{q}}_{n+1} = \dot{\mathbf{q}}_{n+1}(\Delta\mathbf{q}_n) = \frac{\gamma}{\beta}\Delta\mathbf{q}_n + (1 - \frac{\gamma}{\beta})\dot{\mathbf{q}}_n + h(1 - \frac{\gamma}{2\beta})\mathbf{a}_n, \quad (68d)$$

$$\ddot{\mathbf{q}}_{n+1} = \ddot{\mathbf{q}}_{n+1}(\Delta\mathbf{q}_n) = \frac{1 - \alpha_m}{\beta(1 - \alpha_f)}\left(\frac{\Delta\mathbf{q}_n - \dot{\mathbf{q}}_n}{h} - 0.5\mathbf{a}_n\right) + \frac{\mathbf{a}_n - \alpha_f\ddot{\mathbf{q}}_n}{1 - \alpha_f}. \quad (68e)$$

In that way, the nonlinear system (64), (67) is condensed to $n_q + n_\lambda$ nonlinear equations

$$\mathbf{0} = \mathbf{r}_h^{n+1}(\Delta \mathbf{q}_n, h\boldsymbol{\lambda}_{n+1}), \quad (69a)$$

$$\mathbf{0} = \mathbf{g}_h^{n+1}(\Delta \mathbf{q}_n) \quad (69b)$$

in terms of $\Delta \mathbf{q}_n$ and $h\boldsymbol{\lambda}_{n+1}$. The nonlinear functions

$$\begin{aligned} \mathbf{r}_h^{n+1}(\Delta \mathbf{q}_n, h\boldsymbol{\lambda}_{n+1}) &:= \mathbf{M}(\mathbf{q}_{n+1}(\Delta \mathbf{q}_n)) h\dot{\mathbf{q}}_{n+1}(\Delta \mathbf{q}_n) \\ &\quad - h\mathbf{f}(\mathbf{q}_{n+1}(\Delta \mathbf{q}_n), \dot{\mathbf{q}}_{n+1}(\Delta \mathbf{q}_n)) + \mathbf{G}^\top(\mathbf{q}_{n+1}(\Delta \mathbf{q}_n)) h\boldsymbol{\lambda}_{n+1}, \\ \mathbf{g}_h^{n+1}(\Delta \mathbf{q}_n) &:= \frac{1}{h} \mathbf{g}(\mathbf{q}_{n+1}(\Delta \mathbf{q}_n)). \end{aligned}$$

are defined by the constrained equilibrium conditions (67). They are scaled such that the Jacobian

$$\begin{pmatrix} \frac{\partial \mathbf{r}_h^{n+1}}{\partial \Delta \mathbf{q}_n} & \frac{\partial \mathbf{r}_h^{n+1}}{\partial (h\boldsymbol{\lambda}_{n+1})} \\ \frac{\partial \mathbf{g}_h^{n+1}}{\partial \Delta \mathbf{q}_n} & \frac{\partial \mathbf{g}_h^{n+1}}{\partial (h\boldsymbol{\lambda}_{n+1})} \end{pmatrix} = \begin{pmatrix} \frac{1 - \alpha_m}{\beta(1 - \alpha_f)} \mathbf{M}(\mathbf{q}_n) + \mathcal{O}(h) & \mathbf{G}^\top(\mathbf{q}_n) + \mathcal{O}(h) \\ \mathbf{G}(\mathbf{q}_n) + \mathcal{O}(h) & \mathbf{0} \end{pmatrix} \quad (70)$$

and its inverse remain bounded for $h \rightarrow 0$ for algorithmic parameters α_f , α_m , β according to [33] or [51]. Scaling techniques are mandatory for the direct time discretization of higher index DAEs [70], see also [47]. For the application to constrained mechanical systems, they have been studied again more recently in [22].

Note, that the Jacobian in (70) has the characteristic 2×2 block structure that was considered in Lemma 1 above. For sufficiently small time step sizes $h > 0$, it is non-singular since the constraint matrix $\mathbf{G}(\mathbf{q}_n)$ was assumed to have full rank and the positive semi-definite mass matrix $\mathbf{M}(\mathbf{q}_n)$ is positive definite on the null space of $\mathbf{G}(\mathbf{q}_n)$.

Generalized- α and HHT- α methods for constrained systems have been used successfully in large scale practical applications [45, 66]. They may, however, suffer from a strange solution behaviour in transient phases after initialization and step size changes:

Example 8 (see [9, Example 1]). We consider two different initial configurations of the mathematical pendulum with equations of motion (6) and physical parameters $m = 1.0$, $l = 1.0$, $g_{\text{grav}} = 9.81$ (physical units are omitted). The consistent initial values x_0 , y_0 , \dot{x}_0 , \dot{y}_0 , λ_0 are defined such that the total mechanical energy $T + U = m(\dot{x}^2 + \dot{y}^2)/2 + mg_{\text{grav}}y$ at $t = t_0$ is given by $T_0 + U_0 = m/2 - mg_{\text{grav}}l$. In that way, all solution trajectories with initial values $x_0 \geq 0$, $\dot{x}_0 \geq 0$ coincide up to a phase shift to the one with initial values $x_0 = 0.0$, $y_0 = -1.0$, $\dot{x}_0 = 1.0$, $\dot{y}_0 = 0.0$, $\lambda_0 = 10.81$.

Fig. 10 shows the global errors in the Lagrange multiplier λ for the generalized- α method (64), (67) with a damping ratio $\rho_\infty = 0.9$ and algorithmic parameters α_f ,

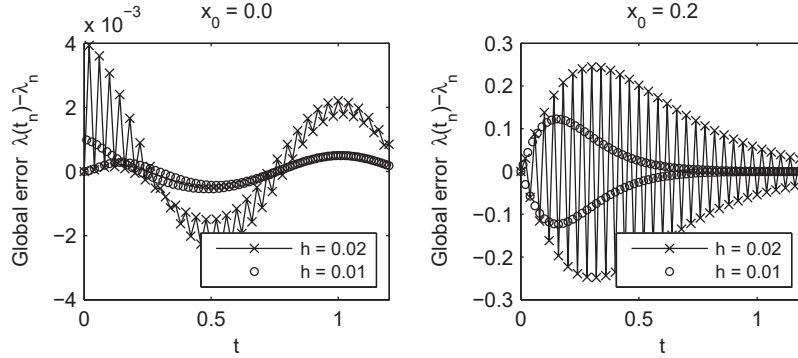


Fig. 10 Global error $\lambda(t_n) - \lambda_n$ of the generalized- α method (64), (67) for the equations of motion (6) of the mathematical pendulum with initial values $x_0 = 0$ (left plot) and $x_0 = 0.2$ (right plot).

α_m , β and γ according to [33]. The left plot shows $\lambda(t_n) - \lambda_n$ for simulations that start at the equilibrium position $(x_0, y_0) = (0, -l)$. Comparing the simulation results for time step size $h = \bar{h} := 0.02$ (marked by “x”) and the ones for time step size $h = \bar{h}/2 = 0.01$ (marked by “o”), we observe second order convergence since the maximum amplitudes are reduced from 4.0×10^{-3} to 1.0×10^{-3} , i.e., by a factor of $2^2 = 4$.

For simulations starting at $x_0 = 0.2$, the global errors are two orders of magnitude larger than before. The right plot of Fig. 10 shows a first order error term with maximum values that are reduced from 0.24 to 0.12 if the time step size is reduced by a factor of 2. This large oscillating error term is damped out after about 100 time steps. The detailed error analysis in [9, Remark 3a] shows that $|\lambda(t_n) - \lambda_n|$ is bounded by $C_1 n^2 \rho_\infty^n |\dot{y}_0| h + C_2 h^2$ with suitable constants $C_1, C_2 > 0$.

The test results in Fig. 10 are not sensitive to the initialization of (64) by starting values $(\mathbf{q}_0, \dot{\mathbf{q}}_0, \ddot{\mathbf{q}}_0, \mathbf{a}_0)$ with $\mathbf{q}_0 = \mathbf{q}(t_0)$, $\dot{\mathbf{q}}_0 = \dot{\mathbf{q}}(t_0)$, $\ddot{\mathbf{q}}_0 = \ddot{\mathbf{q}}(t_0)$ and $\mathbf{a}_0 = \ddot{\mathbf{q}}(t_0) + \mathcal{O}(h)$. In the numerical tests, we used starting values $\mathbf{a}_0 = \ddot{\mathbf{q}}(t_0) + (\alpha_m - \alpha_f)h + \mathcal{O}(h^2)$ that are optimal in the sense that the local truncation error in (64c) is of size $\mathcal{O}(h^2)$ if $(\ddot{\mathbf{q}}_{n+1}, \mathbf{a}_{n+1})$ is substituted by $(\ddot{\mathbf{q}}(t_n + \iota h), \ddot{\mathbf{q}}(t_n + (\iota + \alpha_m - \alpha_f)h))$, $(\iota = 0, 1)$, see, e.g., [55].

Example 8 illustrates that the direct application of generalized- α methods to constrained systems (62) may result in order reduction with a large transient oscillating error term that depends in a nontrivial way on the initial values $\mathbf{q}(t_0)$, $\dot{\mathbf{q}}(t_0)$. Modified starting values $\dot{\mathbf{q}}_0 = \dot{\mathbf{q}}(t_0) + \mathbf{\Delta}_0$ with a correction term $\mathbf{\Delta}_0$ of size $\mathcal{O}(h^2)$ have been proposed to eliminate this first order error term and to regain second order convergence [9].

Newmark type integrators like the HHT- α method and the generalized- α method are tailored to second order systems (62) and (63). They may, however, be extended to models with additional first order differential equations [29, 54]. In multibody

dynamics, such coupled systems of first and second order differential equations are typical of systems with hydraulic components, see Section 3.2.

ODE and DAE time integration methods for first order systems

As an alternative to time integration methods for the second order differential equations from structural dynamics we introduce velocity coordinates $\mathbf{v} := \dot{\mathbf{q}}$ and consider ODE and DAE time integration methods for first order systems that are applied to the linearly implicit DAE

$$\mathbf{0} = \mathbf{F}(t, \mathbf{x}, \dot{\mathbf{x}}) := \begin{pmatrix} \mathbf{M}(\mathbf{q})\dot{\mathbf{v}} - \mathbf{f}(\mathbf{q}, \mathbf{v}) + \mathbf{G}^\top(\mathbf{q})\boldsymbol{\lambda} \\ \mathbf{g}(\mathbf{q}) \end{pmatrix} \quad \text{with } \mathbf{x} := \begin{pmatrix} \mathbf{q} \\ \mathbf{v} \\ \boldsymbol{\lambda} \end{pmatrix} \quad (71)$$

that is equivalent to the constrained system (62), see Remark 3. Implicit Runge-Kutta methods and implicit multi-step methods have originally been developed for the time integration of first order ODEs

$$\dot{\mathbf{x}} = \boldsymbol{\varphi}(t, \mathbf{x}) \quad (72)$$

but may (formally) be applied to DAE (71) as well:

Remark 8. a) An implicit Runge-Kutta method uses s stage vectors

$$\mathbf{X}_{ni} = \mathbf{x}_n + h \sum_{j=1}^s a_{ij} \dot{\mathbf{X}}_{nj}, \quad (i = 1, \dots, s) \quad (73a)$$

to update the numerical solution $\mathbf{x}_n \approx \mathbf{x}(t_n)$ in time step $t_n \rightarrow t_{n+1} = t_n + h$ according to

$$\mathbf{x}_{n+1} = \mathbf{x}_n + h \sum_{i=1}^s b_i \dot{\mathbf{X}}_{ni} \quad (73b)$$

with stage vectors $\dot{\mathbf{X}}_{ni} \approx \dot{\mathbf{x}}(t_n + c_i h)$ that are connected to $\mathbf{X}_{ni} \approx \mathbf{x}(t_n + c_i h)$ by

$$\dot{\mathbf{X}}_{ni} = \boldsymbol{\varphi}(t_n + c_i h, \mathbf{X}_{ni}), \quad (i = 1, \dots, s) \quad (73c)$$

in the ODE case and by

$$\mathbf{0} = \mathbf{F}(t_n + c_i h, \mathbf{X}_{ni}, \dot{\mathbf{X}}_{ni}), \quad (i = 1, \dots, s) \quad (73d)$$

in the application to DAE (71). The method is characterized by nodes c_i , weights b_i and Runge-Kutta parameters a_{ij} , ($i, j = 1, \dots, s$). The application of implicit Runge-Kutta methods to higher index DAEs was studied, e.g., in [69] and [47].

b) For linear k -step methods with parameters α_j, β_j , ($j = 0, 1, \dots, k$), we have

$$\frac{1}{h} \sum_{j=0}^k \alpha_j \mathbf{x}_{n+1-j} = \sum_{j=0}^k \beta_j \dot{\mathbf{x}}_{n+1-j}. \quad (74a)$$

In time step $t_n \rightarrow t_{n+1} = t_n + h$, the vectors $\mathbf{x}_{n+1-j} \approx \mathbf{x}(t_n - (j-1)h)$, $\dot{\mathbf{x}}_{n+1-j} \approx \dot{\mathbf{x}}(t_n - (j-1)h)$, ($j = 1, \dots, k$), are assumed to be known and the numerical solution $\mathbf{x}_{n+1} \approx \mathbf{x}(t_{n+1})$ is defined such that

$$\dot{\mathbf{x}}_{n+1} = \boldsymbol{\varphi}(t_{n+1}, \mathbf{x}_{n+1}) \quad (74b)$$

for ODEs and

$$\mathbf{0} = \mathbf{F}(t_{n+1}, \mathbf{x}_{n+1}, \dot{\mathbf{x}}_{n+1}) \quad (74c)$$

in the application to DAEs (71). Considering k -step methods (74) with parameters $\beta_0 = 1, \beta_j = 0, (j = 1, \dots, k)$, we may eliminate $\dot{\mathbf{x}}_{n+1}$ and get the k -step BDF methods

$$\mathbf{0} = \mathbf{F}(t_{n+1}, \mathbf{x}_{n+1}, \frac{1}{h} \sum_{j=0}^k \alpha_j \mathbf{x}_{n+1-j}). \quad (75)$$

BDF are the most frequently used DAE time integration methods in technical simulation since they may be combined with very efficient step size and order control strategies [26].

For constrained mechanical systems (71), fixed step size BDF (75) define the update of position coordinates \mathbf{q}_n explicitly in terms of \mathbf{v}_{n+1} :

$$\mathbf{q}_{n+1} = \mathbf{q}_{n+1}(\mathbf{v}_{n+1}) = \frac{h}{\alpha_0} \mathbf{v}_{n+1} - \sum_{j=1}^k \frac{\alpha_j}{\alpha_0} \mathbf{q}_{n+1-j}.$$

Similar to generalized- α methods, we may use this expression to eliminate \mathbf{q}_{n+1} in the BDF definition (75) and get a condensed system of $n_q + n_\lambda$ nonlinear equations

$$\mathbf{0} = \mathbf{r}_h^{n+1}(\mathbf{v}_{n+1}, h\boldsymbol{\lambda}_{n+1}), \quad (76a)$$

$$\mathbf{0} = \mathbf{g}_h^{n+1}(\mathbf{v}_{n+1}) \quad (76b)$$

with

$$\begin{aligned} \mathbf{r}_h^{n+1}(\mathbf{v}_{n+1}, h\boldsymbol{\lambda}_{n+1}) &:= \mathbf{M}(\mathbf{q}_{n+1}(\mathbf{v}_{n+1})) \sum_{j=0}^k \alpha_j \mathbf{v}_{n+1-j} \\ &\quad - h\mathbf{f}(\mathbf{q}_{n+1}(\mathbf{v}_{n+1}), \mathbf{v}_{n+1}) + \mathbf{G}^\top(\mathbf{q}_{n+1}(\mathbf{v}_{n+1})) h\boldsymbol{\lambda}_{n+1}, \\ \mathbf{g}_h^{n+1}(\mathbf{v}_{n+1}) &:= \frac{1}{h} \mathbf{g}(\mathbf{q}_{n+1}(\mathbf{v}_{n+1})), \end{aligned}$$

see (69). The Jacobian

$$\begin{pmatrix} \frac{\partial \mathbf{r}_h^{n+1}}{\partial \mathbf{v}_{n+1}} & \frac{\partial \mathbf{r}_h^{n+1}}{\partial (h\boldsymbol{\lambda}_{n+1})} \\ \frac{\partial \mathbf{g}_h^{n+1}}{\partial \mathbf{v}_{n+1}} & \frac{\partial \mathbf{g}_h^{n+1}}{\partial (h\boldsymbol{\lambda}_{n+1})} \end{pmatrix} = \begin{pmatrix} \alpha_0 \mathbf{M}(\mathbf{q}_{n+1}(\mathbf{0})) + \mathcal{O}(h) & \mathbf{G}^\top(\mathbf{q}_{n+1}(\mathbf{0})) + \mathcal{O}(h) \\ \mathbf{G}(\mathbf{q}_{n+1}(\mathbf{0})) + \mathcal{O}(h) & \mathbf{0} \end{pmatrix}$$

has the characteristic 2×2 block structure (18). The Jacobian and its inverse are bounded for $h \rightarrow 0$.

The direct application of implicit Runge-Kutta methods and BDF to the constrained system (71) may again result in order reduction [26, 47]. For variable time step sizes, the numerical solution may even fail to converge [68]:

Example 9 (see [5, Section 5]). The backward Euler method is both a one-stage implicit Runge-Kutta method (73) with parameters $a_{11} = b_1 = c_1 = 1$ and the one-step BDF (75). For equations of motion (71) with mass matrix $\mathbf{M} = \mathbf{I}$, force vector $\mathbf{f} = \mathbf{0}$ and time dependent constraints $\mathbf{0} = \mathbf{g}(t, \mathbf{q}(t)) := \mathbf{C}\mathbf{q}(t) - \mathbf{z}(t)$, it is defined by

$$\begin{aligned} \frac{\mathbf{q}_{n+1} - \mathbf{q}_n}{h_n} &= \mathbf{v}_{n+1}, \\ \frac{\mathbf{v}_{n+1} - \mathbf{v}_n}{h_n} &= -\mathbf{C}^\top \boldsymbol{\lambda}_{n+1}, \\ \mathbf{0} &= \mathbf{C}\mathbf{q}_{n+1} - \mathbf{z}(t_{n+1}) \end{aligned}$$

with h_n denoting the (variable) time step size of time step $t_n \rightarrow t_{n+1} = t_n + h_n$. Straightforward computations show that

$$\boldsymbol{\lambda}_{n+1} = -\frac{h_n + h_{n-1}}{2h_n} (\mathbf{C}\mathbf{C}^\top)^{-1} \ddot{\mathbf{z}}(t_{n+1}) + \mathcal{O}(h_n) + \mathcal{O}\left(\frac{h_{n-1}^2}{h_n}\right)$$

if \mathbf{z} is three times continuously differentiable. For $h_n \rightarrow 0$ (and fixed time step size h_{n-1}), the numerical solution $\boldsymbol{\lambda}_{n+1}$ does *not* converge to the analytical solution $\boldsymbol{\lambda}(t_{n+1}) = -(\mathbf{C}\mathbf{C}^\top)^{-1} \ddot{\mathbf{z}}(t_{n+1})$ that is obtained differentiating the constraints $\mathbf{0} = \mathbf{C}\mathbf{q}(t) - \mathbf{z}(t)$ twice and inserting $\ddot{\mathbf{q}} = -\mathbf{C}^\top \boldsymbol{\lambda}(t)$ afterwards.

The direct application of implicit ODE time integration methods to DAEs (62) and (71) is intuitive and may be extended straightforwardly to more complex model equations including, e.g., non-holonomic constraints or additional algebraic equations $\mathbf{0} = \mathbf{h}(\mathbf{q}, \mathbf{s})$ with non-singular Jacobian $\partial \mathbf{h} / \partial \mathbf{s}$, see (44). Special care is needed in the practical implementation of these methods to address ill-conditioning of iteration matrices [22, 47, 70] and reliable estimation of local errors in step size control algorithms [26, 50].

In Examples 8 and 9, we have verified by two trivial test problems that the direct time discretization of the constrained equations of motion by ODE methods results systematically in poor simulation results for the Lagrange multipliers $\boldsymbol{\lambda}$. For more realistic multibody system models from practical applications, these numerical problems may affect the result accuracy of position and velocity coordinates as well.

In [4], we discussed this numerical effect for test scenarios from railway dynamics. The dynamical behaviour of rail vehicles is strongly influenced by the contact and friction forces between wheel and rail. In a rigid body contact model, the permanent contact between wheel and rail is described by holonomic constraints [84]. In the constrained system (71), the friction forces are part of the force vector \mathbf{f} . They depend nonlinearly on the wheel-rail contact forces $-\mathbf{G}^\top(\mathbf{q})\boldsymbol{\lambda}$, see [57, 84]. As a practical consequence, we get equations of motion (71) with $\mathbf{f} = \mathbf{f}(\mathbf{q}, \mathbf{v}, \boldsymbol{\lambda})$.

We present numerical test results for a rigid wheelset following a straight track, see Fig. 11. These test results were published before in [5, Section 5]:

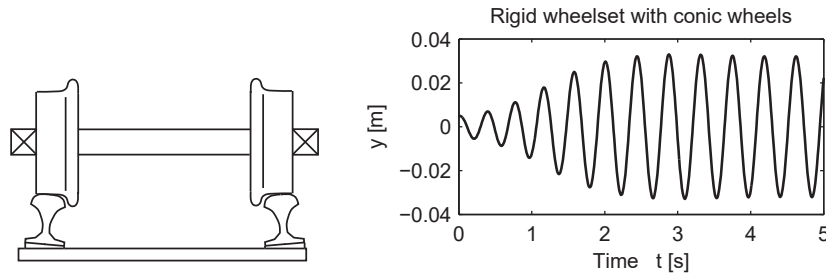


Fig. 11 Lateral displacement $y(t)$ of a rigid wheelset performing a hunting motion [5, Fig. 8].

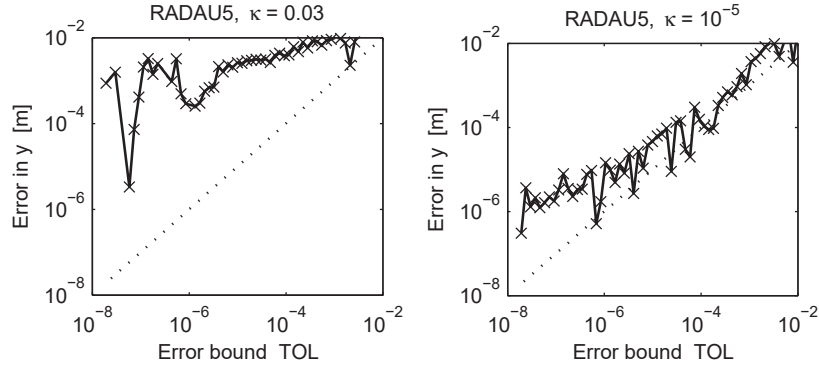


Fig. 12 Global error of the implicit Runge-Kutta solver RADAU5 being applied directly to DAE (71): Hunting motion of a rigid wheelset [5, Fig. 9].

Example 10. We consider the multibody system model of a rigid wheelset with conic wheels moving with constant speed along a straight track. It is a well known phenomenon from railway dynamics that the central position of the wheelset on the track gets unstable if the speed exceeds the so-called critical speed. Starting with

a small initial lateral displacement $y(t_0)$ the wheelset oscillates in lateral direction (*hunting motion*), see Fig. 11.

The rigid wheelset has six degrees of freedom and is described by position coordinates $\mathbf{q}(t) \in \mathbb{R}^6$. The permanent contact between the two wheels and the rails is modelled by two holonomic constraints resulting in contact forces $-\mathbf{G}^\top(\mathbf{q})\boldsymbol{\lambda}$ with $\boldsymbol{\lambda}(t) \in \mathbb{R}^2$.

Fig. 12 shows numerical test results for the implicit Runge-Kutta solver RADAU5 that adjusts its (variable) time step size h_n automatically to meet user-defined error bounds [50]. Practical experience in ODE applications shows that RADAU5 keeps the global error of the numerical solution usually well below these user-defined error tolerances TOL. But in the application to DAE (71), the relative errors remain even for very small error bounds in the size of 0.1 . . . 1.0%. As a typical example, the left plot of Fig. 12 shows the error in the lateral displacement y for various values of TOL.

To analyse these unsatisfactory results, we modify one of the internal solver parameters. BDF (75) and implicit Runge-Kutta methods (73) define \mathbf{x}_{n+1} solving a system of nonlinear equations. In the practical implementation this system is solved iteratively by Newton's method that is stopped if the residual is less than $\kappa \cdot \text{TOL}$. In this stopping criterion the user-defined error tolerance for time integration (TOL) is scaled by a constant $\kappa \leq 1$ that is a free control parameter of the solver. Default values are $\kappa = 0.33$ in the BDF solver DASSL, see [26], and $\kappa = 0.03$ in the implicit Runge-Kutta solver RADAU5, see [50].

The right plot of Fig. 12 shows that the error in time integration is reduced drastically and remains now roughly in the size of the error bounds TOL if κ is set to the very small value $\kappa = 10^{-5}$. The comparison of left and right plot in Fig. 12 illustrates that the direct application of RADAU5 to DAE (71) makes the solver very sensitive to (small) iteration errors in Newton's method. This practical observation coincides with the results of a detailed perturbation analysis for analytical and numerical solution [1].

4.2 Index reduction and projection

In the direct application of ODE time integration methods to DAE (71) the robustness of the solvers may be improved substantially by small values of κ that result in (very) small iteration errors in Newton's method, see the right plot of Fig. 12. On the other hand values of κ that are less than 10^{-3} increase the number of Newton steps per time step substantially and may slow down the solver dramatically.

Instead of applying ODE time integration methods directly to (71) it proved to be much more advantageous to transform the equations of motion analytically before time integration. This *index reduction* is the key to the robust and efficient dynamical simulation of constrained systems. It results in several analytically equivalent DAE formulations of the constrained system that is originally given in its *index-3 formulation* [50]

$$\dot{\mathbf{q}} = \mathbf{v}, \quad (77a)$$

$$\mathbf{M}(\mathbf{q})\dot{\mathbf{v}} = \mathbf{f}(\mathbf{q}, \mathbf{v}) - \mathbf{G}^\top(\mathbf{q})\boldsymbol{\lambda}, \quad (77b)$$

$$\mathbf{0} = \mathbf{g}(\mathbf{q}) \quad (77c)$$

with position coordinates \mathbf{q} , velocity coordinates \mathbf{v} and Lagrange multipliers $\boldsymbol{\lambda}$, see (71) and Remark 3. Note, that the index of (77) is three if the mass matrix $\mathbf{M}(\mathbf{q})$ is positive definite but may be less than three for rank-deficient mass matrices, see Example 5.

Index-2 formulation

Substituting the constraints (77c) by the corresponding hidden constraints

$$\mathbf{0} = \frac{d}{dt}\mathbf{g}(\mathbf{q}(t)) = \frac{\partial \mathbf{g}}{\partial \mathbf{q}}(\mathbf{q}(t))\dot{\mathbf{q}}(t) = \mathbf{G}(\mathbf{q}(t))\mathbf{v}(t) \quad (78)$$

at the level of velocity coordinates, see (8), we get the *index-2 formulation* [50]

$$\dot{\mathbf{q}} = \mathbf{v}, \quad (79a)$$

$$\mathbf{M}(\mathbf{q})\dot{\mathbf{v}} = \mathbf{f}(\mathbf{q}, \mathbf{v}) - \mathbf{G}^\top(\mathbf{q})\boldsymbol{\lambda}, \quad (79b)$$

$$\mathbf{0} = \mathbf{G}(\mathbf{q})\mathbf{v} \quad (79c)$$

that is analytically equivalent to the original equations of motion (77) if the initial values \mathbf{q}_0 are consistent with the holonomic constraints (77c) since $\mathbf{g}(\mathbf{q}_0) = \mathbf{0}$ implies

$$\mathbf{g}(\mathbf{q}(t)) = \underbrace{\mathbf{g}(\mathbf{q}(t_0))}_{=\mathbf{g}(\mathbf{q}_0)=\mathbf{0}} + \int_{t_0}^t \underbrace{\frac{d}{d\tau}\mathbf{g}(\mathbf{q}(\tau))}_{=\mathbf{0}, \text{ see (78) and (79c)}} d\tau = \mathbf{0} \quad (80)$$

for all $t \geq t_0$. Following step by step the index analysis in Remark 3, we see that DAEs (79) with positive definite mass matrices $\mathbf{M}(\mathbf{q})$ have differentiation index and perturbation index two.

Example 11. The perturbation analysis for index-2 systems (79) shows that the numerical solution is much less sensitive w.r.t. small constraint residuals than in the index-3 case [1]. This is nicely illustrated by numerical test results for the wheelset benchmark of Example 10. Applying the implicit Runge-Kutta solver RADAU5 to the index-2 formulation (79) of the equations of motion, we get much smaller errors than before, see Fig. 13. For default solver settings (left plot, $\kappa = 0.03$), the error remains roughly in the size of the user prescribed error tolerances TOL with some error saturation at the level of 10^{-6} for tolerances $\text{TOL} \leq 10^{-6}$. Further improvements are achieved by enforcing very small constraint residuals (right plot, $\kappa = 10^{-5}$) but these highly accurate simulation results require again much more computing time than the simulation with standard solver settings.

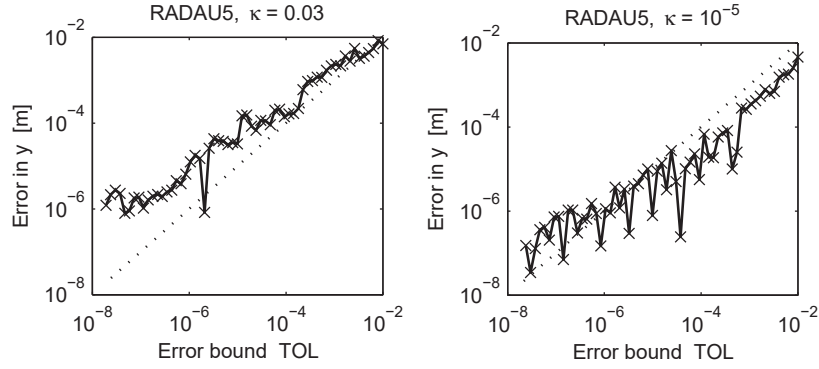


Fig. 13 Global error of the implicit Runge-Kutta solver RADAU5 being applied to the index-2 formulation (79) of the equations of motion: Hunting motion of a rigid wheelset [4, Fig. 2.1].

The time discretization of index-2 DAEs by implicit Runge-Kutta methods and BDF is discussed in the monographs [26, 47, 50]. For generalized- α and HHT- α methods, the combination of index reduction and time discretization is studied, e.g., in [55, 56, 63], see also the recent analysis for configuration spaces with Lie group structure in [9]. The practical implementation of these implicit time integration methods for the index-2 formulation (79) follows the implementation scheme that was discussed in Section 4.1. In the systems of nonlinear equations (69) and (76), equations $\mathbf{0} = \mathbf{g}_h^{n+1}$ have to be substituted by

$$\mathbf{0} = \mathbf{g}_h^{n+1}(\Delta \mathbf{q}_n) := \mathbf{G}(\mathbf{q}_{n+1}(\Delta \mathbf{q}_n)) \dot{\mathbf{q}}_{n+1}(\Delta \mathbf{q}_n)$$

for the generalized- α method and by

$$\mathbf{0} = \mathbf{g}_h^{n+1}(\mathbf{v}_{n+1}) := \mathbf{G}(\mathbf{q}_{n+1}(\mathbf{v}_{n+1})) \mathbf{v}_{n+1}$$

in the BDF case.

Remark 9. For non-stiff constrained systems, the use of *half-explicit* Runge-Kutta methods for the index-2 formulation (79) of the equations of motion proves to be favourable since these methods avoid the solution of systems of nonlinear equations. The s stage half-explicit method has nodes c_i , weights b_i and Runge-Kutta parameters a_{ij} , ($i = 1, \dots, s$, $j = 1, \dots, i-1$). It updates the numerical solution $(\mathbf{q}_n, \mathbf{v}_n, \boldsymbol{\lambda}_n)$ in time step $t_n \rightarrow t_{n+1} = t_n + h$ using stage vectors

$$\mathbf{Q}_{ni} \approx \mathbf{q}(t_n + c_i h), \mathbf{V}_{ni} \approx \mathbf{v}(t_n + c_i h), \dot{\mathbf{V}}_{ni} \approx \dot{\mathbf{v}}(t_n + c_i h), \mathbf{A}_{ni} \approx \boldsymbol{\lambda}(t_n + c_i h),$$

($i = 1, \dots, s$), that are initialized by

$$\mathbf{Q}_{n1} = \mathbf{q}_n, \mathbf{V}_{n1} = \mathbf{v}_n, \dot{\mathbf{V}}_{n1} = \dot{\mathbf{v}}_n, \mathbf{A}_{n1} = \boldsymbol{\lambda}_n \quad (81a)$$

with $\dot{\mathbf{v}}_n$ satisfying the dynamical equations at $t = t_n$:

$$\mathbf{M}(\mathbf{q}_n)\dot{\mathbf{v}}_n = \mathbf{f}(\mathbf{q}_n, \mathbf{v}_n) - \mathbf{G}^\top(\mathbf{q}_n)\boldsymbol{\lambda}_n \quad (81b)$$

The local error analysis shows that the method should start with an explicit stage

$$\mathbf{Q}_{n2} = \mathbf{q}_n + ha_{21}\mathbf{V}_{n1} = \mathbf{q}_n + ha_{21}\mathbf{v}_n \quad (81c)$$

to avoid order reduction [3, 15]. In the remaining $s-1$ stages, we may suppose that the stage vectors \mathbf{Q}_{ni} and $(\mathbf{V}_{nj}, \dot{\mathbf{V}}_{nj})$, ($j = 1, \dots, i-1$), are known such that the stage vectors

$$\mathbf{V}_{ni} = \mathbf{v}_n + h \sum_{j=1}^{i-1} a_{ij} \dot{\mathbf{V}}_{nj}, \quad \mathbf{Q}_{n,i+1} = \mathbf{q}_n + h \sum_{j=1}^i a_{i+1,j} \mathbf{V}_{nj} \quad (81d)$$

may be computed explicitly. (For $i = s$ we use for simplicity $a_{s+1,j} := b_j$.)

According to [25], a half-explicit Runge-Kutta stage for index-2 systems (79) is defined by the dynamical equations (79b) at $t = t_n + c_i h$ and by the constraints (79c) that are evaluated at $t = t_n + c_{i+1} h$ using the stage vector $\mathbf{Q}_{n,i+1}$ from (81d):

$$\mathbf{M}(\mathbf{Q}_{ni})\dot{\mathbf{V}}_{ni} = \mathbf{f}(\mathbf{Q}_{ni}, \mathbf{V}_{ni}) - \mathbf{G}^\top(\mathbf{Q}_{ni})\boldsymbol{\Lambda}_{ni},$$

$$\mathbf{0} = \mathbf{G}(\mathbf{Q}_{n,i+1})\mathbf{V}_{n,i+1} \quad \text{with} \quad \mathbf{V}_{n,i+1} = \mathbf{v}_n + h \sum_{j=1}^i a_{i+1,j} \dot{\mathbf{V}}_{nj}.$$

These equations are linear in the unknown stage vectors $\dot{\mathbf{V}}_{ni}$, $\boldsymbol{\Lambda}_{ni}$ and may be summarized to a system of $n_q + n_\lambda$ linear equations:

$$\begin{pmatrix} \mathbf{M}(\mathbf{Q}_{ni}) & \mathbf{G}^\top(\mathbf{Q}_{ni}) \\ \mathbf{G}(\mathbf{Q}_{n,i+1}) & \mathbf{0} \end{pmatrix} \begin{pmatrix} \dot{\mathbf{V}}_{ni} \\ \boldsymbol{\Lambda}_{ni} \end{pmatrix} = \begin{pmatrix} \mathbf{f}(\mathbf{Q}_{ni}, \mathbf{V}_{ni}) \\ -\frac{1}{ha_{i+1,i}} \mathbf{G}(\mathbf{Q}_{n,i+1})(\mathbf{v}_n + h \sum_{j=1}^{i-1} a_{i+1,j} \dot{\mathbf{V}}_{nj}) \end{pmatrix}. \quad (81e)$$

With (81d) and (81e) we compute stage by stage vectors $\mathbf{Q}_{n,i+1}$, \mathbf{V}_{ni} , $\dot{\mathbf{V}}_{ni}$ and $\boldsymbol{\Lambda}_{ni}$ for $i = 2, \dots, s$. Finally, the numerical solution at $t = t_{n+1}$ is given by

$$\mathbf{q}_{n+1} = \mathbf{q}_n + h \sum_{i=1}^s b_i \mathbf{V}_{ni}, \quad \mathbf{v}_{n+1} = \mathbf{v}_n + h \sum_{i=1}^s b_i \dot{\mathbf{V}}_{ni}, \quad \boldsymbol{\lambda}_{n+1} = \sum_{i=1}^s d_i \boldsymbol{\Lambda}_{ni} \quad (81f)$$

with new algorithmic parameters d_i , ($i = 1, \dots, s$), being defined by order conditions and by a contractivity condition that has to be satisfied to guarantee zero-stability and convergence [3, 15], see also [50, Section VII.6].

The 5th order explicit Runge-Kutta method of Dormand and Prince [34] has $s = 6$ stages and may be extended to a half-explicit Runge-Kutta method (81) of order $p = 5$ with $\hat{s} = 7$ stages that was implemented in the solver HEDOP5 for non-stiff constrained systems [3]. Numerical tests for a wheel suspension benchmark problem [81] illustrate that half-explicit solvers like HEDOP5 are superior to the

implicit BDF solver DASSL if the equations of motion (79) are non-stiff [3, 15]. On the other hand, implicit solvers are more flexible and may, e.g., be applied as well to systems with force vectors $\mathbf{f} = \mathbf{f}(\mathbf{q}, \mathbf{v}, \boldsymbol{\lambda})$ that contain friction forces depending nonlinearly on the Lagrange multipliers $\boldsymbol{\lambda}$.

Index-1 formulation

The index-2 formulation (79) was obtained substituting the holonomic constraints (77c) by their first time derivative. For index reduction, the second time derivative

$$\mathbf{0} = \frac{d^2}{dt^2} \mathbf{g}(\mathbf{q}(t)) = \mathbf{G}(\mathbf{q}(t)) \dot{\mathbf{v}}(t) + \mathbf{g}(\mathbf{q}(t))(\mathbf{v}(t), \mathbf{v}(t)) \quad (82)$$

may be used as well. These hidden constraints at the level of acceleration coordinates have been used in Section 2.2 to prove the unique solvability of initial value problems for consistent initial values. They define the constraints in the *index-1 formulation* of the equations of motion:

$$\dot{\mathbf{q}} = \mathbf{v}, \quad (83a)$$

$$\mathbf{M}(\mathbf{q}) \dot{\mathbf{v}} = \mathbf{f}(\mathbf{q}, \mathbf{v}) - \mathbf{G}^\top(\mathbf{q}) \boldsymbol{\lambda}, \quad (83b)$$

$$\mathbf{0} = \mathbf{G}(\mathbf{q}) \dot{\mathbf{v}} + \mathbf{g}_{qq}(\mathbf{q})(\mathbf{v}, \mathbf{v}). \quad (83c)$$

Using similar arguments as in (80), we may verify that this index-1 formulation is equivalent to the original equations of motion (77) for any consistent initial values $\mathbf{q}_0, \mathbf{v}_0$ satisfying $\mathbf{g}(\mathbf{q}_0) = \mathbf{G}(\mathbf{q}_0) \mathbf{v}_0 = \mathbf{0}$.

The index-1 formulation is attractive from the numerical point of view since $\dot{\mathbf{v}}(t)$ and $\boldsymbol{\lambda}(t)$ may be eliminated from (83) solving a system of $n_q + n_\lambda$ linear equations, see (17). Therefore, position and velocity coordinates may be obtained from the first order ODE

$$\dot{\mathbf{q}} = \mathbf{v}, \quad (84a)$$

$$\dot{\mathbf{v}} = \mathbf{a}(\mathbf{q}, \mathbf{v}) \quad (84b)$$

with the right hand side $\mathbf{a}(\mathbf{q}, \mathbf{v})$ being defined by

$$\begin{pmatrix} \mathbf{M}(\mathbf{q}) & \mathbf{G}^\top(\mathbf{q}) \\ \mathbf{G}(\mathbf{q}) & \mathbf{0} \end{pmatrix} \begin{pmatrix} \mathbf{a} \\ \boldsymbol{\lambda} \end{pmatrix} = \begin{pmatrix} \mathbf{f}(\mathbf{q}, \mathbf{v}) \\ -\mathbf{g}_{qq}(\mathbf{q})(\mathbf{v}, \mathbf{v}) \end{pmatrix}. \quad (84c)$$

Initial value problems for (84) can be solved straightforwardly by any ODE time integration method including higher order explicit Runge-Kutta methods and predictor-corrector methods of Adams type.

Remark 10. Half-explicit Runge-Kutta methods for the index-1 formulation (83) of the equations of motion compute a numerical solution $(\mathbf{q}_n, \mathbf{v}_n)$ that is updated in time step $t_n \rightarrow t_{n+1} = t_n + h$ by s half-explicit stages. A half-explicit stage for the

index-1 formulation (83) combines the explicit update

$$\mathbf{Q}_{ni} = \mathbf{q}_n + h \sum_{j=1}^{i-1} a_{ij} \mathbf{V}_{nj}, \quad \mathbf{V}_{ni} = \mathbf{v}_n + h \sum_{j=1}^{i-1} a_{ij} \dot{\mathbf{V}}_{nj} \quad (85a)$$

with a system of $n_q + n_\lambda$ linear equations in terms of $\dot{\mathbf{V}}_{ni}$ and Λ_{ni} :

$$\begin{pmatrix} \mathbf{M}(\mathbf{Q}_{ni}) & \mathbf{G}^\top(\mathbf{Q}_{ni}) \\ \mathbf{G}(\mathbf{Q}_{ni}) & \mathbf{0} \end{pmatrix} \begin{pmatrix} \dot{\mathbf{V}}_{ni} \\ \Lambda_{ni} \end{pmatrix} = \begin{pmatrix} \mathbf{f}(\mathbf{Q}_{ni}, \mathbf{V}_{ni}) \\ -\mathbf{g}_{qq}(\mathbf{Q}_{ni})(\mathbf{V}_{ni}, \mathbf{V}_{ni}) \end{pmatrix}. \quad (85b)$$

With (85a) and (85b) we compute stage by stage vectors \mathbf{Q}_{ni} , \mathbf{V}_{ni} , $\dot{\mathbf{V}}_{ni}$ and Λ_{ni} for $i = 1, \dots, s$. Finally, the numerical solution at $t = t_{n+1}$ is given by

$$\mathbf{q}_{n+1} = \mathbf{q}_n + h \sum_{i=1}^s b_i \mathbf{V}_{ni}, \quad \mathbf{v}_{n+1} = \mathbf{v}_n + h \sum_{i=1}^s b_i \dot{\mathbf{V}}_{ni}. \quad (85c)$$

This solution strategy was implemented, e.g., in the half-explicit Runge-Kutta solver MDOP5 [80] that is based on the 5th order explicit Runge-Kutta method of Dormand and Prince [34]. For non-stiff problems, MDOP5 is as efficient as the half-explicit solver HEDOP5, see Remark 9. Numerical tests have shown that MDOP5 is slightly more efficient than HEDOP5 if the curvature term $\mathbf{g}_{qq}(\mathbf{v}, \mathbf{v})$ may be evaluated with moderate numerical effort. On the other hand, the index-2 solver HEDOP5 is superior for problems with time consuming function evaluations $\mathbf{g}_{qq}(\mathbf{v}, \mathbf{v})$ like the wheel suspension benchmark [81], see [3, 4].

Drift-off effect

Index reduction by differentiation does not only improve the robustness of implicit solvers substantially but offers additionally the chance to use explicit and half-explicit methods as well. The main drawback of index reduced formulations like (79) and (83) are large constraint residuals $\mathbf{g}(\mathbf{q}_n)$ in long-term simulations. This *drift-off effect* is illustrated by the numerical test results in Fig. 14 that show linearly growing constraint residuals of size 10^{-6} for the index-2 formulation (79) and quadratically growing constraint residuals of size 5.0×10^{-4} for the index-1 formulation (83).

Because of (80), the *analytical* solution of the index-2 formulation satisfies the original constraints $\mathbf{g}(\mathbf{q}) = \mathbf{0}$ exactly for all $t \geq t_0$. In the *numerical* solution the integrand $(d\mathbf{g}/dt)(\mathbf{q}(\tau))$ in (80) is still bounded by a small constant $\varepsilon > 0$ but because of discretization and round-off errors it does *not* vanish identically. Therefore, the error in (77c) may increase linearly in time t :

$$\|\mathbf{g}(\mathbf{q}_n)\| \leq \|\mathbf{g}(\mathbf{q}_0)\| + \int_{t_0}^{t_n} \varepsilon \, dt = \varepsilon \cdot (t_n - t_0). \quad (86)$$

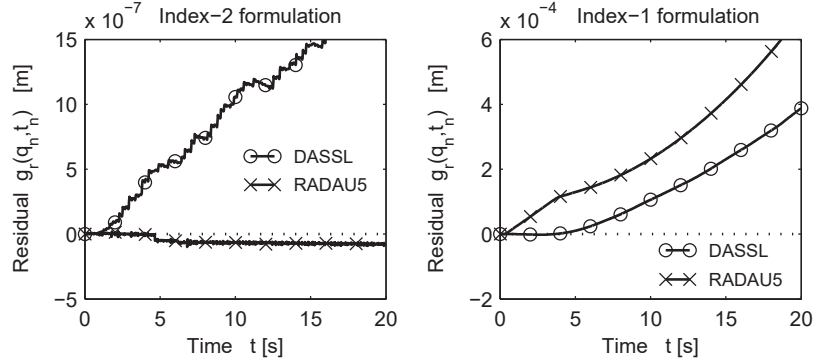


Fig. 14 Drift-off effect in the dynamical simulation of the rigid wheelset of Fig. 11 resulting in an increasing distance $g_r(\mathbf{q})$ between the right wheel and the rail, i.e., in an increasing error in the constraints $\mathbf{0} = \mathbf{g} = (g_l, g_r)^\top$ that are defined by the contact conditions for left and right wheel [5, Fig. 10].

The numerical solution \mathbf{q}_n drifts off the manifold $\mathfrak{M} = \{\boldsymbol{\eta} : \mathbf{g}(\boldsymbol{\eta}) = \mathbf{0}\}$ that is defined by the constraints (77c) on position level. The error bound ε summarizes discretization and round-off errors and the iteration errors of Newton's method.

For the index-1 formulation (83) a quadratic error growth

$$\|\mathbf{g}(\mathbf{q}_n)\| \leq \varepsilon \cdot (t_n - t_0)^2$$

has to be expected since the constraints (77c) on position level are substituted by their second derivatives (83c). Practical experience shows that ε depends on the solver and on the user-defined error tolerances TOL. In general, however, there is always a linear drift in the time integration of the index-2 formulation and a quadratic drift for the index-1 formulation.

Projection techniques and Baumgarte stabilization

An early attempt to avoid both the numerical problems for the index-3 formulation (77) and the drift-off effect in the index-2 and index-1 formulation goes back to the work of Baumgarte [21] who substituted the constraints (77c) by a linear combination of all three constraints (77c), (79c) and (83c). Because of the problems to select suitable coefficients for this linear combination (*Baumgarte coefficients*) the practical use of Baumgarte's approach is restricted to small scale models, see also the detailed analysis in [18].

A Baumgarte like method that substitutes the original constraints (77c) by a linear combination of (77c) and (79c) proved to be more favourable:

$$\dot{\mathbf{q}} = \mathbf{v}, \quad (87a)$$

$$\mathbf{M}(\mathbf{q})\dot{\mathbf{v}} = \mathbf{f}(\mathbf{q}, \mathbf{v}) - \mathbf{G}^\top(\mathbf{q})\boldsymbol{\lambda}, \quad (87b)$$

$$\mathbf{0} = \alpha_0 \mathbf{g}(\mathbf{q}) + \mathbf{G}(\mathbf{q})\mathbf{v}. \quad (87c)$$

This *index-2 Baumgarte approach* is used successfully for fixed step size computations in real-time applications. Here, the Baumgarte parameter should be set to $\alpha_0 = C/h$ with a suitable constant $C > 0$, see [10, 87].

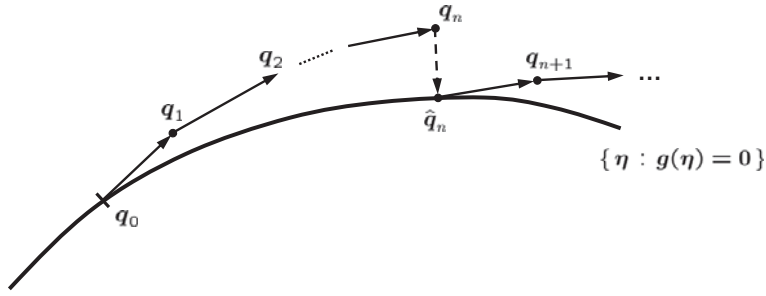


Fig. 15 Time integration with projection steps [5, Fig. 11].

In off-line simulation, it is state-of-the-art to avoid the drift-off effect by *projection* techniques [35, 61]. During the time integration of index reduced formulations like (79) and (83), the residual $\|\mathbf{g}(\mathbf{q}_n)\|$ in the constraints $\mathbf{g}(\mathbf{q}) = \mathbf{0}$ is monitored. If the residual exceeds at $t = t_n$ some user-defined small error bound $\varepsilon_g > 0$ then \mathbf{q}_n is projected onto the manifold $\mathfrak{M} = \{\boldsymbol{\eta} : \mathbf{g}(\boldsymbol{\eta}) = \mathbf{0}\}$ resulting in projected position coordinates $\hat{\mathbf{q}}_n$, see Fig. 15. In a second stage, the velocity coordinates \mathbf{v}_n are projected to the tangent space $T_{\mathbf{q}}\mathfrak{M}$ at $\mathbf{q} = \hat{\mathbf{q}}_n$. Finally, the position and velocity coordinates $(\mathbf{q}_n, \mathbf{v}_n)$ are substituted by their projections $(\hat{\mathbf{q}}_n, \hat{\mathbf{v}}_n)$ and the time integration is continued with the next time step.

For nonlinear constraints $\mathbf{g}(\mathbf{q}) = \mathbf{0}$, the projected position coordinates $\hat{\mathbf{q}}_n$ have to be computed iteratively. Following the approach of [61], we study the constrained minimization problem

$$\min \left\{ \frac{1}{2} \|\boldsymbol{\eta} - \mathbf{q}_n\|_{\mathbf{M}(\mathbf{q}_n)}^2 : \mathbf{g}(\boldsymbol{\eta}) = \mathbf{0} \right\} \quad (88)$$

with the semi-norm $\|\boldsymbol{\eta}\|_{\mathbf{M}(\mathbf{q}_n)} := (\boldsymbol{\eta}^\top \mathbf{M}(\mathbf{q}_n) \boldsymbol{\eta})^{1/2}$ that considers the mass distribution in the multibody system model. The constraints $\mathbf{g}(\boldsymbol{\eta}) = \mathbf{0}$ are coupled to the objective function by Lagrange multipliers $\boldsymbol{\mu}$ resulting in

$$\mathcal{L}(\boldsymbol{\eta}, \boldsymbol{\mu}) := \frac{1}{2} (\boldsymbol{\eta} - \mathbf{q}_n)^\top \mathbf{M}(\mathbf{q}_n) (\boldsymbol{\eta} - \mathbf{q}_n) + \boldsymbol{\mu}^\top \mathbf{g}(\boldsymbol{\eta}).$$

The necessary conditions

$$\begin{aligned}\mathbf{0} &= \nabla_{\boldsymbol{\eta}} \mathcal{L}(\boldsymbol{\eta}, \boldsymbol{\mu}) = \mathbf{M}(\mathbf{q}_n)(\boldsymbol{\eta} - \mathbf{q}_n) + \mathbf{G}^\top(\boldsymbol{\eta}) \boldsymbol{\mu}, \\ \mathbf{0} &= \nabla_{\boldsymbol{\mu}} \mathcal{L}(\boldsymbol{\eta}, \boldsymbol{\mu}) = \mathbf{g}(\boldsymbol{\eta})\end{aligned}$$

for a local minimum of (88) motivate a projection step $\mathbf{q}_n \mapsto \hat{\mathbf{q}}_n$ with $\hat{\mathbf{q}}_n$ being defined by the nonlinear system

$$\begin{aligned}\mathbf{0} &= \mathbf{M}(\mathbf{q}_n)(\hat{\mathbf{q}}_n - \mathbf{q}_n) + \mathbf{G}^\top(\mathbf{q}_n) \boldsymbol{\mu}, \\ \mathbf{0} &= \mathbf{g}(\hat{\mathbf{q}}_n)\end{aligned}$$

that may be solved iteratively by a simplified Newton method without re-evaluating the constraint matrix \mathbf{G} . The iteration matrix has the characteristic 2×2 block structure (18), see [61]:

$$\begin{pmatrix} \mathbf{M}(\mathbf{q}_n) & \mathbf{G}^\top(\mathbf{q}_n) \\ \mathbf{G}(\mathbf{q}_n) & \mathbf{0} \end{pmatrix} \begin{pmatrix} \hat{\mathbf{q}}_n^{(k+1)} - \hat{\mathbf{q}}_n^{(k)} \\ \boldsymbol{\mu}^{(k+1)} \end{pmatrix} = - \begin{pmatrix} \mathbf{M}(\mathbf{q}_n)(\hat{\mathbf{q}}_n^{(k)} - \mathbf{q}_n) \\ \mathbf{g}(\hat{\mathbf{q}}_n^{(k)}) \end{pmatrix}. \quad (89)$$

The method is initialized by $\hat{\mathbf{q}}_n^{(0)} := \mathbf{q}_n$ and needs typically only a few simplified Newton steps (89) to get an iterate $\hat{\mathbf{q}}_n = \hat{\mathbf{q}}_n^{(k)}$ satisfying $\|\mathbf{g}(\hat{\mathbf{q}}_n)\| \leq \varepsilon_g$, see [61].

The projection of \mathbf{v}_n to the tangent space $T_{\mathbf{q}}\mathfrak{M}$ at $\mathbf{q} = \hat{\mathbf{q}}_n$ does not require the iterative solution of nonlinear equations because the hidden constraints $\mathbf{G}(\hat{\mathbf{q}}_n)\mathbf{v} = \mathbf{0}$ are linear in the velocity coordinates \mathbf{v} . The constrained minimization problem

$$\min \left\{ \frac{1}{2} \|\boldsymbol{\eta} - \mathbf{v}_n\|_{\mathbf{M}(\hat{\mathbf{q}}_n)}^2 : \mathbf{G}(\hat{\mathbf{q}}_n)\boldsymbol{\eta} = \mathbf{0} \right\} \quad (90)$$

may be solved directly and defines the projected velocity coordinates $\hat{\mathbf{v}}_n$ by

$$\begin{pmatrix} \mathbf{M}(\hat{\mathbf{q}}_n) & \mathbf{G}^\top(\hat{\mathbf{q}}_n) \\ \mathbf{G}(\hat{\mathbf{q}}_n) & \mathbf{0} \end{pmatrix} \begin{pmatrix} \hat{\mathbf{v}}_n - \mathbf{v}_n \\ \bar{\boldsymbol{\mu}} \end{pmatrix} = \begin{pmatrix} \mathbf{0} \\ -\mathbf{G}(\hat{\mathbf{q}}_n)\mathbf{v}_n \end{pmatrix}. \quad (91)$$

Stabilized index-2 formulation

In complex applications, the use of classical projection methods like (89) and (91) is restricted to Runge-Kutta, generalized- α and other one-step methods since the efficient implementation of projection steps in advanced BDF solvers with order and step size control is non-trivial.

Instead of implementing explicit projection steps in the solver, the index reduced formulations of the equations of motion are reformulated in a way that contains implicitly the projection onto the constraint manifold $\mathfrak{M} = \{\mathbf{q} : \mathbf{g}(\mathbf{q}) = \mathbf{0}\}$ and its tangent space $T_{\mathbf{q}}\mathfrak{M}$. For the index-2 formulation (79), this approach goes back to the work of Gear, Gupta and Leimkuhler [44] who proposed to consider the (hidden) constraints (77c) and (79c) on position and velocity level simultaneously:

$$\dot{\mathbf{q}} = \mathbf{v} - \mathbf{G}^\top(\mathbf{q}) \boldsymbol{\mu}, \quad (92a)$$

$$\mathbf{M}(\mathbf{q}) \dot{\mathbf{v}} = \mathbf{f}(\mathbf{q}, \mathbf{v}) - \mathbf{G}^\top(\mathbf{q}) \boldsymbol{\lambda}, \quad (92b)$$

$$\mathbf{0} = \mathbf{g}(\mathbf{q}), \quad (92c)$$

$$\mathbf{0} = \mathbf{G}(\mathbf{q}) \mathbf{v}. \quad (92d)$$

The increasing number of equations in this *stabilized index-2 formulation* [26] of the equations of motion is compensated by a correction term $-\mathbf{G}^\top(\mathbf{q}) \boldsymbol{\mu}$ with auxiliary variables $\boldsymbol{\mu}(t) \in \mathbb{R}^{n_\lambda}$. The correction term vanishes identically for the analytical solution since (92a,d) and the time derivative of (92c) imply

$$\mathbf{0} = \frac{d}{dt} \mathbf{g}(\mathbf{q}(t)) = \frac{\partial \mathbf{g}}{\partial \mathbf{q}}(\mathbf{q}) \dot{\mathbf{q}} = \mathbf{G}(\mathbf{q}) (\mathbf{v} - \mathbf{G}^\top(\mathbf{q}) \boldsymbol{\mu}) = -[\mathbf{G}\mathbf{G}^\top](\mathbf{q}) \boldsymbol{\mu}$$

and the matrix product $[\mathbf{G}\mathbf{G}^\top](\mathbf{q})$ is non-singular for any full rank matrix $\mathbf{G}(\mathbf{q})$. Therefore, $\boldsymbol{\mu}(t) \equiv \mathbf{0}$. For the numerical solution, the correction term remains in the size of the user-defined error tolerances TOL.

Eqs. (92) form an index-2 DAE that may be solved robustly and efficiently by BDF [44] and implicit Runge-Kutta methods [50]. However, the error estimates in classical ODE solvers tend to overestimate the local errors in the algebraic components $\boldsymbol{\lambda}$, $\boldsymbol{\mu}$ of DAE (92), see [68]. Therefore the components $\boldsymbol{\lambda}$ and $\boldsymbol{\mu}$ should not be considered in the automatic step size control of BDF solvers [70]. For implicit Runge-Kutta solvers the error estimates for $\boldsymbol{\lambda}$ and $\boldsymbol{\mu}$ are scaled by the small factor h , see [50].

In implicit methods, the correction term $-\mathbf{G}^\top(\mathbf{q}) \boldsymbol{\mu}$ may be evaluated efficiently taking into account the block structure of the iteration matrix in the corrector iteration [5, Section 5]. This implementation scheme goes back to the work of Führer [40] who considered furthermore a stabilized index-1 formulation in BDF time integration [41].

The stabilized index-2 formulation may be defined as well for the more complex model equations (44) with additional algebraic equations $\mathbf{0} = \mathbf{h}(\mathbf{q}, \mathbf{s})$ but the structure of the correction term needs to be adapted carefully [2, 5]. This generalization of the classical approach of Gear, Gupta and Leimkuhler is closely related to the first index reduction step in the index reduction algorithm according to Kunkel and Mehrmann [58].

Stabilized index reduced formulations have also been investigated in the context of generalized- α and HHT- α methods [9, 55, 56, 63, 91]. Here, we consider the generalized- α method (64) for the stabilized index-2 formulation (92) of the equations of motion [9]. The constrained equilibrium conditions

$$\mathbf{M}(\mathbf{q}_{n+1}) \ddot{\mathbf{q}}_{n+1} = \mathbf{f}(\mathbf{q}_{n+1}, \dot{\mathbf{q}}_{n+1}) - \mathbf{G}^\top(\mathbf{q}_{n+1}) \boldsymbol{\lambda}_{n+1}, \quad (93a)$$

$$\mathbf{0} = \mathbf{g}(\mathbf{q}_{n+1}), \quad (93b)$$

$$\mathbf{0} = \mathbf{G}(\mathbf{q}_{n+1}) \mathbf{v}_{n+1} \quad (93c)$$

define a numerical solution $(\mathbf{q}_{n+1}, \mathbf{v}_{n+1})$ that satisfies both the holonomic constraints at the level of position coordinates and the hidden constraints at the level of velocity coordinates. A correction term $-\mathbf{G}^\top(\mathbf{q}_n)\boldsymbol{\mu}_n$ is added to the update formula (64a) of the position coordinates, i.e., we get $\mathbf{q}_{n+1} = \mathbf{q}_n + h\Delta\mathbf{q}_n$ with the scaled increment

$$\Delta\mathbf{q}_n := \dot{\mathbf{q}}_n - \mathbf{G}^\top(\mathbf{q}_n)\boldsymbol{\mu}_n + h(0.5 - \beta)\mathbf{a}_n + h\beta\mathbf{a}_{n+1}, \quad (94a)$$

see (68a). Using again the functions $\mathbf{q}_{n+1}(\Delta\mathbf{q}_n), \dots$ that were introduced in (68b-e), we may express $\mathbf{q}_{n+1}, \mathbf{a}_{n+1}, \dot{\mathbf{q}}_{n+1}$ and $\ddot{\mathbf{q}}_{n+1}$ in terms of $\Delta\mathbf{q}_n$ and $\boldsymbol{\mu}_n$:

$$\mathbf{q}_{n+1} = \mathbf{q}_{n+1}(\Delta\mathbf{q}_n), \quad (94b)$$

$$\mathbf{a}_{n+1} = \mathbf{a}_{n+1}(\Delta\mathbf{q}_n + \mathbf{G}^\top(\mathbf{q}_n)\boldsymbol{\mu}_n), \quad (94c)$$

$$\dot{\mathbf{q}}_{n+1} = \dot{\mathbf{q}}_{n+1}(\Delta\mathbf{q}_n + \mathbf{G}^\top(\mathbf{q}_n)\boldsymbol{\mu}_n), \quad (94d)$$

$$\ddot{\mathbf{q}}_{n+1} = \ddot{\mathbf{q}}_{n+1}(\Delta\mathbf{q}_n + \mathbf{G}^\top(\mathbf{q}_n)\boldsymbol{\mu}_n). \quad (94e)$$

In each time step, the numerical solution is obtained solving the system of $n_q + 2n_\lambda$ nonlinear equations

$$\begin{aligned} \mathbf{0} &= \mathbf{r}_h^{n+1}(\Delta\mathbf{q}_n, h\boldsymbol{\lambda}_{n+1}, \boldsymbol{\mu}_n), \\ \mathbf{0} &= \mathbf{g}_h^{n+1}(\Delta\mathbf{q}_n), \\ \mathbf{0} &= \dot{\mathbf{g}}_h^{n+1}(\Delta\mathbf{q}_n, \boldsymbol{\mu}_n) \end{aligned}$$

with

$$\begin{aligned} \mathbf{r}_h^{n+1}(\Delta\mathbf{q}_n, h\boldsymbol{\lambda}_{n+1}, \boldsymbol{\mu}_n) &:= \mathbf{M}(\mathbf{q}_{n+1}(\Delta\mathbf{q}_n))h\ddot{\mathbf{q}}_{n+1}(\Delta\mathbf{q}_n + \mathbf{G}^\top(\mathbf{q}_n)\boldsymbol{\mu}_n) \\ &\quad - h\mathbf{f}(\mathbf{q}_{n+1}(\Delta\mathbf{q}_n), \dot{\mathbf{q}}_{n+1}(\Delta\mathbf{q}_n + \mathbf{G}^\top(\mathbf{q}_n)\boldsymbol{\mu}_n)) \\ &\quad + \mathbf{G}^\top(\mathbf{q}_{n+1}(\Delta\mathbf{q}_n))h\boldsymbol{\lambda}_{n+1}, \\ \mathbf{g}_h^{n+1}(\Delta\mathbf{q}_n) &:= \frac{1}{h}\mathbf{g}(\mathbf{q}_{n+1}(\Delta\mathbf{q}_n)), \\ \dot{\mathbf{g}}_h^{n+1}(\Delta\mathbf{q}_n) &:= \mathbf{G}(\mathbf{q}_{n+1}(\Delta\mathbf{q}_n))\dot{\mathbf{q}}_{n+1}(\Delta\mathbf{q}_n + \mathbf{G}^\top(\mathbf{q}_n)\boldsymbol{\mu}_n). \end{aligned}$$

These equations are scaled again such that the Jacobian

$$\left(\begin{array}{ccc} \frac{1 - \alpha_m}{\beta(1 - \alpha_f)}\mathbf{M}(\mathbf{q}_n) + \mathcal{O}(h) & \mathbf{G}^\top(\mathbf{q}_n) + \mathcal{O}(h) & \frac{1 - \alpha_m}{\beta(1 - \alpha_f)}[\mathbf{M}\mathbf{G}^\top](\mathbf{q}_n) + \mathcal{O}(h) \\ \mathbf{G}(\mathbf{q}_n) + \mathcal{O}(h) & \mathbf{0} & \mathbf{0} \\ \frac{\gamma}{\beta}\mathbf{G}(\mathbf{q}_n) + \mathcal{O}(h) & \mathbf{0} & \frac{\gamma}{\beta}[\mathbf{G}\mathbf{G}^\top](\mathbf{q}_n) + \mathcal{O}(h) \end{array} \right)$$

and its inverse remain bounded for $h \rightarrow 0$.

The generalized- α method (93), (94) converges with order $p = 2$ for all solution components if the starting values $\mathbf{q}_0, \dot{\mathbf{q}}_0$ and $\ddot{\mathbf{q}}_0$ are second order accurate and

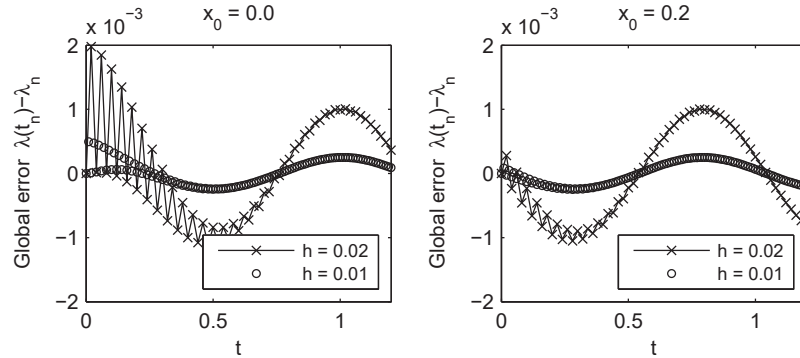


Fig. 16 Global error $\lambda(t_n) - \lambda_n$ of the generalized- α method (93), (94) for the stabilized index-2 formulation of the equations of motion for the mathematical pendulum with initial values $x_0 = 0$ (left plot) and $x_0 = 0.2$ (right plot).

$\mathbf{a}_0 = \ddot{\mathbf{q}}(t_0 + (\alpha_m - \alpha_f)h) + \mathcal{O}(h^2)$, see [9]. In Fig. 16 this second order convergence result is illustrated for the application to the equations of motion of the mathematical pendulum, see Example 8. For the stabilized index-2 formulation, the global error $\lambda(t_n) - \lambda_n$ remains in the size of 2.0×10^{-3} for both initial configurations. A step size reduction by a factor of two results approximately in a reduction of global errors by the factor of $2^2 = 4$.

The stabilized index-2 formulation of the equations of motion may be extended straightforwardly to model equations with more complex structure including, e.g., nonholonomic constraints or additional differential or algebraic equations. In that sense it is considered to be the most flexible general purpose approach to time integration in multibody dynamics that combines robustness with numerical efficiency. In a practical implementation, the stabilized index-2 formulation is discretized by BDF, by implicit Runge-Kutta methods or by Newmark type methods resulting in nonlinear corrector equations that have to be solved in each time step.

5 Summary

Analysis and numerical solution of constrained mechanical systems have been an important subject of DAE theory for more than 25 years. The well structured higher index model equations have inspired the development of very efficient index reduction and time integration methods. These DAE solution techniques offer much flexibility to multibody system dynamics w.r.t. model setup and choice of coordinates. Model equations with redundant coordinates resulting from a generic network approach for model setup or from kinematically closed loops in the multibody system model may be solved efficiently by a combination of index reduction techniques

with time integration methods from nonlinear system dynamics (BDF, Runge-Kutta methods) or structural dynamics (generalized- α and HHT- α methods).

Half-explicit methods prove to be efficient in the non-stiff case but are typically restricted to the simulation of N -body systems. The model equations in multibody system dynamics may have a substantially more complex structure including nonlinear configuration spaces, additional differential and algebraic equations, rank-deficient mass matrices and redundant constraints. Often, they may be solved more efficiently by implicit methods. The combination of BDF, implicit Runge-Kutta methods or generalized- α methods with the stabilized index-2 formulation of the equations of motion is the method of choice in industrial multibody system simulation.

References

1. M. Arnold. A perturbation analysis for the dynamical simulation of mechanical multibody systems. *Applied Numerical Mathematics*, 18:37–56, 1995.
2. M. Arnold. Numerical problems in the dynamical simulation of wheel-rail systems. *Z. Angew. Math. Mech.*, 76(S3):151–154, 1996.
3. M. Arnold. Half-explicit Runge–Kutta methods with explicit stages for differential-algebraic systems of index 2. *BIT Numerical Mathematics*, 38:415–438, 1998.
4. M. Arnold. *Zur Theorie und zur numerischen Lösung von Anfangswertproblemen für differentiell-algebraische Systeme von höherem Index*. Fortschritt-Berichte VDI Reihe 20, Nr. 264. VDI-Verlag, Düsseldorf, 1998.
5. M. Arnold. Numerical methods for simulation in applied dynamics. In M. Arnold and W. Schiehlen, editors, *Simulation Techniques for Applied Dynamics*, volume 507 of *CISM Courses and Lectures*, pages 191–246. Springer, Wien New York, 2009.
6. M. Arnold. Algorithmic aspects of singularly perturbed multibody system models. *GACM Report*, Summer 2013:10–16, 2013.
7. M. Arnold. A recursive multibody formalism for systems with small mass and inertia terms. *Mech. Sci.*, 4:221–231, 2013.
8. M. Arnold and O. Brüls. Convergence of the generalized- α scheme for constrained mechanical systems. *Multibody System Dynamics*, 18:185–202, 2007.
9. M. Arnold, O. Brüls, and A. Cardona. Error analysis of generalized- α Lie group time integration methods for constrained mechanical systems. *Numerische Mathematik*, 129:149–179, 2015.
10. M. Arnold, B. Burgermeister, and A. Eichberger. Linearly implicit time integration methods in real-time applications: DAEs and stiff ODEs. *Multibody System Dynamics*, 17:99–117, 2007.
11. M. Arnold, B. Burgermeister, C. Führer, G. Hippmann, and G. Rill. Numerical methods in vehicle system dynamics: State of the art and current developments. *Vehicle System Dynamics*, 49:1159–1207, 2011.
12. M. Arnold, A. Cardona, and O. Brüls. Order reduction in time integration caused by velocity projection. In *Proc. of The 3rd Joint International Conference on Multibody System Dynamics and the 7th Asian Conference on Multibody Dynamics, June 30 – July 3, 2014*, BEXCO, Busan, Korea, 2014. - In revised version online available as Technical Report 02-2015, Martin Luther University Halle-Wittenberg, Institute of Mathematics, 2015.
13. M. Arnold, A. Cardona, and O. Brüls. A Lie algebra approach to Lie group time integration of constrained systems. Accepted for publication in P. Betsch, editor, *Structure-Preserving Integrators in Nonlinear Structural Dynamics and Flexible Multibody Dynamics*, *CISM Courses and Lectures*. Springer, Wien New York. - Online available as Technical Report 01-2015, Martin Luther University Halle-Wittenberg, Institute of Mathematics, 2015.

14. M. Arnold, A. Fuchs, and C. Führer. Efficient corrector iteration for DAE time integration in multibody dynamics. *Comp. Meth. Appl. Mech. Eng.*, 195:6958–6973, 2006.
15. M. Arnold and A. Murua. Non-stiff integrators for differential-algebraic systems of index 2. *Numerical Algorithms*, 19:25–41, 1998.
16. M. Arnold and W. Schiehlen, editors. *Simulation Techniques for Applied Dynamics*, volume 507 of *CISM Courses and Lectures*. Springer, Wien New York, 2009.
17. V.I. Arnold. *Mathematical Methods of Classical Mechanics*. Number 60 in Graduate Texts in Mathematics. Springer-Verlag, New York Berlin Heidelberg, 2nd edition, 1989.
18. U.M. Ascher, H. Chin, and S. Reich. Stabilization of DAEs and invariant manifolds. *Numer. Math.*, 67:131–149, 1994.
19. D.S. Bae and E.J. Haug. A recursive formulation for constrained mechanical system dynamics: Part II. Closed loop systems. *Mechanics of Structures and Machines*, 15:481–506, 1987.
20. O.A. Bauchau. *Flexible Multibody Dynamics*. Springer, Dordrecht Heidelberg London New York, 2011.
21. J. Baumgarte. Stabilization of constraints and integrals of motion in dynamical systems. *Computer Methods in Applied Mechanics and Engineering*, 1:1–16, 1972.
22. C.L. Bottasso, O.A. Bauchau, and A. Cardona. Time-step-size-independent conditioning and sensitivity to perturbations in the numerical solution of index three differential algebraic equations. *SIAM J. Sci. Comp.*, 29:397–414, 2007.
23. C.L. Bottasso and M. Borri. Integrating finite rotations. *Comput. Methods Appl. Mech. Engrg.*, 164:307–331, 1998.
24. H. Brandl, R. Johanni, and M. Otter. A very efficient algorithm for the simulation of robots and similar multibody systems without inversion of the mass matrix. In P. Kopacek, I. Troch, and K. Desoyer, editors, *Theory of Robots*, pages 95–100, Oxford, 1988. Pergamon Press.
25. V. Brasey. A half-explicit method of order 5 for solving constrained mechanical systems. *Computing*, 48:191–201, 1992.
26. K.E. Brenan, S.L. Campbell, and L.R. Petzold. *Numerical solution of initial-value problems in differential-algebraic equations*. SIAM, Philadelphia, 2nd edition, 1996.
27. O. Brüls, M. Arnold, and A. Cardona. Two Lie group formulations for dynamic multibody systems with large rotations. In *Proceedings of IDETC/MSNDC 2011, ASME 2011 International Design Engineering Technical Conferences*, Washington, USA, 2011.
28. O. Brüls and A. Cardona. On the use of Lie group time integrators in multibody dynamics. *J. Comput. Nonlinear Dynam.*, 5:031002, 2010.
29. O. Brüls and J.C. Golinval. The generalized- α method in mechatronic applications. *ZAMM - Journal of Applied Mathematics and Mechanics / Zeitschrift für Angewandte Mathematik und Mechanik*, 86:748–758, 2006.
30. S.L. Campbell and C.W. Gear. The index of general nonlinear DAEs. *Numerische Mathematik*, 72:173–196, 1995.
31. A. Cardona and M. Géradin. Time integration of the equations of motion in mechanism analysis. *Computers and Structures*, 33:801–820, 1989.
32. E. Celledoni and B. Owren. Lie group methods for rigid body dynamics and time integration on manifolds. *Computer Methods in Applied Mechanics and Engineering*, 192:421–438, 2003.
33. J. Chung and G. Hulbert. A time integration algorithm for structural dynamics with improved numerical dissipation: The generalized- α method. *ASME Journal of Applied Mechanics*, 60:371–375, 1993.
34. J.R. Dormand and P.J. Prince. A family of embedded Runge–Kutta formulae. *J. Comp. Appl. Math.*, 6:19–26, 1980.
35. E. Eich. Convergence results for a coordinate projection method applied to mechanical systems with algebraic constraints. *SIAM J. Numer. Anal.*, 30:1467–1482, 1993.
36. E. Eich-Soellner and C. Führer. *Numerical Methods in Multibody Dynamics*. Teubner-Verlag, Stuttgart, 1998.
37. A. Eichberger. Transputer-based multibody system dynamic simulation: Part I. The residual algorithm – a modified inverse dynamic formulation. *Mech. Struct. & Mach.*, 22:211–237, 1994.

38. R. Featherstone. The calculation of robot dynamics using articulated-body inertias. *The International Journal of Robotics Research*, 2:13–30, 1983.
39. J. Fraćzek and M. Wojtyra. On the unique solvability of a direct dynamics problem for mechanisms with redundant constraints and Coulomb friction in joints. *Mechanism and Machine Theory*, 46:312–334, 2011.
40. C. Führer. *Differential-algebraische Gleichungssysteme in mechanischen Mehrkörpersystemen. Theorie, numerische Ansätze und Anwendungen*. PhD thesis, TU München, Mathematisches Institut und Institut für Informatik, 1988.
41. C. Führer and B.J. Leimkuhler. Numerical solution of differential-algebraic equations for constrained mechanical motion. *Numerische Mathematik*, 59:55–69, 1991.
42. J. García de Jalón and M.D. Gutiérrez-López. Multibody dynamics with redundant constraints and singular mass matrix: existence, uniqueness, and determination of solutions for accelerations and constraint forces. *Multibody System Dynamics*, 30:311–341, 2013.
43. C.W. Gear. Maintaining solution invariants in the numerical solution of ODEs. *SIAM J. Sci. Stat. Comput.*, 7:734–743, 1986.
44. C.W. Gear, B. Leimkuhler, and G.K. Gupta. Automatic integration of Euler–Lagrange equations with constraints. *J. Comp. Appl. Math.*, 12&13:77–90, 1985.
45. M. Géradin and A. Cardona. *Flexible Multibody Dynamics: A Finite Element Approach*. John Wiley & Sons, Ltd., Chichester, 2001.
46. G.H. Golub and Ch.F. van Loan. *Matrix Computations*. The Johns Hopkins University Press, Baltimore London, 3rd edition, 1996.
47. E. Hairer, Ch. Lubich, and M. Roche. *The numerical solution of differential-algebraic systems by Runge–Kutta methods*. Lecture Notes in Mathematics, 1409. Springer–Verlag, Berlin Heidelberg New York, 1989.
48. E. Hairer, Ch. Lubich, and G. Wanner. *Geometric Numerical Integration. Structure–Preserving Algorithms for Ordinary Differential Equations*. Springer–Verlag, Berlin Heidelberg New York, 2nd edition, 2006.
49. E. Hairer, S.P. Nørsett, and G. Wanner. *Solving Ordinary Differential Equations. I. Nonstiff Problems*. Springer–Verlag, Berlin Heidelberg New York, 2nd edition, 1993.
50. E. Hairer and G. Wanner. *Solving Ordinary Differential Equations. II. Stiff and Differential-Algebraic Problems*. Springer–Verlag, Berlin Heidelberg New York, 2nd edition, 1996.
51. H.M. Hilber, T.J.R. Hughes, and R.L. Taylor. Improved numerical dissipation for time integration algorithms in structural dynamics. *Earthquake Eng. and Struct. Dynamics*, 5:283–292, 1977.
52. M. Hoschek, P. Rentrop, and Y. Wagner. Network approach and differential-algebraic systems in technical applications. *Surveys on Math. in Industry*, 9:49–75, 1999.
53. A. Iserles, H.Z. Munthe-Kaas, S. Nørsett, and A. Zanna. Lie-group methods. *Acta Numerica*, 9:215–365, 2000.
54. K.E. Jansen, C.H. Whiting, and G.M. Hulbert. A generalized- α method for integrating the filtered Navier-Stokes equations with a stabilized finite element method. *Computer Methods in Applied Mechanics and Engineering*, 190:305–319, 2000.
55. L.O. Jay and D. Negrut. Extensions of the HHT-method to differential-algebraic equations in mechanics. *Electronic Transactions on Numerical Analysis*, 26:190–208, 2007.
56. L.O. Jay and D. Negrut. A second order extension of the generalized- α method for constrained systems in mechanics. In C. Bottasso, editor, *Multibody Dynamics. Computational Methods and Applications*, volume 12 of *Computational Methods in Applied Sciences*, pages 143–158. Springer, Dordrecht, 2008.
57. J.J. Kalker. *Three-Dimensional Elastic Bodies in Rolling Contact*. Kluwer Academic Publishers, Dordrecht Boston London, 1990.
58. P. Kunkel and V. Mehrmann. *Differential-Algebraic Equations. Analysis and Numerical Solution*. EMS Textbooks in Mathematics. European Mathematical Society, Zurich, 2006.
59. P. Lötstedt. Mechanical systems of rigid bodies subject to unilateral constraints. *SIAM J. Appl. Math.*, 42:281–296, 1982.

60. P. Lötstedt and L.R. Petzold. Numerical solution of nonlinear differential equations with algebraic constraints I: convergence results for backward differentiation formulas. *Math. of Comp.*, 46:491–516, 1986.
61. Ch. Lubich, Ch. Engstler, U. Nowak, and U. Pöhle. Numerical integration of constrained mechanical systems using MEXX. *Mech. Struct. Mach.*, 23:473–495, 1995.
62. Ch. Lubich, U. Nowak, U. Pöhle, and Ch. Engstler. MEXX – Numerical software for the integration of constrained mechanical multibody systems. Technical Report SC 92–12, ZIB Berlin, 1992.
63. C. Lunk and B. Simeon. Solving constrained mechanical systems by the family of Newmark and α -methods. *Z. Angew. Math. Mech.*, 86:772–784, 2006.
64. M. Möller and C. Glocker. Rigid body dynamics with a scalable body, quaternions and perfect constraints. *Multibody System Dynamics*, 27:437–454, 2012.
65. A. Müller and Z. Terze. The significance of the configuration space Lie group for the constraint satisfaction in numerical time integration of multibody systems. *Mechanism and Machine Theory*, 82:173–202, 2014.
66. D. Negrut, R. Rampalli, G. Ottarsson, and A. Sajdak. On the use of the HHT method in the context of index 3 differential algebraic equations of multi-body dynamics. In J.M. Goicolea, J. Cuadrado, and J.C. García Orden, editors, *Proc. of Multibody Dynamics 2005 (ECCOMAS Thematic Conference)*, Madrid, Spain, 2005.
67. N. Orlandea. *Development and Application of Node–Analogous Sparsity–Oriented Methods for Simulation of Mechanical Dynamic Systems*. PhD thesis, University of Michigan, 1973.
68. L.R. Petzold. Differential/algebraic equations are not ODEs. *SIAM J. Sci. Stat. Comput.*, 3:367–384, 1982.
69. L.R. Petzold. Order results for implicit Runge–Kutta methods applied to differential/algebraic systems. *SIAM J. Numer. Anal.*, 23:837–852, 1986.
70. L.R. Petzold and P. Lötstedt. Numerical solution of nonlinear differential equations with algebraic constraints II: Practical implications. *SIAM J. Sci. Stat. Comput.*, 7:720–733, 1986.
71. W.C. Rheinboldt. Differential-algebraic systems as differential equations on manifolds. *Math. Comp.*, 43:473–482, 1984.
72. W.C. Rheinboldt. On the existence and uniqueness of solutions of nonlinear semi-implicit differential-algebraic equations. *Nonlinear Analysis: Theory Methods & Applications*, 16:647–661, 1991.
73. W. Rulka. *Effiziente Simulation der Dynamik mechatronischer Systeme für industrielle Anwendungen*. PhD thesis, Vienna University of Technology, Department of Mechanical Engineering, 1998.
74. W. Schiehlen. Multibody system dynamics: roots and perspectives. *Multibody System Dynamics*, 1:149–188, 1997.
75. W. Schiehlen and P. Eberhard. *Applied Dynamics*. Springer, Dordrecht, 2014.
76. W.O. Schiehlen, editor. *Multibody Systems Handbook*. Springer–Verlag, Berlin Heidelberg New York, 1990.
77. R. Schwertassek and O. Wallrapp. *Dynamik flexibler Mehrkörpersysteme*. Vieweg, 1999.
78. A.A. Shabana. Flexible multibody dynamics: Review of past and recent developments. *Multibody System Dynamics*, 1:189–222, 1997.
79. A.A. Shabana. *Dynamics of Multibody Systems*. Cambridge University Press, Cambridge, 2nd edition, 1998.
80. B. Simeon. MBSPACK – Numerical integration software for constrained mechanical motion. *Surveys on Mathematics for Industry*, 5:169–202, 1995.
81. B. Simeon. On the numerical solution of a wheel suspension benchmark problem. *Comp. Appl. Math.*, 66:443–456, 1996.
82. B. Simeon. *Computational Flexible Multibody Dynamics: A Differential-Algebraic Approach*. Differential-Algebraic Equations Forum. Springer–Verlag, Berlin Heidelberg, 2013.
83. B. Simeon. On the History of Differential-Algebraic Equations. A Retrospective with Personal Sidetraps. submitted for publication, <https://kluedo.ub.uni-kl.de/frontdoor/index/index/docId/4106>, 2016.

84. B. Simeon, C. Führer, and P. Rentrop. Differential-algebraic equations in vehicle system dynamics. *Surveys on Mathematics for Industry*, 1:1–37, 1991.
85. J.C. Simo and L. Vu-Quoc. On the dynamics in space of rods undergoing large motions – A geometrically exact approach. *Computer Methods in Applied Mechanics and Engineering*, 66:125–161, 1988.
86. F.E. Udewadia and P. Phohomsiri. Explicit equations of motion for constrained mechanical systems with singular mass matrices and applications to multi-body dynamics. *Proc. R. Soc. A*, 462:2097–2117, 2006.
87. M. Valášek, Z. Šika, and O. Vaculín. Multibody formalism for real-time application using natural coordinates and modified state space. *Multibody System Dynamics*, 17:209–227, 2007.
88. R. von Schwerin. *MultiBody System SIMulation – Numerical Methods, Algorithms, and Software*, volume 7 of *Lecture Notes in Computational Science and Engineering*. Springer, Berlin Heidelberg, 1999.
89. R.A. Wehage and E.J. Haug. Generalized coordinate partitioning for dimension reduction in analysis of constrained dynamic systems. *J. Mech. Design*, 104:247–255, 1982.
90. R.A. Wehage, A.A. Shabana, and Y.L. Hwang. Projection methods in flexible multibody dynamics. Part II: Dynamics and recursive projection methods. *International Journal for Numerical Methods in Engineering*, 35:1941–1966, 1992.
91. J. Yen, L.R. Petzold, and S. Raha. A time integration algorithm for flexible mechanism dynamics: The DAE α -method. *Computer Methods in Applied Mechanics and Engineering*, 158:341–355, 1998.

Index

- Baumgarte stabilization, 52
 - index-2 Baumgarte approach, 53
- BDF, 43
 - BDF solver DASSL, 37, 46
- Consistent initial values, 12
- Constraint matrix, 4, 28
 - rank-deficient constraint matrix, 14, 17
- Constraints
 - hidden constraints, 8, 28
 - holonomic constraints, 4
 - inconsistent constraints, 17
 - redundant constraints, 17
 - rheonomic constraints, 10
 - scleronomic constraints, 8
- Coordinate partitioning, 12
- Coordinates
 - position coordinates, 3
 - velocity coordinates, 3
- Derivative array, 8
- Force vector, 4, 32
 - condensed force vector, 36
- Generalized- α method, 38
- Hamilton's principle, 4, 22, 30
- Hessenberg form
 - index-3 DAE in Hessenberg form, 13, 18, 38
- HHT- α method, 39
- Index reduction, 46
- Index-1 formulation, 50
- Index-2 formulation, 47
- Index-3 formulation, 46
- Lagrange multipliers, 4
- Lagrangian, 4
- Lie group, 20
 - special orthogonal group $SO(3)$, 20
- Loops
 - closed kinematical loops, 37
- Mass matrix, 3
 - body mass matrix, 32
 - condensed mass matrix, 36
 - rank-deficient mass matrix, 3, 14
- Multibody formalisms, 30, 31
 - $\mathcal{O}(N)$ -formalisms, 34
 - explicit $\mathcal{O}(N)$ -formalism, 37
 - recursive multibody formalisms, 32
 - residual formalisms, 36
- Newton-Euler equations, 30
- Projection techniques, 53
- Runge-Kutta methods
 - half-explicit Runge-Kutta methods, 48, 50
 - half-explicit Runge-Kutta solver HEDOP5, 49
 - half-explicit Runge-Kutta solver MDOP5, 51
 - implicit Runge-Kutta methods, 42
 - implicit Runge-Kutta solver RADAU5, 46, 47
- Stabilized index-2 formulation, 55
- Tilde operator, 21
- Topology, 30
- Tree structure, 31

Reports of the Institutes 2015

- 01-15.** M. Arnold, A. Cardona and O. Brüls, *A Lie algebra approach to Lie group time integration of constrained systems*
- 02-15.** M. Arnold, A. Cardona and O. Brüls, *Order reduction in time integration caused by velocity projection*
- 03-15.** Sh. Alzorba, Chr. Günther, N. Popovici and Chr. Tammer, *A new algorithm for solving planar multiobjective location problems involving the Manhattan norm*
- 04-15.** B. Soleimani and R. Weiner, *A class of implicit peer methods for stiff systems*
- 05-15.** E. Köbis and M. A. Köbis, *Treatment of set order relations by means of a nonlinear scalarization functional: A full characterization*